Copyright

by

Hongyi Dang

2000

CO_2 Absorption Rate and Solubility in Monoethanolamine/Piperazine/Water

by

Hongyi Dang, B.S.

Thesis

Presented to the Faculty of the Graduate School of
The University of Texas at Austin
in Partial Fulfillment
of the Requirements
of the Degree of

Master of Science of Engineering

The University of Texas at Austin
May, 2001

CO_2 Absorption Rate and Solubility in Monoethanolamine/Piperazine/Water

APPROVED BY

Gary Rochelle

Gary T. Rochelle

Keith P. Johnston

Keith P. Johnston

To my husband

Acknowledgments

I would like to express my appreciation to Dr. Gary T. Rochelle who served as my thesis supervisor. He has provided guidance, encouragement, and especially insight. His comments and suggestions are always constructive and invariably improve the quality of the work.

I would like to express my appreciation to all those people who contributed to my education. I appreciated especially the invaluable help from Sanjay Bishnoi.

I would like to acknowledge the Separations Research Program of the University of Texas at Austin for providing financial support and research funding.

Finally, my deepest thanks and gratitude must go to my husband for his love and his moral and psychological support. He is the source of my strength. He is my treasure for ever.

ABSTRACT

CO_2 ABSORPTION RATE AND SOLUBILITY IN MONOETHANOLAMINE/PIPERAZINE/WATER

HONGYI DANG, M.S.E.

SUPERVISOR: GARY T. ROCHELLE

The solubility and absorption rate of carbon dioxide into monoethanolamine/ piperazine/water were measured in a wetted wall column at 40-60°C. The total amine concentration was varied from 1.0 M to 5.0 M with monoethanolamine blends containing 0 to 1.2 M piperazine. CO_2 solubility and solution speciation were simulated by 9 equilibrium reactions. Two of the equilibrium constants were adjusted to match literature data. The rate of absorption was predicted by the theory of diffusion with fast chemical reaction. Piperazine at 24 mol% of the total amine decreases CO_2 equilibrium pressure by 50% and enhances CO_2 absorption rate by 50% to 100%. The CO_2 enhancement factor decreases by a factor of 0.6 to 2 as loading decreases from 0 to 0.5 moles CO_2/mole amine.

TABLE OF CONTENTS

Acknowledgements.....v

Abstract.....vi

List of Tables.....x

List of Figures.....xii

Chapter One: Introduction.....1

1.1 Introduction of CO_2 Removal Processes..... 1

1.2 CO_2 Removal From Flue Gas.....4

1.3 Scope and Outline of the Present Work..... 6

Chapter Two: Vapor-Liquid Equilibrium Models and Solubility Data.....10

2.1 Literature Review of VLE Models and Solubility Data.....10

2.1.1 Thermodynamic Models.....10

2.1.2 Summary of Solubility Data of CO_2 in MEA Aqueous Solution.....17

2.2 Simple Vapor-Liquid Equilibrium Model.....17

2.2.1 Model Development.....19

2.2.2 Model Parameter Fitting and Solubility Prediction.....22

2.2.2.1 VLE of CO_2 in MEA at 60°C.....24

2.2.2.2 VLE Model Extension.....30

2.2.2.3 VLE of CO_2 in MEA/PZ at 40°C.....34

Chapter Three: Simple Rate Model..... .37

3.1 Literature Review..... .37

3.2 Simple Rate Model Structure.....39

3.2.1 Pseudo-First Order Enhancement Factor.....40

3.2.2 Instantaneous Enhancement Factor.....41
3.2.3 Total Enhancement Factor.....43
3.3 Rate Model Prediction.....44

Chapter Four: Solubility and Absorption Rate of CO_2 in MEA/PZ/H_2O.....50
4.1 Experimental Apparatus and Methods.....50
4.2 Data Analysis 55
4.2.1 Physical Properties.....55
4.2.2 Liquid Phase and Gas Phase Mass Transfer Coefficients..59
4.2.3 Calculation of Enhancement Factor.....60
4.3. Experimental Results and Discussion.....61
4.3.1 Solubility of CO_2 in MEA/PZ/H_2O.....62
4.3.2 Rate of CO_2 Absorption in MEA/PZ/H_2O.....67

Chapter Five: Conclusions.....75
5.1 Conclusions.....75
5.2 Recommendations.....76

Appendix A: Fortran Codes of VLE and Rate Models.....79
A.1 VLE Model (3.8 M MEA/1.2 M PZ at 60°C).....79
A.2 Pseudo-First Order Enhancement Factor (3.8 M MEA/1.2 M PZ at 60°C).....86
A.3 Instantaneous Enhancement Factor (3.8 M MEA/1.2 M PZ at 60°C).....88

Appendix B: CO_2 Equilibrium Partial Pressure and Speciation of MEA, PZ and $PZCOO^-$.....89

Appendix C: Contributions of Important Species to CO_2 Total Absorption Rate.....99

Appendix D: Calibrations of Mass Flow Rate Controllers.....102

Appendix E: Detailed Experimental Result.....103

Nomenclature.....121

Reference.....123

Vita.....129

List of Tables

Table 2.1. Summary of CO_2 solubility data in MEA aqueous solution.....18

Table 2.2. Temperature dependence of the equilibrium constants.....23

Table 2.3. Summary of fitted model parameters and literature values.....23

Table 2.4. CO_2 solubility in 5 M MEA at 60°C, data from Jou et al. (1995), values predicted by parameters in Table 2.3.....25

Table 2.5. CO_2 solubility in 2.5 M MEA at 60°C, data from Lee et al. (1976), values predicted by parameters in table 2.3.....28

Table 2.6. CO_2 solubility in 1.0 M MEA at 60°C, data from Jou et al. (1995), values predicted by parameters in Table 2.3.....28

Table 2.7. CO_2 solubility in 5.0 M MEA at 40°C, data from Jou et al. (1995), values predicted by parameters in Table 2.3.....35

Table 4.1. Experimental conditions in this work.....62

Table 4.2. Summary of CO_2 solubility in MEA/PZ/H_2O of this work.....64

Table 4.3. Measured and predicted enhancement factors for CO_2 absorption in MEA/PZ/H_2O.....68

Table B.1. P_{CO2} and MEA speciation in CO_2/MEA/H_2O systems.....89

Table B.2. P_{CO2} and speciation in 0.4 M MEA/0.6 M PZ/H_2O systems at 60°C.....91

Table B.3. P_{CO2} and speciation in 1.9 M MEA/0.6 M PZ/H_2O systems at 60°C.....93

Table B.4. P_{CO2} and speciation in 3.8 M MEA/1.2 M PZ/H_2O systems at 60°C.....95

Table B.5. P_{CO2} and speciation in 3.8 M MEA/1.2 M PZ/H_2O systems at 40°C.....97

Table D. Calibrations of mass flow rate controllers.....102

Table E.1. CO_2 in 0.4 M MEA/0.6 M PZ at 60°C (Low loading).....106

Table E.2. CO_2 in 0.4 M MEA/0.6 M PZ at 60°C (Medium loading).....107

Table E.3. CO_2 in 1.9 M MEA/0.6 M PZ at 60°C (Zero loading).....108

Table E.4. CO_2 in 1.9 M MEA/0.6 M PZ at 60°C (Medium loading).....109

Table E.5. CO_2 in 1.9 M MEA/0.6 M PZ at 60°C (High loading).....110

Table E.6. CO_2 in 2.5 M MEA at 60°C (Zero loading).....111

Table E.7. CO_2 in 2.5 M MEA at 60°C (Medium loading).....112

Table E.8. CO_2 in 2.5 M MEA at 60°C (High loading).....113

Table E.9. CO_2 in 3.8 M MEA/1.2 PZ at 40°C (High loading).....114

Table E.10. CO_2 in 3.8 M MEA/1.2 PZ at 40°C (High loading).....115

Table E.11. CO_2 in 3.8 M MEA/1.2 PZ at 60°C (High loading).....116

Table E.12. CO_2 in 5.0 M MEA at 40°C (Medium loading).....117

Table E.13. CO_2 in 5.0 M MEA at 40°C (High loading).....118

Table E.14. CO_2 in 5.0 M MEA at 60°C (Medium loading).....119

Table E.15. CO_2 in 5.0 M MEA at 60°C (Medium loading).....120

List of Figures

Figure 1.1. Commonly used alkanolamines in gas treating processes.....3

Figure 1.2. Simplified process flow diagram of CO_2 removal from flue gas.....6

Figure 2.1. Chemical and physical equilibria in a closed aqueous weak electrolyte system.....11

Figure 2.2. Figure 2.2. CO_2 solubility in 5 M amine (MEA+PZ) at 60°C and 40°C, predicted by parameters in table 2.3, data from Jou et al. (1995).....24

Figure 2.3. Predicted speciation of CO_2 in 5 M MEA at 60°C, data from Jou (1995).....26

Figure2.4. CO_2 solubility in 2.5 M amine (MEA+PZ) and 1.0 M amine (MEA+PZ) at 60°C, data from Lee (1976), 2.0 predicted by parameters in table 2.3.....27

Figure 2.5. Predicted speciation of CO_2 in 2.5 M MEA at 60°C, data from Lee (1976).....29

Figure 2.6. Predicted speciation of CO_2 in 1.0 M MEA at 60°C, data from Lee (1976).....29

Figure 2.7. Predicted speciation of CO_2 in 2.5 M MEA at 60°C, values predicted by parameters fitted by data from Jou et al. (1995) at 5 M MEA.....31

Figure 2.8. Predicted speciation of CO_2 in 1.0 M MEA at 60°C, values predicted by parameters fitted by data from Jou et al. (1995) at 5 M MEA.....31

Figure 2.9. Predicted speciation of CO_2 in 4.4 M MEA/0.6 M PZ at 60°C.....32

Figure 2.10. Predicted speciation of CO_2 in 1.9 M MEA/0.6 M PZ at 60°C....33

Figure 2.11. Predicted speciation of CO_2 in 0.4 M MEA/0.6 M PZ at 60°C....33

Figure 2.12. Predicted speciation of CO_2 in 3.8 M MEA/1.2 M PZ at 60°C....34

Figure 2.13. Predicted speciation of CO_2 in 5.0 M MEA at 40°C....36

Figure 2.14. Predicted speciation of CO_2 in 3.8 M MEA/1.2 M PZ at 40°C....36

Figure 3.1 Pseudo-first order assumption of CO_2 absorption in amine solution....43

Figure 3.2 Physical model of CO_2 absorption in amine solution....44

Figure 3.3 Predicted enhancement of CO_2 absorption in 0.4 M MEA/0.6 M PZ at 60°C, and k_l^o =1.6E(-4)....44

Figure 3.4. Enhancement of CO_2 absorption in 1.0 M MEA/PZ at 60°C....46

Figure 3.5. Enhancement of CO_2 absorption in 2.5 M MEA/PZ at 60°C....46

Figure 3.6. Enhancement of CO_2 absorption in 5.0 M MEA/PZ at 60°C....47

Figure 3.7. Enhancement of CO_2 absorption in 5.0 M MEA/PZ at 40°C....47

Figure 3.8. Enhancement of CO_2 absorption in 5.0 M MEA/PZ at 60°C and 40°C....48

Figure 3.9. CO_2 absorption rate contribution of MEA, PZ and $PZCOO^-$ in 3.8 M MEA/1.2 M PZ at 60°C....49

Figure 4.1. Detailed column diagram.....51

Figure 4.2. Overall experimental flowsheet.....51

Figure 4.3. Extraction of CO_2 solubility in 5.0 M MEA at 40 °C, P_{CO2}*=22.1Pa, loading=0.299.....63

Figure 4.4. Comparison of predicted CO_2 solubility, literature data, and the experimental data of this work in 5.0 M MEA blends with 0 or 1.2 M PZ at 60°C and 40°C.....65

Figure 4.5. Comparison of predicted CO_2 solubility, literature data, and the experimental data of this work in 2.5 M MEA blends with 0 or 0.6 M PZ at 60°C.....66

Figure 4.6. Comparison of predicted CO_2 solubility, literature data, and the experimental data of this work in 1.0 M MEA blends with 0 or 0.6 M PZ at 60°C.....66

Figure 4.7. Linear relation between flux and ($P_{CO2,i}$ – P_{CO2}*) for CO_2 absorption in 0.4M MEA/0.6MPZ at loading of 0.138, 60°C....69

Figure 4.8. CO_2 absorption rate in 1.0 M MEA blends containing with 0 or 0.6M PZ at 60°C, curves predicted by the rate model with the listed constants.....71

Figure 4.9. CO_2 absorption rate in 2.5 M MEA blends containing with 0 or 0.6M PZ at 60°C, curves predicted by the rate model with the listed constants.....72

Figure 4.10. CO_2 absorption rate in 5.0 M MEA blends containing with 0 or 1.2 M PZ at 60°C, curves predicted by the rate model with the listed constants, line segments connected values of equal loading.....72

Figure 4.11. CO_2 absorption rate in 5.0 M MEA blends containing with 0 or 1.2 M PZ at 40°C, curves predicted by the rate model with the listed constants, line segments connected values of equal loading.....73

Figure C.1. CO_2 absorption rate contribution of MEA, PZ and $PZCOO^-$ in 0.4 M MEA/0.6 M PZ at 60°C.....100

Figure C.2. CO_2 absorption rate contribution of MEA, PZ and $PZCOO^-$ in 1.9 M MEA/0.6 M PZ at 60°C.....100

Figure C.3. CO_2 absorption rate contribution of MEA, PZ and $PZCOO^-$ in 3.8 M MEA/1.2 M PZ at 60°C.....101

Figure C.4. CO_2 absorption rate contribution of MEA, PZ and $PZCOO^-$ in 3.8 M MEA/1.2 M PZ at 40°C.....101

Chapter One

Introduction

1.1 Introduction of CO_2 Removal Processes

Removal of CO_2 from fuel gas and H_2 has been practiced in many industrial processes including oil and gas purification, ammonia manufacture, coal gasification, and hydrogen production. CO_2 must be removed from natural gas because it acts as diluent, increasing transportation costs and reducing the energy level per unit gas. CO_2 has to be separated from syn-gas in the production of ammonia to avoid poisoning catalyst in the ammonia converter. Now, CO_2 is considered to be a major greenhouse gas, so the separation of CO_2 from fuel gas and flue gas is desired to reduce greenhouse gas emissions. Furthermore the interest in the removal of CO_2 is also being propelled in use in the merchant CO_2 market and the renewed interest in enhanced oil recovery (EOR).

Aqueous alkanolamine solutions are widely used for the removal of CO_2 from source gas streams. Alkanolamines are characterized as containing both hydroxyl groups and amine groups. The hydroxyl groups of the alkanolamines reduce the vapor pressure and increase the water solubility while the amine groups provide the necessary alkalinity in the aqueous solution to react with the acid gas.

The chemical reactions of alkanolamine with CO_2 have two distinct effects on the gas absorption processes. The first effect is the increase in solubility of the acid

gas in the liquid phase, since the dissolved gas exists in both chemically combined and original forms. The second effect is the increase in the absorption rate of the acid gas due to the reaction of the gas with the basic species in the boundary layer. The increased solubility allows for a lower liquid-phase flow rate, which decreases pumping and regeneration costs and permits preferential absorption of the acid gas relative to nonacidic gases such as methane or hydrogen, which can also be present in the gas streams. Furthermore, the increased absorption rate of the acid gases permits smaller column design.

Commercially used alkanolamines include monoethanolamine (MEA), diethanolamine (DEA), and methyldiethanolamine (MDEA). Aqueous MEA solution has been used extensively for the removal of CO_2 from gas streams. It has several advantages over other commercial alkanolamines. First, it is a relative strong base with a fast reaction rate, yielding the lowest CO_2 concentration, which makes it most suitable for processing natural gas, synthesis gas, and hydrogen. MEA has the lowest molecular weight and thus the highest absorption capacity on a weight basis. MEA is very thermally stable and less likely to undergo thermal degradation. It has a relative low solubility for hydrocarbon, which reduces the hydrocarbon loss when processing natural gas and refinery gas streams. But MEA has a high heat of reaction with CO_2 that leads to higher stripping energy consumption. It suffers more vaporization loss than other alkanolamines because of

its higher vapor pressure. Another disadvantage of MEA is that it is appreciably more corrosive than many other alkanolamines.

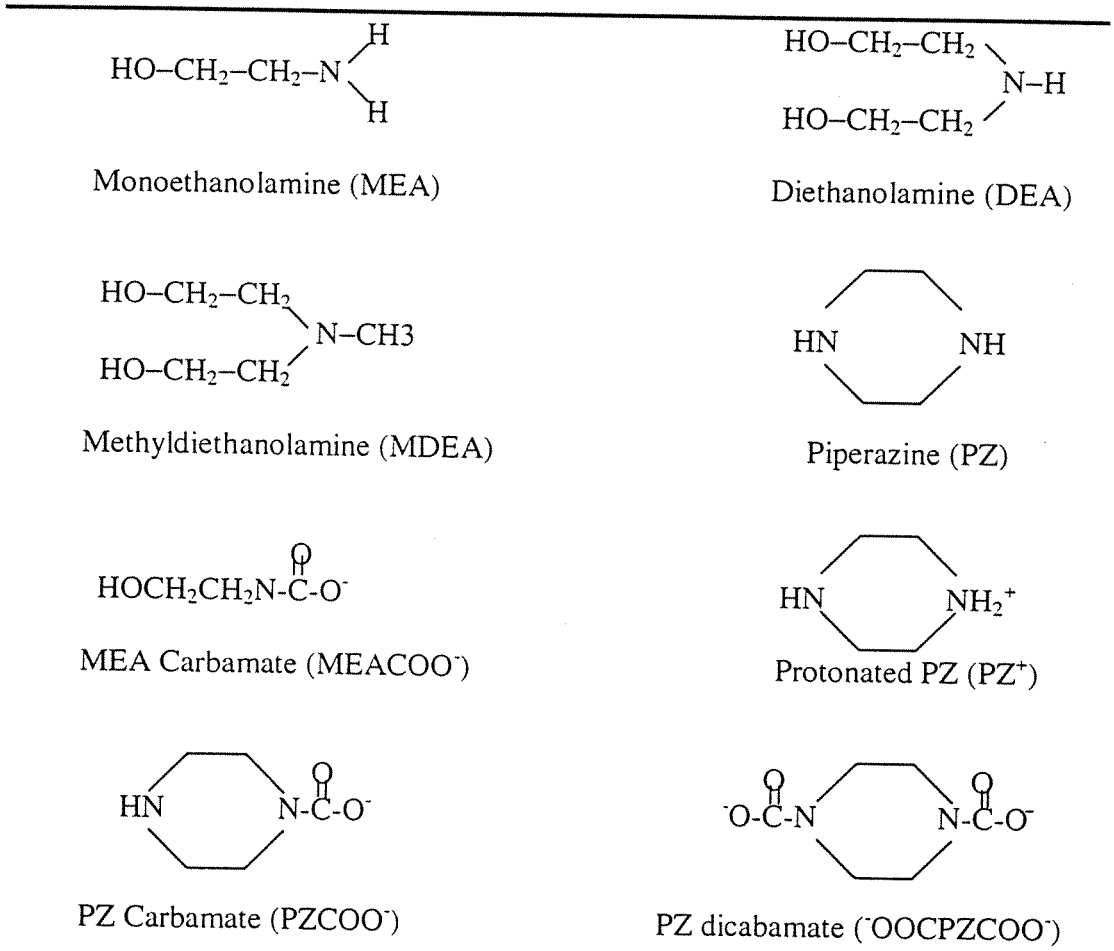

Figure 1.1. Commonly used alkanolamines in gas treating processes.

Aqueous solutions of diethanolamine (DEA) have been used for many years for the treatment of refinery gases which normally contain appreciable amounts of COS and CS_2, besides CO_2. Generally, secondary amines are much less reactive

with COS and CS_2 than primary amine, and the reaction products are not particularly corrosive. Consequently, DEA and other secondary amines are the better choice for treating gas streams containing COS and CS_2. The low vapor pressure of DEA makes it suitable for low-pressure operations as vaporization losses are quite negligible. One disadvantage of DEA solution is that the reclaiming of contaminated solutions may require vacuum distillation. Another disadvantage of DEA is that DEA undergoes numerous irreversible reactions with CO_2, forming corrosive degradation products, and for this reason, DEA may not be the optimum choice for treating gas with a high CO_2 content. The heat of absorption of CO_2 is typically about 16 kcal/mol (Kohl and Nielsen, 1997).

MDEA, a tertiary amine, reacts at a much slower rate with an enthalpy of reaction of 11.6 kcal/mol (Kohl and Nielsen, 1997). MDEA has a higher capacity to absorb CO_2 and is less volatile than DEA or MEA. Its smaller enthalpy of reaction and greater capacity lead to lower energy requirements for regeneration while the lower vapor pressure results in smaller losses of solvent by vaporization. Due to the corrosion problems, MEA is used in less that 20 wt% without corrosion inhibitors and DEA is used in 20-35 wt%. MDEA is less corrosive and can be used at concentrations up to 50 wt%. This higher concentration compensates to some extent for its slower rate of reaction; therefore, MDEA can be considered for bulk removal of acid gases as well. Another advantage of MDEA is that it does not

degrade readily to form higher molecular weight compounds that accumulate in the solution.

1.2 CO_2 Removal From Flue Gas

The chemical solvents play a very important role for the removal of CO_2 from flue gas. Flue gas is generally at atmospheric pressure. The CO_2 partial pressure of the residue gases required to achieve the desired separation is extremely small, e.g., 5 to 10 mmHg. Thoroughly regenerated chemical solvent is needed to bring the CO_2 partial pressures down to this low level. The recovered CO_2 must be recompressed or/and condensed to transport the product to the end user for enhanced oil recovery, beverage-manufacturing or for remote disposal in the case of greenhouse mitigation.

Figure 1.2 shows a simplified gas treating process that employs an aqueous alkanolamine solution in an absorption/stripping process. In this process, a flue gas containing CO_2 is introduced at the bottom of the absorber where it contacts countercurrently with an aqueous solution of alkanolamine that is introduced at the top of the absorber. As the alkanolamine solution travels down the column, it becomes loaded with CO_2 and leaves the bottom of the absorber as rich alkanolamine. The alkanolamine solution rich in absorbed CO_2 is pumped from the bottom of the absorber through heat exchangers where the temperature is raised. The amine solution is then introduced at the top of a stripper where it countercurrently contacts steam at a reduced pressure and at a high temperature.

The steam produced in a reboiler, provides the energy necessary to reverse the reactions of the CO_2 with alkanolamine, increasing the CO_2 partial pressure and, simultaneously, stripping the CO_2 from the solution. The lean alkanolamine solution is then pumped through a heat exchanger, where it is cooled and reintroduced at the top of the absorber. The stripped CO_2 is sent for further processing.

For flue gas processing, a typical inlet concentration of CO_2 is about 10 mol%. Usually, CO_2 must be removed down to about 1%. The absorber operates at a temperature range of 40°C-60°C. Lower temperature is hard to achieve without refrigeration and can also inhibit absorption kinetics. Higher temperature reduces equilibrium solubility and solution capacity. The absorber is near atmospheric pressure. The stripper removes acid gases by increasing the temperature of the amine. Typical operating temperatures of the stripper are around 120°C. The stripper pressure is usually determined by the backpressure required for the acid gas stream to be further processed.

1.3 Scope and Outline of the Present Work

Due to the high rate of reaction of the primary or secondary amines with CO_2 and the low reaction heat of CO_2 with tertiary amines, mixtures of primary or secondary amines (such as MEA and DEA) with tertiary amines (MDEA) can be attractive alternatives for acid gas absorption and have found widespread application in the absorption of CO_2 from process gases. The kinetics of CO_2

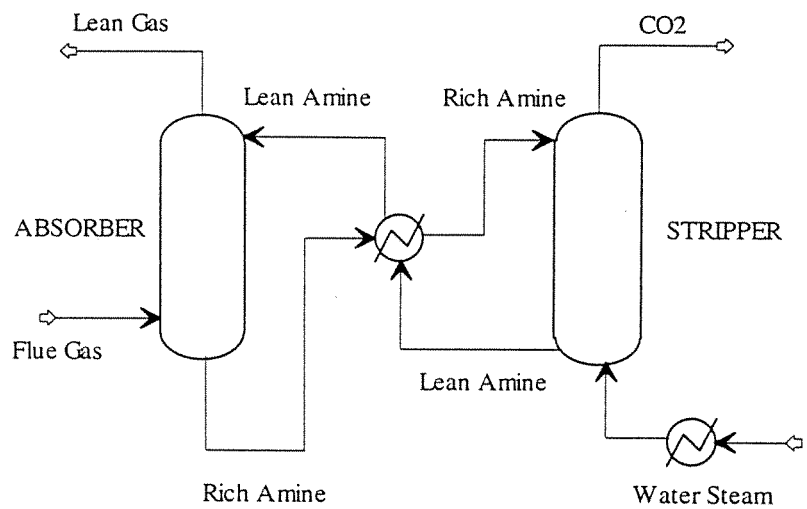

Figure1.2. Simplified process flow diagram of CO_2 removal from flue gas.

absorption into mixtures of MDEA and DEA has been studied by Mshewa and Rochelle (1995). They measured the rates of absorption and desorption of CO_2 in a 50 wt% solution of MDEA over a wide range of temperature and partial pressures. The results were used with literature values of DEA reactions to develop a model for CO_2 absorption in DEA and mixture of DEA and MDEA. The model predicts that the overall gas phase coefficient for CO_2 absorption in a solution containing 40% MDEA and 10% DEA is 1.7 to 3.4 times greater than that for CO_2 absorption in a 50% MDEA solution under typical absorption column conditions. A commercial process using this phenomenon was disclosed by BASF Aktiengesellschaft and described by Meissner (1983) and by Meissner and Wagner (1983).

The BASF Activated MDEA process employs a 2.5 to 4.5 M MDEA solution containing up to 0.8 M piperazine as promoter (Bartholome et al., 1971; Appl et al., 1980). Piperazine is a cyclic secondary alkanolamine with two amine groups. Its molecular structure is shown in figure 1.1. Its carbamate stability constant is comparable to other secondary alkanolamine such DEA but the apparent second order rate constant is an order of magnitude higher than that of primary alkanolamines such as MEA or DGA (Bishnoi, 1999). Several studies have been done for piperazine activated MDEA (Appl et al., 1982, Xu et al., 1992, 1995, 1998). This blend of amines has been used successfully for high capacity carbon dioxide removal in ammonia plant. They have been effective at much lower promoter concentration than conventional blends (DGA/MDEA).

This work deals with CO_2 absorption in MEA solution and in blends of MEA and piperazine for the purpose of increasing the absorption rate and absorption capacity. Currently, the tray efficiency of an absorption column for the CO_2 removal is about 10-20%. Because of the high apparent second order rate constant and two amine groups in one molecule, the addition of PZ is expected to absorb more CO_2 at the a faster rate with the same amine concentration as MEA or achieve the same degree of CO_2 removal at a lower total amine concentration. This will increase the tray efficiency and decrease the number of trays of the absorption column.

This work begins by the discussion of the vapor-liquid-equilibrium model of CO_2 absorption in MEA/H_2O and in blends of MEA/PZ/H_2O in chapter 2. The outline will be similar to the model of Bishnoi (1999) for the CO_2 absorption in PZ/H_2O. Chapter 3 presents a rate model using the speciation/solubility model of chapter 2. The rate model uses the pseudo first order assumption with the correction of instantaneous reactions to represent the effect of fast reactions in the liquid film. The most important part of this work is the measurement of the solubility and absorption rate of CO_2 in MEA/H_2O and MEA/PZ/H_2O. Chapter 4 summarizes the results of those measurements and compares them with the model predictions.

Chapter Two

Vapor-Liquid Equilibrium Models and Solubility Data

The design of acid gas absorption/stripping systems requires a correct knowledge of the vapor-liquid equilibrium behavior of the aqueous acid gas-alkanolamine system. There exists a large body of vapor-liquid equilibrium data for aqueous acid gas-alkanolamine systems reported in the literature. However, most of these data were measured at high acid gas loading. Only small fraction of the data is at low acid gas loading which determines the limitation of the sweet gas purity. Consequently, thermodynamic models are needed to interpolate and extrapolate available experimental data. Furthermore, a successful VLE model is not only needed for equilibrium stage design calculations, but also for rate-based models, in which liquid phase concentrations enter into kinetic expressions affecting mass transfer at the liquid-vapor interface.

This chapter will review the VLE models of acid gases in alkanolamine solutions and solubility data of CO_2 in MEA solutions. A simple VLE model will be introduced to provide a guide to the measurement of the solubility of CO_2 in monoethanolamine and monoethanolamine/piperazine aqueous solutions.

2.1 Literature Review of VLE Models and Solubility Data

2.1.1 Thermodynamic Models

Before going into the details of these VLE models, a physical model is introduced first. As mentioned above, acid gases and alkanolamines are weak electrolytes, which partially dissociate in the aqueous phase to form a complex mixture of nonvolatile or moderately volatile solvent species (water and alkanolamine), highly volatile molecular species (such as CO_2), and nonvolatile ionic species.

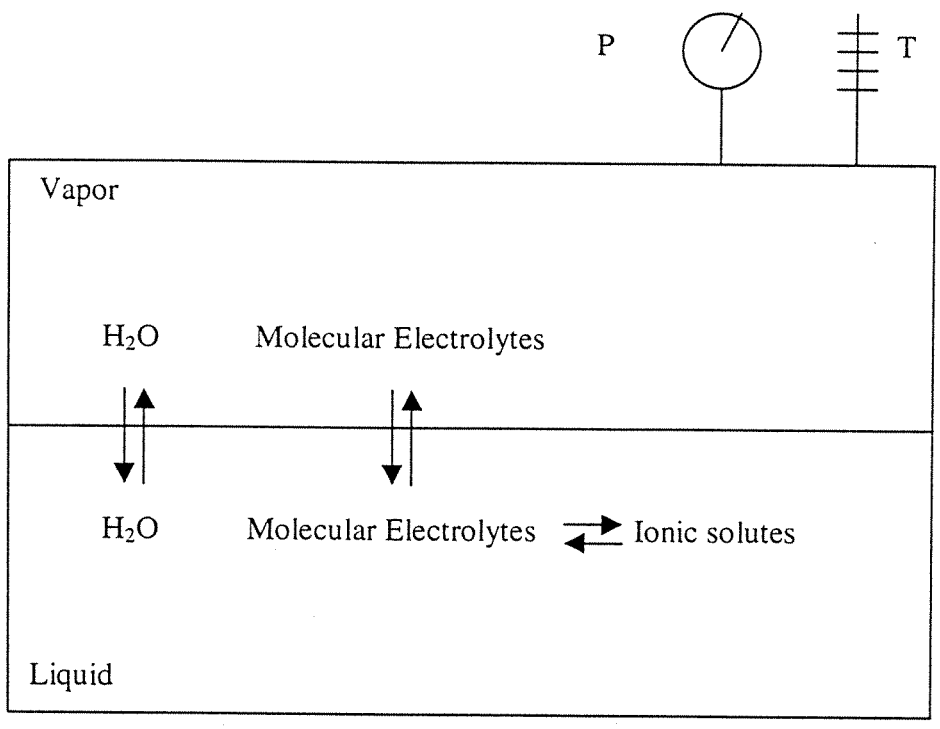

Figure 2.1. Chemical and physical equilibria in a closed aqueous weak electrolyte system.

Figure 2.1 illustrates the phase and chemical equilibria of a weak electrolyte system such as the acid gas-alkanolamine-water system. In a closed system, at constant temperature and pressure, the phase equilibrium governs the distribution of molecular species between the liquid and vapor phases, while chemical reactions occur in the liquid phase between acid gases and alkanolamines to produce a number of ionic species. As shown in figure 2.1, phase and chemical equilibria are highly coupled in this system so that the degree of dissociation of the weak electrolytes in the liquid phase is influenced by the partial pressure of an acid gas in the vapor phase and vice versa. Hence, representation of the vapor-liquid equilibrium behavior of acid gas-alkanolamine-water systems is complicated due to the large number of chemical reactions that occur in this system. Therefore representation of phase equilibria for such system requires that both phase and chemical equilibria be accounted for.

In the early stage of developing VLE models for weak electrolyte solutions, most models set all activity coefficients of all species to unity. With the development of several semi-empirical excess Gibbs energy models or activity coefficient models for aqueous electrolyte systems, several thermodynamically rigorous VLE models for the alkanolamine-water-acid gas system have been developed. Following are the VLE models that have played important roles in simulating the alkanolamine-acid gas-water system.

Kent and Eisenberg (1976) created the first equilibrium model that received widespread use. Their model was based on pseudo-equilibrium constants and Henry's law. They regressed the pseudo-equilibrium constants for the amine protonation and carbamate reversion reactions for MEA and DEA systems to fit experimental vapor-liquid equilibrium data. This resulted in a model which has only two parameters per acid gas to account for the ionic strength dependencies of the acid gas partial pressure. The model was reasonably accurate at loading greater that 0.1, but was inaccurate at lower loading due to the manipulations of amine equilibrium constants. Another drawback of this model was that it could not be used to find ionic species concentrations. By regressing the equilibrium constants they have effectively combined the activity coefficients with species mole fractions making independent determinations of either impossible. Only MEA and DEA systems were studied in their paper and they report a reasonable predictive agreement with mixed acid gas data.

Edwards et al. (1975, 1978) developed a model for aqueous solutions of ammonia with CO_2, H_2O, SO_2, and hydrogen cyanide. These chemical systems are similar to the typical gas treating chemical system, alkanolamine-H_2O-CO_2-H_2S. They also compiled chemical equilibrium and Henry's constants in water for the various compounds as a function of temperature. Austgen (1989) based many of his constants on this compilation. Their equation for activity coefficients is the basis for the Deshmukh-Mather model.

Deshmukh and Mather (1981) produced a more thermodynamically rigorous model based on extended Debye-Hückel theory and the work of Edwards et al. (1975, 1978) and Beutier and Renon (1978). Their activity coefficient equation had one term to account for electrostatic forces by the Debye-Hückel law and another term with adjustable parameters to account for short range interactions.

The Peng-Robinson equation of state was used to determine vapor phase fugacity coefficients. They assumed the activity coefficient of water to be 1.0. In fact, the water activity coefficient can be different from 1.0 and is highly correlated with the amine activity coefficient. A 5% change in water activity coefficient can result in a large change in the amine activity coefficient.

To simplify their regressions, species having small concentrations were removed from the mass balances and their parameters were set to zero so that they had no effect on the model. As an example, for the MEA-CO_2-H_2O system, CO_2, OH^-, H^+, and CO_3^{2-} would be neglected. These assumptions leave questions about the validity of the model at the low loading where the above neglected species are important. Deshmukh and Mather neglect any mixed acid gas parameters and state that combining the single acid gas systems sufficiently predicts mixed acid gas equilibrium. Weiland (1993, 1995) used the Deshmukh-Mather model to predict CO_2 and H_2S equilibrium for MEA, DEA, DGA® and MDEA.

Austgen (1989) developed a rigorous physical-chemical model for representing liquid phase chemical equilibria of acid gas/alkanolamine/water systems. The

model framework requires an input of the equilibrium constants for all solution reactions, Henry's constant for gases, and binary interaction parameters for all important solution species.

Austgen and Rochelle (1991) used the electrolyte-NRTL equation to correlate most of the available data on acid gas equilibria in aqueous solution of the common alkanolamines. In developing the model parameters for the acid gas-alkanolamine-water system, they regressed amine-water total pressure data to obtain amine-water parameters, and regressed acid gas solubility data to obtain the interaction parameters of bisulfide or bicarbonate salt with water. All other activity parameters were set to default values. Furthermore, because the MDEA/H_2O parameters did not give a successful fit of the acid gas solubility data and because the MDEA/H_2O data did not appear to be reliable, Austgen arbitrarily chosen to set the MDEA/H_2O parameters to zero rather than their regressed values.

Posey and Rochelle (1994) used data for total pressure, freezing point, heat of mixing and vapor-liquid equilibrium to find parameters of the Nonrandom Two-Liquid (NRTL) model for the binary alkanolamine-water systems, MEA-H_2O, DEA-H_2O and MDEA-H_2O. Later Posey and Rochelle (1997) regressed the electrolyte NRTL model parameters for MDEA-CO_2-H_2S-H_2O with the VLE data supplemented by pH and conductivity data by using the data regression system (DSA) of Aspen Plus to improve confidence in model predictions at low acid gas loading.

Liu et al. (1999) discussed the effects of chemical equilibrium constants, Henry's law constant, experimental data, and data regression on the representation of the VLE of the acid gas-alkanolamine-water system.

Lee (1992, 1994) developed a modified group contribution model for equilibrium predictions for gas treating systems. His model is modified from previous group contribution methods in that it can account for gas molecules such as CO_2 and H_2S that cannot be broken into groups. The possible benefits of his model would be the ability to predict the behavior of new proposed alkanolamine molecules for which there is no data. A drawback of the group contribution method is that it requires accurate data for a series of chemically similar compounds to generate the group constants. Accurate data is often hard to find for the amines of interest, such as MDEA, and data for the other amines in a series, which have no industrial use, are non-existent. Since the parameters of his model are also regressed on acid gas VLE data, it has the same data discrepancy problems to contend with as do other models.

In addition to the VLE models mentioned above, there are other approaches for the VLE modeling concept. For example, Posy et al. (1996) developed a model that is simple enough to use in a hand held calculator, but its structure is derived from theory. Parameters are given for the MDEA-H_2O-H_2S-CO_2 and DEA-H_2O-H_2S system. Zuo and Fürst (1998) extended the electrolyte equation of state developed by Fürst and Renon(1993) to mixed-solvent electrolyte system. Kuranov et al.

(1997) proposed a method for modeling vapor-liquid equilibria in ternary aqueous systems containing acid gas and alkanolamine with an equation of state describing both phases. A hole quasichemical model is modified for chemical reactions and electrostatic interactions in the liquid solution. The model was carried out for CO_2-MDEA-H_2O and H_2S-MDEA-H_2O systems.

2.1.2 Summary of Solubility Data of CO_2 in MEA Aqueous Solution

In order to improve the quality of thermodynamic models, thermodynamic data of high quality is required. However, the existing database contained in the literature has been found to be inadequate to meet this industrial demand, especially for the mixed amine solutions, mixed acid gases, and in the low-pinch regions (Rochelle, 1991; Weiland et al., 1993). Moreover, the available literature data show significant discrepancies among the result of different authors. The available VLE data for CO_2/MEA/H2O is summarized in table 2.1

2.2 Simple Vapor-Liquid Equilibrium Model

One of the main objectives of the present work is to measure the solubility and absorption rate of CO_2 in MEA/PZ/H_2O. An effective VLE model is required to select experimental gas and liquid compositions and to interpret rate results. In this work, a simple VLE model was developed to predict the thermodynamic behavior of the CO_2/MEA/PZ/H_2O system with acceptable accuracy.

Table 2.1. Summary of CO_2 solubility data in MEA aqueous solution.

Data source	MEA Concentration	Temperature Range	Partial Pressure	Acid Loading
Bottoms(1931)	5.3M	25~ 55 °C	<760mm-Hg	
Mason(1936)	0.5~12.5M	0.~ 75°C	10-760mm-Hg	0.047-1.112
Reed(1941)	2.5M	100~140°C	20-250Psia	
Lyudkovskaya(1949)	0.5, 2, 5M	20~75°C	2.5-40atm	
Atadan(1954)	2.5~10.0M	30~100°C	15-500Psia	
Monnahan(1957)	2.5M	25, 100°C	<1000mmHg	0.136-0.74
Goldman(1959)	6~30wt%	75~140°C	0.3-467kPa	
Jones(1959)	15.3wt%	40~140°C	<6206mmHg	0.017-0.728
Murzin(1971)	0.5~3.4M	30~80°C	<13.5Psia	
Lee(1974)	15, 30wt%	40, 100°C	<6620kPa	
Lee(1976)	1.0~5.0M	25~120°C	<6616kPa	0.09-2.0
Lawson(1976)	15wt%	104~284°C	<20900mmHg	0.110-0.929
Nasir(1977)	15, 30wt%	60~100°C	0.001-1.3kPa	
Isaacs(1980)	2.5M	80, 100°C	0.01-1.75kPa	0.037-0.315
Shen(1992)	15.3, 30wt%	40~100°C	<2550kPa	0.227-1.049
Jou(1995)	30%	0~150°C	<20,000kPa	0.003-1.324

2.2.1 Model Development

The focus of this work is the CO_2/MEA/PZ/H_2O system. A VLE model for CO_2 absorption in MEA aqueous solution was developed first and then extended to CO_2 absorption in MEA/PZ solution.

There are two kinds of equilibria in the MEA aqueous solution: phase equilibrium and chemical equilibrium. The phase equilibrium governs the distribution of molecular species between the liquid and gas phase and can be represented by Henry's law:

$$P^*_{CO_2} = H_{CO_2} X_{CO_2} \tag{2.1}$$

Where, P_{CO2}* is the equilibrium partial pressure of CO_2 in the gas phase, H_{CO2} is the Henry's law constant of CO_2 in the MEA solution. X_{CO2} is the mole fraction of CO_2 molecule in the liquid phase.

Equilibrium reactions determine speciation in the liquid phase. Most of these equilibrium reactions can be written as chemical dissociation:

Ionization of water

$$2H_2O \xleftrightarrow{K_{H_2O}} H_3O^+ + OH^- \tag{2.2}$$

Dissociation of carbon dioxide

$$2H_2O + CO_2 \xleftrightarrow{K_{a,CO_2}} H_3O^+ + HCO_3^- \tag{2.3}$$

Dissociation of bicarbonate

$$H_2O + HCO_3^- \xleftrightarrow{K_{a,HCO_3^-}} H_3O^+ + CO_3^{2-} \tag{2.4}$$

Dissociation of protonated MEA

$$H_2O + MEAH^+ \xleftrightarrow{K_{a,MEA}} H_3O^+ + MEA \tag{2.5}$$

The above reactions occur very rapidly and are often assumed instantaneous with respect to mass transfer. As a primary amine, MEA reacts directly with CO_2 to form a stable carbamate:

$$H_2O + MEA + CO_2 \xleftrightarrow{K_{MEACOO^-}} H_3O^+ + MEACOO^- \tag{2.6}$$

There are ten variables in the above phase and chemical equilibria. In order to calculate the concentration of each species and the equilibrium partial pressure of CO_2, another four equations must be found in addition to the six equilibrium equations, which correspond to the above equilibrium reactions. There are three material balance equations for CO_2, MEA, and the whole solution respectively:

$$X_{CO2,T} = X_{CO2} + X_{HCO_3^-} + X_{CO_3^{2-}} + X_{MEACOO^-} \tag{2.7}$$

$$X_{MEA,T} = X_{MEA} + X_{MEAH^+} + X_{MEACOO^-} \tag{2.8}$$

$$1 = X_{CO2} + X_{H_2O} + X_{MEA} + X_{MEAH^+} + X_{H_3O^+} + X_{HCO_3^-} + X_{CO_3^{2-}} + X_{OH^-} + X_{MEACOO^-} \quad (2.9)$$

where, $X_{CO2,T}$ is the mole fraction of CO_2 in the liquid phase, including CO_2 molecule, HCO_3^-, CO_3^{2-}, and $MEACOO^-$. The same definition for $X_{MEA,T}$.

Because the solution is neutral, there exists a charge balance equation for the liquid solution:

$$0 = 2X_{CO_3^{2-}} + X_{HCO_3^-} + X_{OH^-} + X_{MEACOO^-} - X_{H_3O^+} - X_{MEAH^+} \quad (2.10)$$

Assuming that the Henry's law constant and the equilibrium constants of the chemical reactions are available, the equilibrium partial pressure of CO_2 in the gas phase and the mole fractions of each species in the liquid phase can be calculated. However the literature values for the reaction equilibrium constants are for infinite dilution in water. In this work, the MEA solution is concentrated and the strong ionic effects will change the system behavior. This work uses literature values for the water dissociation constant, CO_2 dissociation constant, and HCO_3^- dissociation constant on one hand, and on the other hand, adjusts the pK_a value of MEA (reaction (5)) and the carbamate stability constant of MEA (reaction (6)), to account for the all of the nonideality of the system.

The Henry's law constant is approximated by the following equations (Licht and Weiland, 1989):

$$H_{CO_2,MEA}(atm/mole \cdot L) = R \cdot \exp[(\frac{-2625}{T(K)}) + 12.2] \quad (2.11)$$

$$R = \exp[(\frac{A}{T(K)} + B)X_I + hI] \quad (2.12)$$

where, X_I is the mole fraction of amine in unloaded solution, h is the Van Krevelen constant, I is the ionic strength which is typically equal to concentration of CO_2 in solution, and the model parameters A=5076 and B =-16.699. This work simplified the correlation by ignoring the hI term.

The equilibrium constants of other reactions are listed in table 2.2. Because these equilibrium constants were defined in terms of mole fraction and activity coefficients, they are dimensionless.

2.2.2 Model Parameter Fitting and Solubility Prediction

The resulting model has only two parameters. In order to regress the model parameters, a FORTRAN code was developed. An initial Fortran code was developed by Bishnoi for the CO_2/MDEA/PZ/H_2O system. This work adapted this code to the CO_2/MEA/PZ/H_2O system. The adapted code is given in Appendix A. First, the code uses the Jacobian method to linearize the nonlinear equations and then uses the Guassian elimination algorithm to solve the equilibrium concentration of each species at given loading. The "do loop" accomplishes the calculations for a range of loading in order to get a continuous spectrum of speciation. The model parameters have been adjusted to fit solubility data of CO_2 in 5 M MEA at 60°C

and 40°C (Jou et al., 1995), and in 2.5 M MEA and 1.0 M MEA at 60°C (Lee et al., 1976). Their values are listed in table 2.3.

Table 2.2. Temperature dependence of the equilibrium constants.
$LnK=C_1+C_2/T(K)+C_3LnT(K)$

reaction	C_1	C_2	C_3	Source
K_{H2O}	132.899	-13445.9	-22.4773	Maurer, 1980
$K_{a,CO2}$	231.465	-12092.1	-36.7816	Edwards et al., 1978
K_{a,HCO^-}	216.049	-12431.7	-35.4819	Edwards et al., 1978
$K_{a,PZ}$	-11.91	-4350.6	0	Bishnoi et al., 1998
K_{PZCOO^-}	-29.308	5614.64	0	Bishnoi et al., 1998
$K_{PZ(COO^-)2}$	-30.777	5614.64	0	Bishnoi et al., 1998

Table 2.3. Summary of fitted model parameters and literature values.

	pK_a (fitted)	pK_a (ref.)	K_{MEACOO^-} (fitted)	K_{MEACOO^-} (ref.)	Source of data
*5.0M MEA, 60°C	9.18E-12	1.45E-11	5.84E-6	2.87E-5	Jou et al. (1995)
2.5M MEA, 60°C	2.23E-11	1.45E-11	8.67E-6	2.87E-5	Lee et al. (1976)
1.0M MEA, 60°C	2.63E-11	1.45E-11	9.63E-6	2.87E-5	Lee et al. (1976)
*5.0M MEA, 40°C	1.26E-12	3.51E-12	5.03E-6	5.51E-5	Jou et al. (1976)

* parameters used in the rate model

2.2.2.1 VLE of CO_2 in MEA at 60°C

The VLE model was fitted to solubility data of CO_2 in 5 M MEA at 60°C (Jou et al., 1995), with CO_2 partial pressure varying from 0.004 kPa to 19893 kPa. The results are shown in table 2.4 and figure 2.2.

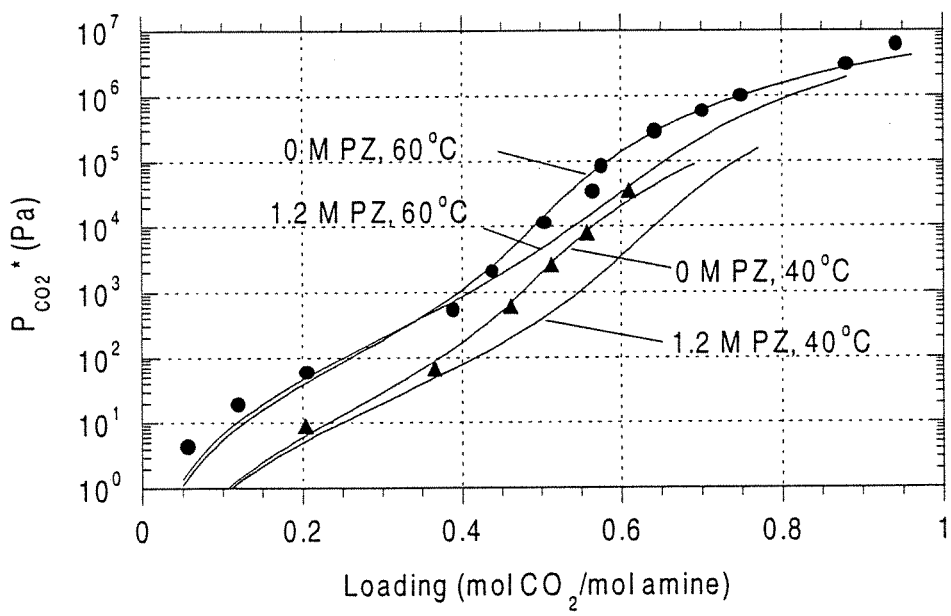

Figure 2.2. CO_2 solubility in 5 M amine (MEA+PZ) at 60°C and 40°C, predicted by parameters in table 2.3, data from Jou et al. (1995).

Table 2.4. CO_2 solubility in 5 M MEA at 60°C, data from Jou et al. (1995), values predicted by parameters in Table 2.3.

CO_2 Loading	P_{CO2}(Pa)		Error
(Moles CO_2/mol amine)	Experimental	Predicted	(Pred.-Exp.)/Exp.
0.0564	4.28	1.45	-0.66
0.119	1.93E+1	8.63	-0.55
0.206	5.79E+1	4.27E+1	-0.26
0.389	5.28E+2	8.82E+2	0.67
0.438	2.01E+3	2.55E+3	0.27
0.504	1.10E+4	1.48E+4	0.35
0.575	8.20E+4	8.72E+4	0.064
0.642	2.82E+5	2.81E+5	-0.0050
0.701	5.82E+5	5.90E+5	0.014
0.749	9.82E+5	9.49E+5	-0.034
0.88	2.98E+6	2.38E+6	-0.20
0.942	5.97E+6	3.25E+6	-0.45

The VLE model fits the literature data well at medium and high loading, but not very well at low loading. Large relative error may be expected in the experimental loading and/or pressure at low loading. Another possible reason may be related to the ionic strength of the solution. With the increase of loading, the ionic strength of the solution increases. If the VLE model with the fitted parameters can predict the vapor-liquid equilibrium well at high ionic strength situation, it may do a poor job at low ionic strength.

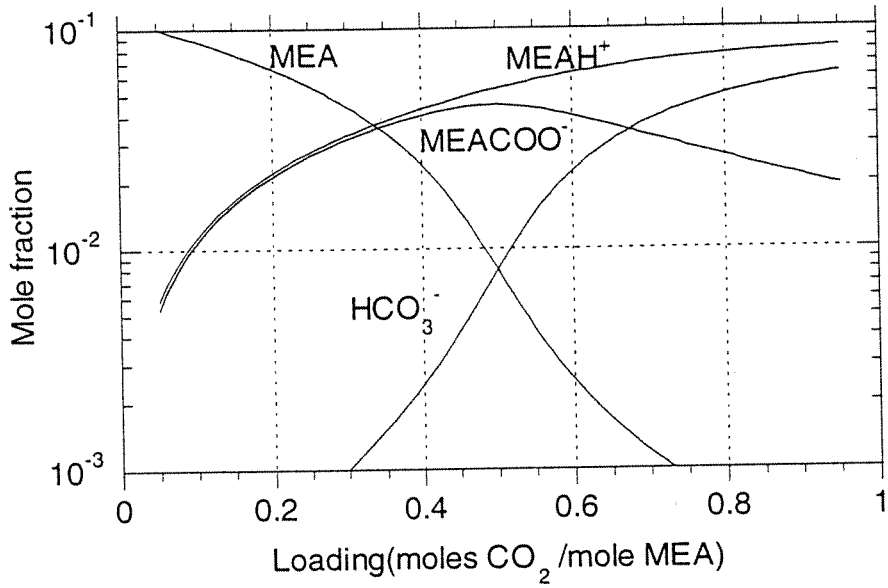

Figure 2.3. Predicted speciation of CO_2 in 5 M MEA at 60°C, data from Jou (1995).

Figure 2.3 gives the predicted speciation in 5 M MEA at 60°C. With an increase of CO_2 loading, the mole fraction of MEA decreases because of reactions with CO_2 and H_3O^+. With the increase of loading, more and more CO_2 enters into liquid phase and dissociates, so the concentration of H_3O^+ increases. With more protonation of MEA and a resulting decrease in free amine, the concentration of MEA carbamate also increases with loading. However, at loading greater than 0.5, the mole fraction of MEA carbamate decreases.

Parameters of the model were also adjusted to fit data from Lee et al. (1976) at 60°C in 2.5 M MEA and in 1.0 M MEA. Tables 2.5 and 2.6, and figure 2.4 show the results. Figures 2.5 and 2.6 give the prediction of the speciation for these two cases.

The model fits the 2.5 M MEA and 1.0 M MEA data very well. One of the reasons is the data used is not the real measured data but the smoothed data (The data were smoothed by the preparation of cross-plots with respect to temperature and normality, Lee et al., 1976).

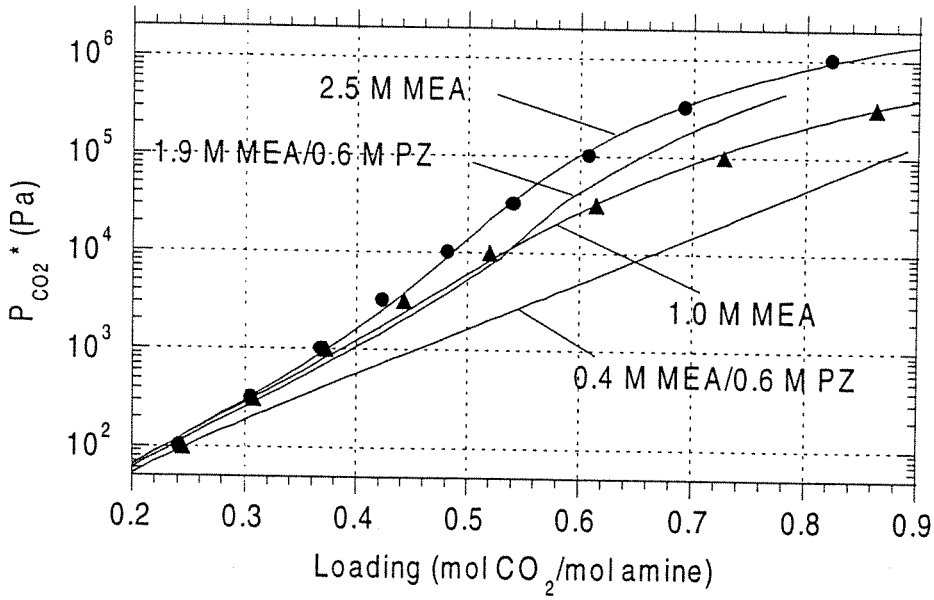

Figure 2.4. CO_2 solubility in 2.5 M amine (MEA+PZ) and 1.0 M amine (MEA+PZ) at 60°C, data from Lee (1976), predicted by parameters in table 2.3.

Table 2.5. CO_2 solubility in 2.5 M MEA at 60°C, smoothed data from Lee et al.(1976), values predicted by parameters in table 2.3.

CO_2 Loading	PCO_2(pa)		Error
(mol CO_2/ mol amine)	Experimental	Predicted	(Pred.-Exp.)/Exp.
0.241	1.00E+2	1.21E+2	0.214
0.305	3.16E+2	3.26E+2	0.030
0.368	1.00E+3	9.11E+2	-0.089
0.423	3.16E+3	2.54E+3	-0.195
0.482	1.00E+4	8.96E+3	-0.104
0.541	3.16E+4	3.55E+4	0.124
0.607	1.00E+5	1.21E+5	0.214
0.692	3.16E+5	3.57E+5	0.130
0.822	1.00E+6	9.02E+5	-0.008

Table 2.6 CO_2 solubility in 1.0 M MEA at 60°C, data from Jou et al. (1995), values predicted by parameters in Table 2.3.

CO_2 Loading	P_{CO2}(Pa)		Error
(Moles CO_2/mol amine)	Experimental	Predicted	(Pred.-Exp.)/Exp.
0.244	1.00E+2	1.27E+2	0.212
0.307	3.16E+2	3.16E+2	0.00
0.372	1.00E+3	8.13E+2	-0.230
0.442	3.16E+3	2.38E+3	-0.327
0.520	1.00E+4	8.24E+3	-0.213
0.614	3.16E+4	3.20E+4	0.013
0.727	1.00E+5	1.12E+5	0.109
0.862	3.16E+5	3.19E+5	0.010

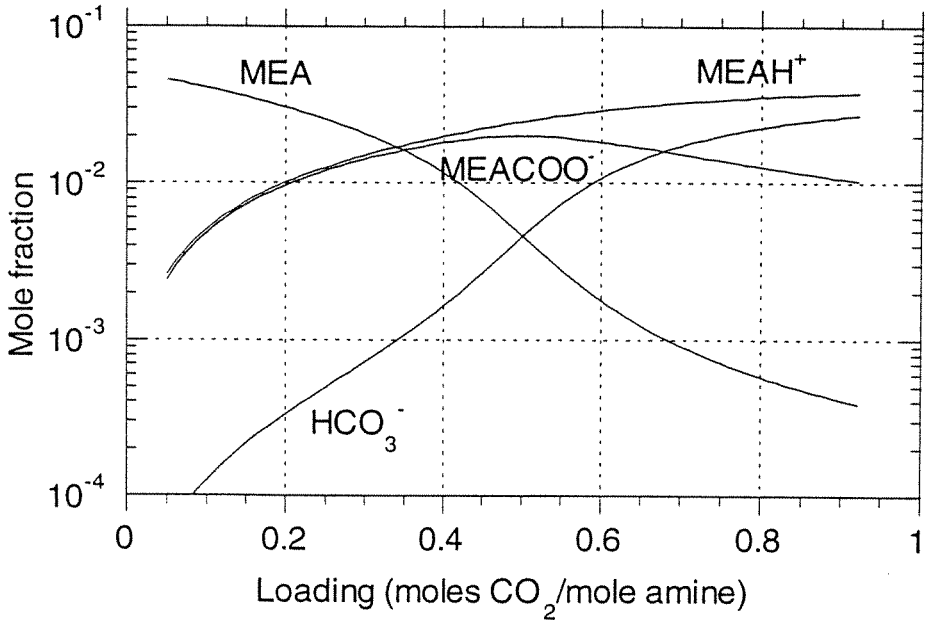

Figure 2.5. Predicted speciation of CO_2 in 2.5 M MEA at 60°C, data from Lee (1976).

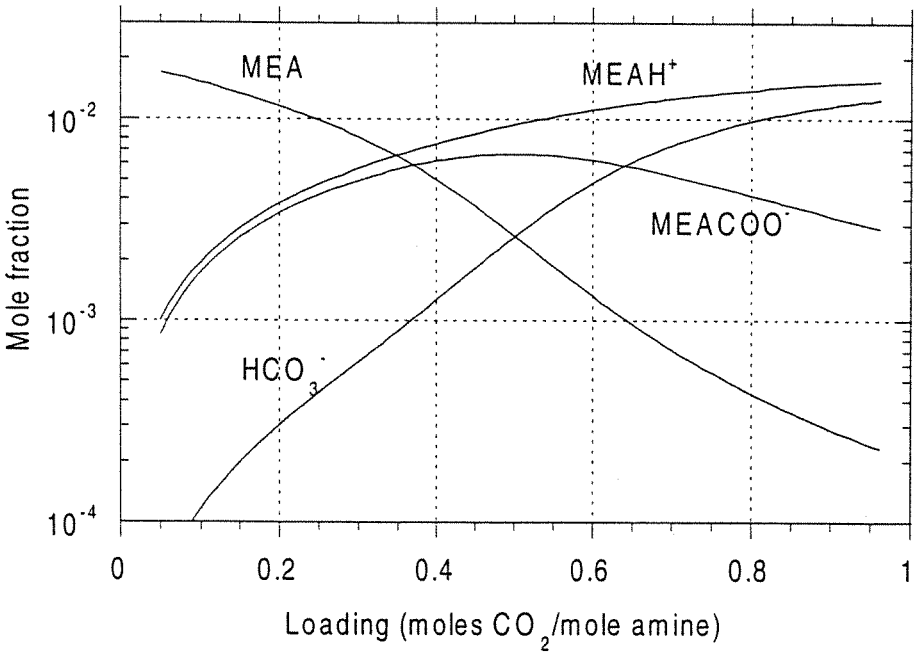

Figure 2.6. Predicted speciation of CO_2 in 1.0 M MEA at 60°C, data from Lee (1976).

In order to check the sensitivity of the VLE model to the data from different sources, CO_2 solubility in 2.5 M MEA and 1.0 M MEA was predicted by using model parameters fitted to the solubility data of CO_2 in 5 M MEA (Jou et al., 1995). The predictions of the speciation are shown in figures 2.7 and 2.8. Comparing figure 2.5 with figure 2.7 and figure 2.6 with figure 2.8, it can be seen that the difference of the MEA mole fraction between the two predictions is less than 10%.

We chose to use the unique model parameters which were fitted to the data from Jou et al. (1995) for all three amine concentrations. The speciation of MEA is tabulated in appendix B.

2.2.2.2 VLE Model Extension

The VLE model was extended to predict CO_2 solubility in a mixture of MEA and PZ. The introduction of PZ adds the following reactions:

Dissociation of protonated PZ (molecular structures are in figure 1.1)

$$H_2O + PZH^+ \xleftrightarrow{K_{a,PZ}} H_3O^+ + PZ \qquad (2.13)$$

PZ carbamate formation

$$H_2O + PZ + CO_2 \xleftrightarrow{K_{PZCOO^-}} H_3O^+ + PZCOO^- \qquad (2.14)$$

PZ dicarbamate formation

$$H_2O + PZCOO^- + CO_2 \xleftrightarrow{K_{PZ(COO^-)_2}} H_3O^+ + {}^-OOCPZCOO^- \qquad (2.15)$$

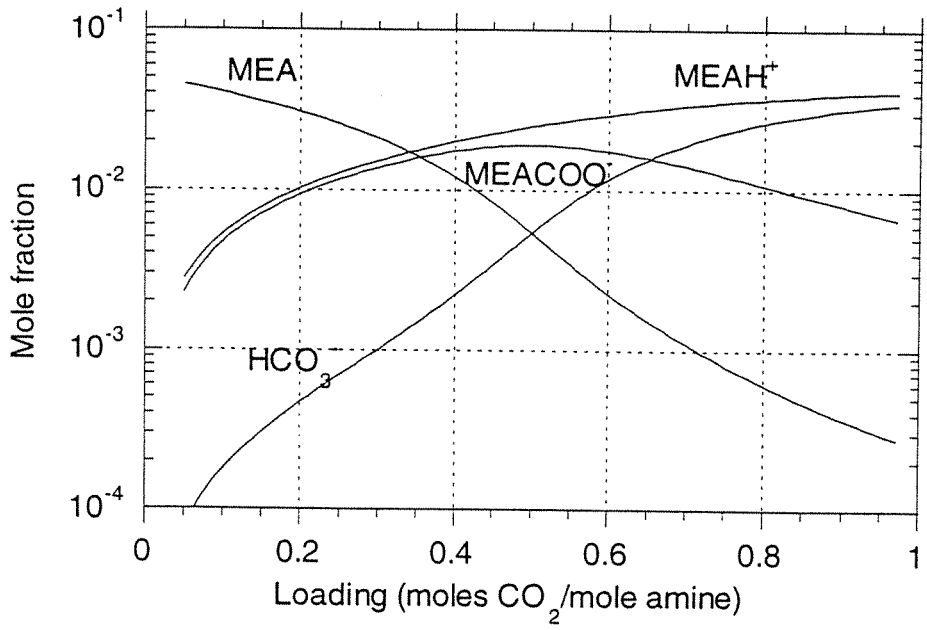

Figure 2.7. Predicted speciation of CO_2 in 2.5 M MEA at 60°C, values predicted by parameters fitted by data from Jou et al. (1995) at 5 M MEA.

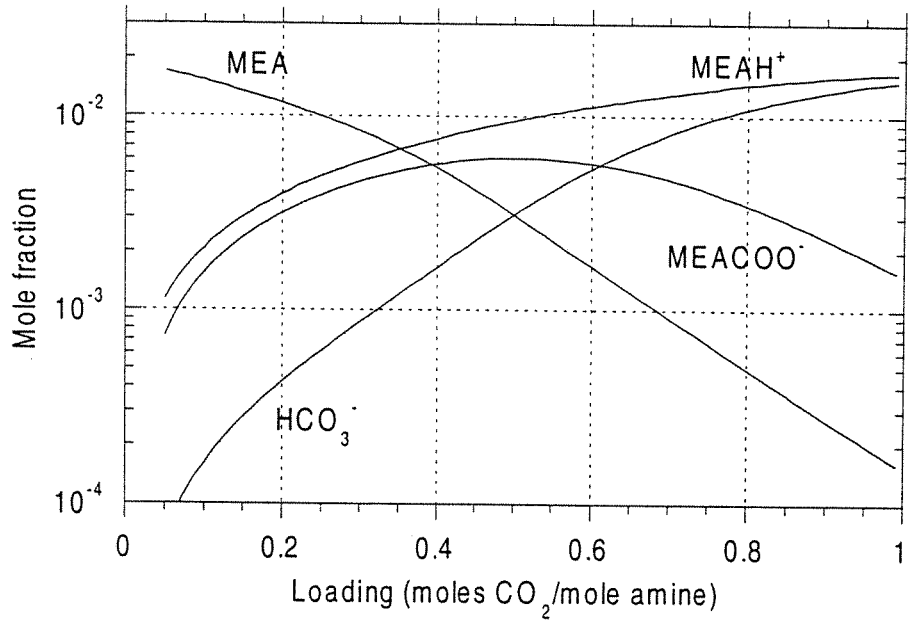

Figure 2.8. Predicted speciation of CO_2 in 1.0 M MEA at 60°C, values predicted by parameters fitted by data from Jou et al. (1995) at 5 M MEA.

The equilibrium constants of reaction (2.13), (2.14), and (2.15) were taken from Bishnoi and Rochelle (1998) and are listed in table 2.2. The $K_{a,MEA}$ and K_{MEACOO^-} values fitted to the data of Jou et al. (1995) are used. The other equilibrium constants keep the same values as before. The extended model was used to speciate CO_2 in 4.4 M MEA/0.6 M PZ, 1.9 M MEA/0.6 M PZ, 0.4 M MEA/0.6 MPZ, and 3.8 M MEA/ 1.2 M PZ. The predicted speciation is shown in figures 2.9 to 2.12. The predicted CO_2 solubilities in 3.8 M MEA/1.2 M PZ, 1.9 M MEA/0.6 M PZ, and 0.4 M MEA/0.6 M PZ are shown in figures 2.2 and 2.4 respectively. Comparing the predicted CO_2 solubility in blends with those in MEA with the same amine concentrations, the effect of PZ on CO_2 solubility can been seen. At low loading, PZ has no significant effect on CO_2 solubility. But at medium and high loading, PZ decreases the CO_2 equilibrium partial pressure by a factor of about 2.

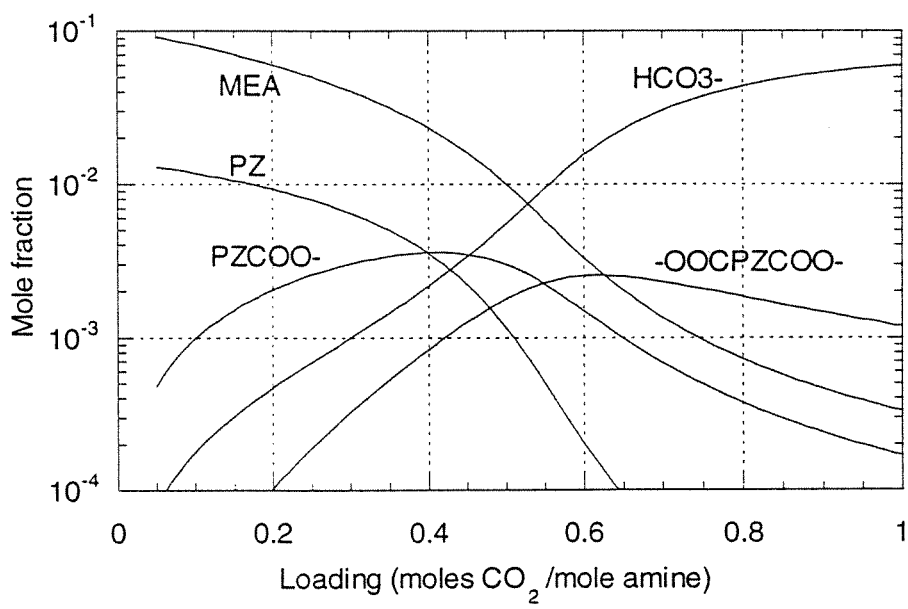

Figure 2.9. Predicted speciation of CO_2 in 4.4 M MEA/0.6 M PZ at 60°C.

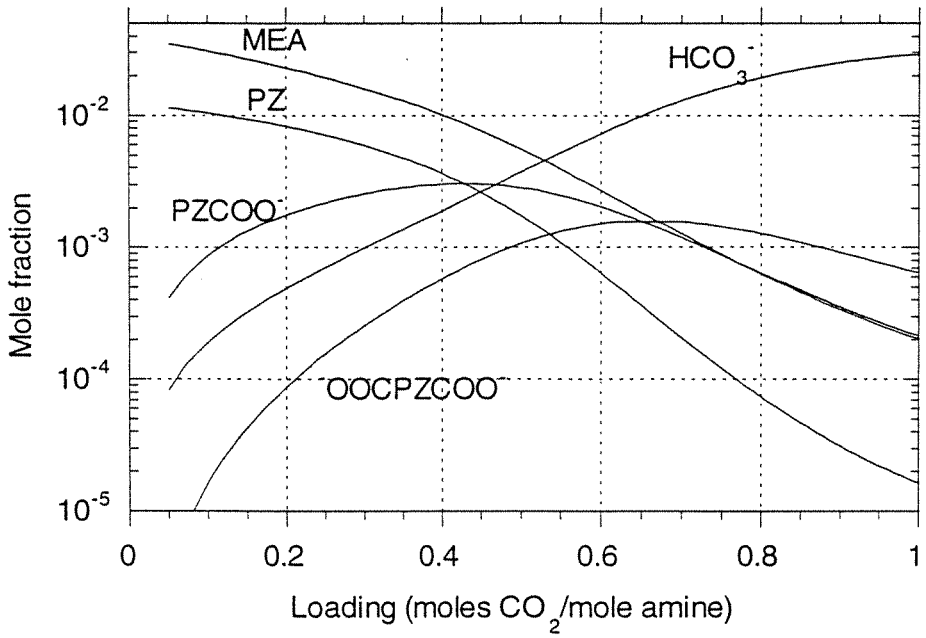

Figure 2.10. Predicted speciation of CO_2 in 1.9 M MEA/0.6 M PZ at 60°C.

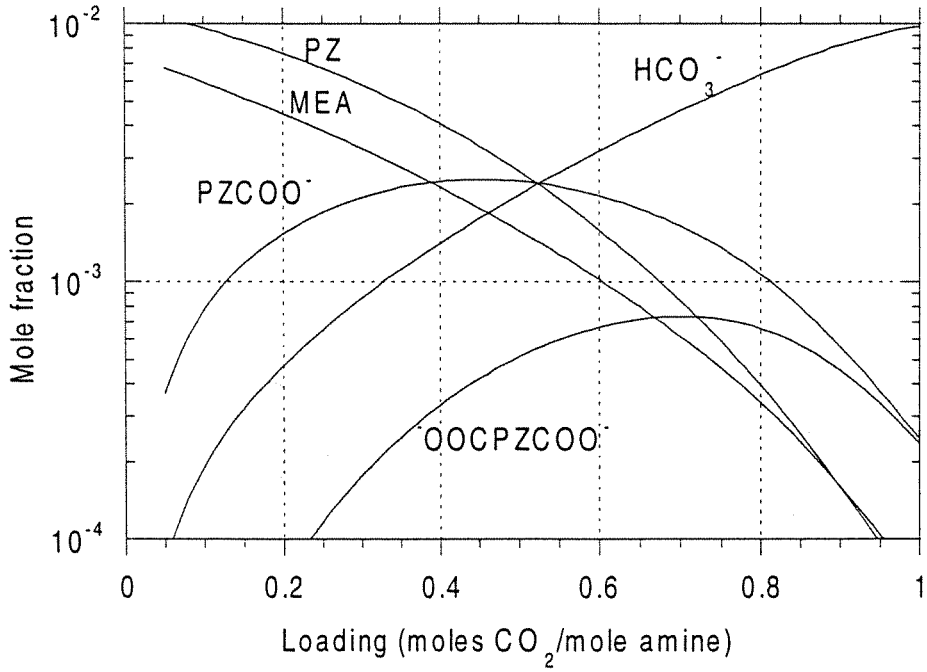

Figure 2.11. Predicted speciation of CO_2 in 0.4 M MEA/0.6 M PZ at 60°C.

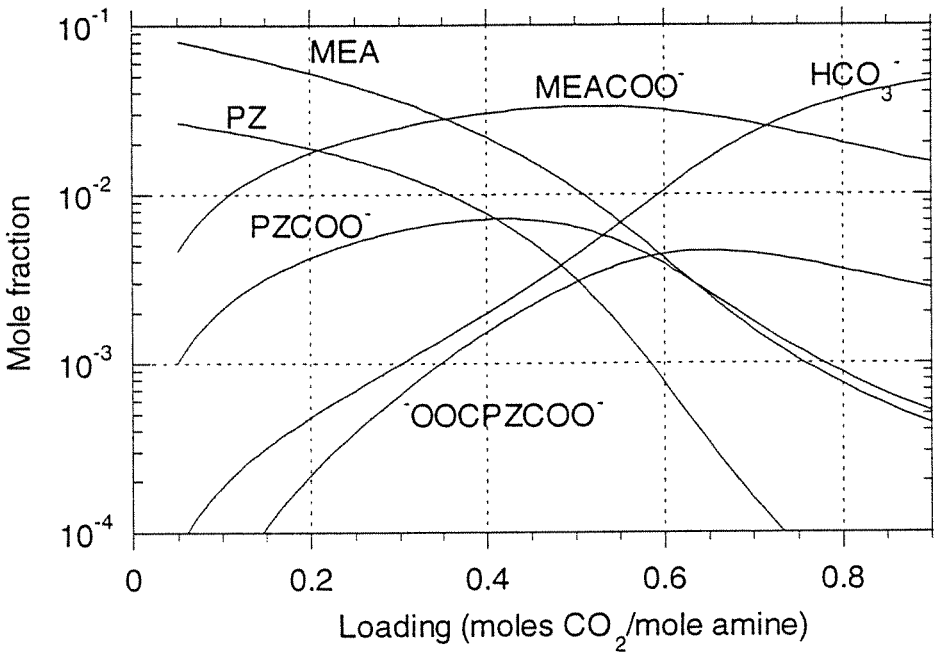

Figure 2.12. Predicted speciation of CO_2 in 3.8 M MEA/1.2 M PZ at 60°C.

The values of MEA, PZ, and $PZCOO^-$ are tabulated in appendix B.

From figure 2.9 to 2.12, we can see that the mole fractions of MEA, $MEACOO^-$, and HCO_3^- follow the same trends as in the MEA solution. Free PZ decreases with loading, $PZCOO^-$ approaches its maximum at a loading of 0.4, and then $^-OOCPZCOO^-$ reaches its maximum at a loading of about 0.6. The sum of the concentrations of PZ and $PZCOO^-$ is considerable at a loading up to 0.4~0.5, this will benefit the CO_2 absorption rate because of the high rate constants of PZ and $PZCOO^-$ with CO_2 compared to the rate constant of MEA with CO_2.

2.2.2.3 VLE of CO_2 in MEA/PZ at 40°C

In industrial processes for CO_2 absorption, the temperature is 40°C to 60°C. CO_2 solubility was also modeled at 40°C. The result of parameter fitting is shown

in figure 2.2 and table 2.7. The fitted parameters and the literature values are listed in table 2.3. From table 2.3, we can see the decrease of temperature will decrease the basicity of MEA and increase the MEA carbamate stability. So, lower temperature will increase the CO_2 solubility although the absorption rate will decrease.

Figure 2.13 shows the VLE model prediction of CO_2 solubility in 5 M MEA at 40°C. Then the VLE model was extended to CO_2 solubility in the mixture of MEA and PZ solution. Figure 2.14 shows the model prediction of CO_2 in 3.8 M MEA/1.2 M PZ at 40°C. All the species keep the same trends as at 60°C.

Table 2.7. CO_2 solubility in 5.0 M MEA at 40°C, data from Jou et al. (1995), values predicted by parameters in Table 2.3.

CO_2 Loading	P_{CO2}(Pa)		Error
(Moles CO_2/mol amine)	Experimental	Predicted	(Pred.-Exp.)/Exp.
0.203	8.96	6.46	-0.279
0.365	6.77E+1	8.83E+1	0.304
0.461	6.04E+2	6.90E+2	0.142
0.513	2.57E+3	2.79E+3	0.085
0.557	8.09E+3	8.52E+3	0.054
0.609	3.61E+4	2.51E+4	-0.304

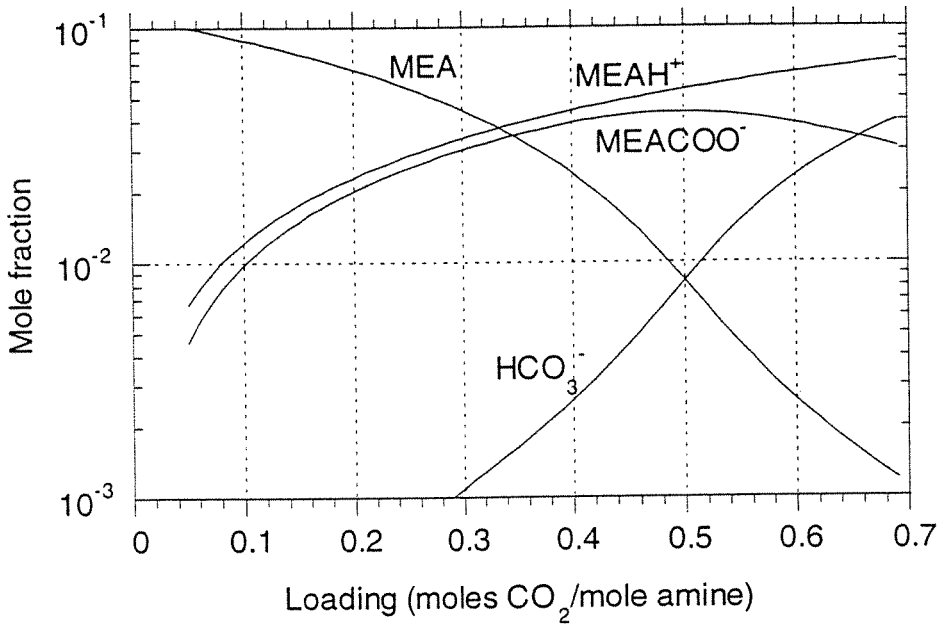

Figure 2.13. Predicted speciation of CO_2 in 5.0 M MEA at 40°C.

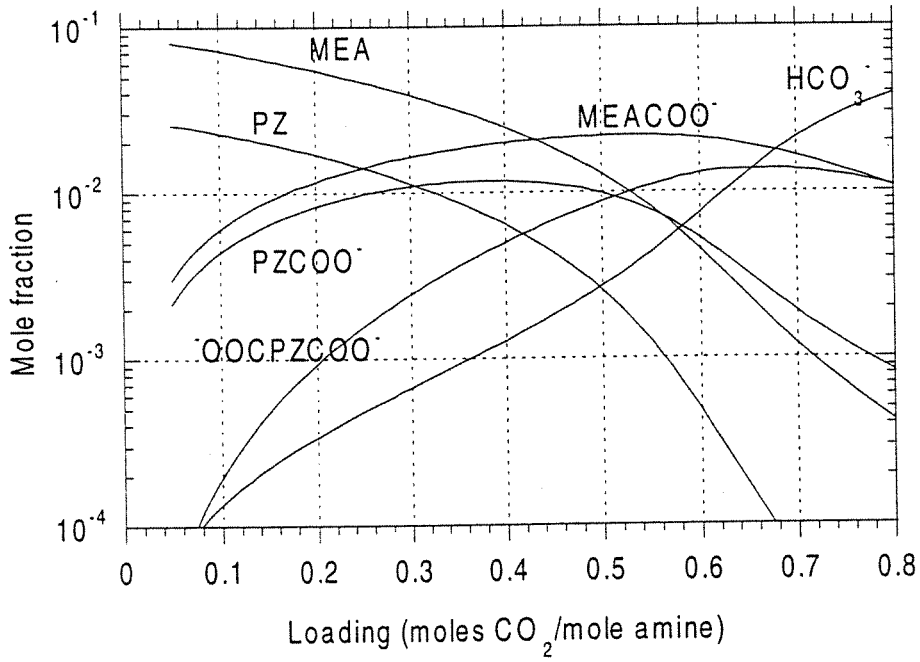

Figure 2.14. Predicted speciation of CO_2 in 3.8 M MEA/1.2 M PZ at 40°C.

Chapter Three

Simple Rate Model

3.1 Literature Review

The design of absorbers and strippers requires information about mass transfer and kinetics mechanisms, and the related rate expressions. Much work has been done with respect to modeling and calculating the rate of mass transfer in absorption of gases followed by complex chemical reactions.

In the cases of single reversible or irreversible first order reaction, instantaneous or not, analytical expressions based on film or penetration theory have been presented for the mass-transfer rate (Secor and Beutler, 1967). The major drawback of these models is that their validities are limited due to the assumptions involved. When no analytical or approximate solution is available, it is necessary to use numerical methods to estimate the effect of reaction rate on absorption or to estimate a rate constant from absorption data.

Cornelisse et al. (1980) have studied the simultaneous absorption of CO_2 and H_2S in a secondary amine. The CO_2 absorption rate was enhanced by the reaction with amine to form carbamate, and the H_2S reaction with amine was assumed to be instantaneous. They used a Newton-Raphson method to linearize the nonlinear reaction terms. This technique decoupled the simultaneous differential equations and allowed them to be solved as a set of linear equations. Little et al. (1991) have

used fundamentally the same method to describe the simultaneous absorption of H_2S and CO_2 in a solution of a primary or secondary amine and a tertiary amine.

In the model presented by Glasscock and Rochelle (1989) for the absorption of CO_2 into MDEA aqueous solutions, multiple reactions and the diffusion of ionic species were taken into account. The coupling between positive and negative ions was described by the Nernst-Planck equation. For gas absorption accompanied by second-order reversible reaction and the CO_2 absorption in MDEA, comparisons were made between the enhancement factor obtained for film theory, Higbie's penetration theory, Danckwert's surface renewal theory, and simplified eddy diffusivity theory. For the steady state theories, the equations are transformed into a large set of coupled, nonlinear algebraic equations. For the unsteady-state theories, a spatial discretization results in a set of coupled ordinary differential/algebraic equations which are integrated through time by DDASSL (petzold, 1983).

Rinker et al. (1995) presented a study in order to determine the significant reactions involved in the absorption of CO_2 into MDEA aqueous solutions, in particular the effect of including or neglecting the CO_2/OH^- reaction on the estimation of the forward rate coefficient of the MDEA-catalyzed hydrolysis reaction. The method of lines was used to transform each partial differential equation into a system of ordinary differential equations which were then solved by DDASSL (Petzold, 1983). The same numerical method was used by Hagewiesche et al. (1995) to estimate the rate coefficient of the reaction between CO_2 and MEA

at 313 K from experimentally measured absorption rates of CO_2 into blends of MDEA and MEA.

Cadours and Bouallou (1998) developed a general model for the diffusion/reaction processes. They considered a rigorous approach of taking into account the electrostatic potential gradient terms with unequal diffusion coefficients for the ionic species even if much computational effort is required. This model allows them to consider reactions with finite rate and instantaneous reactions with respect to mass transfer. They assume reversibility, generalized reaction rate expressions, and generalized stoichiometry. The applicability of their model is not limited by the type of reactions modeled. The main advantage lives in the simple of the numerical treatment because no numerical method is needed to transform each partial differential equation into a system of ordinary differential equations. Optimization using a Levenberg-Marquardt algorithm provides the rate coefficients for different kinetic mechanisms, from experimental data. In their work, the model had been applied to investigate the discrepancies between different works reported in the literature for the CO_2 absorption into MDEA aqueous solutions, especially at high temperature.

3.2 Simple Rate Model Structure

This work used a simple approximation for the enhancement factor, E, for CO_2 absorption in MEA/PZ aqueous solution, which combines the pseudo-first order enhancement factor and the instantaneous enhancement factor in a series resistance.

3.2.1 Pseudo-First Order Enhancement Factor

In the CO_2/MEA/PZ/H_2O system, three finite-rate, reversible reactions are important:

$$MEA + CO_2 + H_2O \leftrightarrow MEACOO^- + H_3^+O \tag{3.1}$$

$$PZ + CO_2 + H_2O \leftrightarrow PZCOO^- + H_3^+O \tag{3.2}$$

$$PZCOO^- + CO_2 + H_2O \leftrightarrow {}^-OOCPZCOO^- + H_3^+O \tag{3.3}$$

If the MEA, PZ and PZCOO- concentration gradients in the liquid film are ignored and represented by their bulk values respectively, the analytical expression for the pseudo-first order enhancement factor can be derived by shell balance:

$$E_l = \frac{\sqrt{(k_{MEA}[MEA] + k_{PZ}[PZ] + k_{PZCOO^-}[PZCOO^-])D_{CO_2}}}{k_l^o} \tag{3.4}$$

Where, E_l is the pseudo first order enhancement factor. [MEA], [PZ], and [PZCOO$^-$] are the concentrations of these species at the interface. Under pseudo first order assumption, they are equal to their bulk concentrations. k_{MEA}, k_{PZ}, and k_{PZCOO^-} are the second order rate constants of MEA, PZ, and PZCOO$^-$ with CO_2 respectively. k_{MEA} and k_{PZ} were calculated by equations 3.5(Hikita et al, 1977) and 3.6 (Bishnoi and Rochelle, 1999). k_{PZCOO^-} was assumed to be one fourth of k_{PZ} unless specified otherwise in order fit the measured data, which is shown in chapter four.

$$Log_{10}(0.001 * k_{MEA}(m^3 / mole \cdot s)) = 10.99 - 2152/T(K) \tag{3.5}$$

$$k_{PZ}(m^3/mol \cdot s) = 0.001 * k_{25^oC} \exp[\frac{-\Delta H_a}{R}(\frac{1}{T(K)} - \frac{1}{298})] \quad (3.6)$$

where, k_{25^oC}=5.37E4 m^3/kmol, ΔH_a=3.36E4kJ/kmol, and R=8.314. k_l^o is the liquid film mass transfer coefficient. k_l^o was calculated for each amine concentration and temperature and varied from 0.8E-4 to 1.6E-4m/s.

D_{CO2} is the diffusion coefficient of CO_2 in liquid phase and was calculated by N_2O analogy, namely,

$$(D_{CO2,amine})=C_1(D_{N2O,amine}) \quad (3.7)$$

with

$$C_1=D_{CO2,H2O}/D_{N2O,H2O} \quad (3.8)$$

where, $D_{i,amine}$ is the diffusion coefficient of i in amine solution, and $D_{i,H2O}$ is the diffusion coefficient of i in water. $D_{CO2,H2O}$ and $D_{N2O,H2O}$ were calculated by the following expressions (Versteeg and Van Swaaij, 1988):

$$D_{CO2,H2O} = 2.35 \times 10^{-6} \exp(-2119/T(K)) \quad (3.9)$$

$$D_{N2O,H2O} = 5.07 \times 10^{-6} \exp(-2371/T(K)) \quad (3.10)$$

D is in m^2/s. The diffusion coefficient of N_2O in amine solution was then estimated according to the modified Stokes-Einstein relation:

$$(D_{N2O}\,\mu^{0.8})amine = (D_{N2O}\,\mu^{0.8})_{H2O} \quad (3.11)$$

The assumptions are demonstrated in figure 3.1 and the real physical process is shown in figure 3.2.

3.2.2 Instantaneous Enhancement Factor

The pseudo-first enhancement factor accounts for the enhancement of CO_2 absorption by chemical reactions. It does not include the effect of the diffusion of

reactants and products to the mass transfer process. But at high loading, the diffusion of the reactants and products plays a very important role in the mass transfer process. So, the instantaneous enhancement factor was introduced:

$$E_{inst} k^{o}_{l,CO2} \frac{(P_{CO2,i} - P^{*}_{CO2,b})}{H_{CO_2}} = C_{amine}(\text{loading}^{*}_{i} - \text{loading}_{b}) k^{o}_{l,prod} \tag{3.12}$$

where, C_{amine} is the total amine concentration in M, H_{CO2} is the Henry's law constant of CO_2 in amine solution, which is calculated by equation 2.11 and 2.12. $k_{l,CO2}^{o}$ and $k_{l,prod}^{o}$ are the liquid phase mass transfer coefficients of CO_2 and reaction products, P_{CO2}* is the equilibrium partial pressure of CO_2 at certain loading, and i means interface. Generally,

$$\frac{k^{o}_{l,CO_2}}{k^{o}_{l,prod}} = \sqrt{\frac{D_{CO_2}}{D_{prod}}} \tag{3.13}$$

where, D_{CO2} and D_{prod} are the diffusion coefficients of CO_2 and reaction products respectively. So,

$$E_{inst} = C_{amine} H_{CO_2} \frac{\Delta(\text{loading})}{\Delta(P^{*}_{CO_2})} \sqrt{\frac{D_{CO_2}}{D_{product}}} \tag{3.14}$$

If the changes of loading and P_{CO2}* are small enough, equation 3.14 becomes:

$$E_{inst} = C_{amine} H_{CO_2} \frac{\partial(\text{loading})}{\partial(P^{*}_{CO_2})} \sqrt{\frac{D_{CO_2}}{D_{product}}} \tag{3.15}$$

In this model, equation 3.14 was approximated by equation 3.15 based on the VLE model prediction of this work. This means E_{inst} in this work is a global instantaneous enhancement factor which assumes that the reactions of MEA, PZ, and $PZCOO^-$ with CO_2 are all instantaneous. The ratio of D_{CO2} to $D_{product}$ was approximated by a value of 2.0.

3.2.3 Total Enhancement Factor

If the reaction occurs near the interface, then the reaction enhancement, E_l, is in series with instantaneous enhancement E_{inst}.

$$\frac{1}{E} = \frac{1}{E_l} + \frac{1}{E_{inst}} \qquad (3.16)$$

Equation 3.12 can also be interpreted another way:

$$flux = E_l([CO_2]_i - [CO_2]_i^*)k_l^o \qquad (3.17)$$

$$flux = E_{inst}([CO_2]_i^* - [CO_2]_b^*)k_l^o \qquad (3.18)$$

$$flux = E([CO_2]_i - [CO_2]_b^*)k_l^o \qquad (3.19)$$

by combining equations 3.17, 3.18, and 3.19, equation 3.16 is derived.

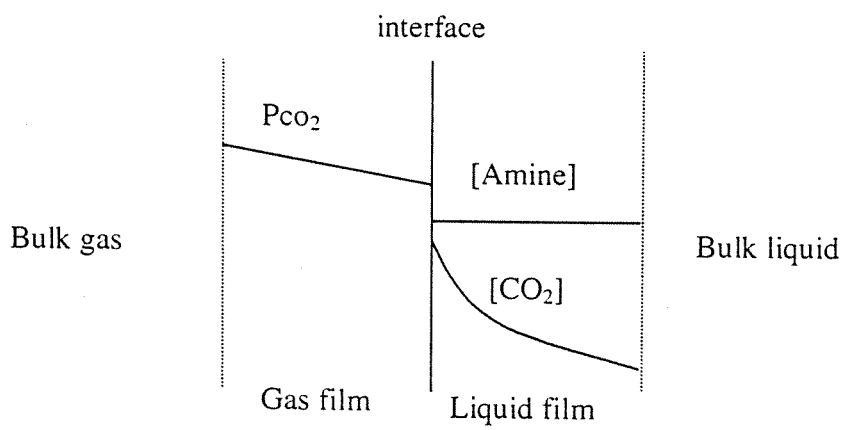

Figure 3.1. Pseudo-first order assumption of CO_2 absorption in amine solution.

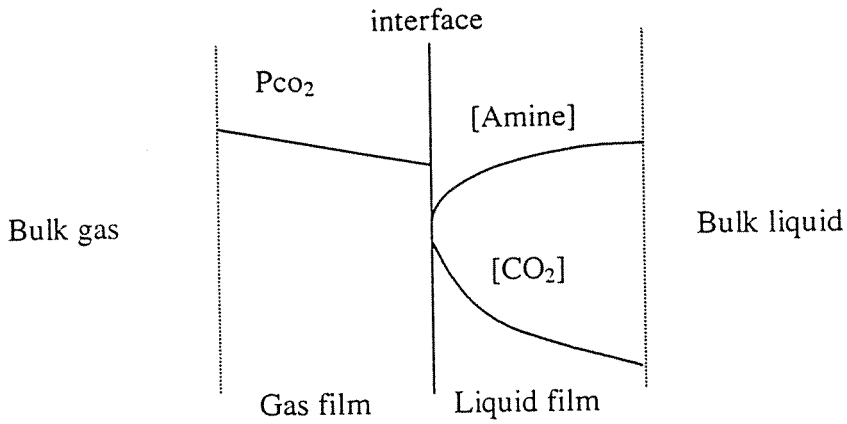

Figure 3.2. Physical model of CO_2 absorption in amine solution.

3.3 Rate Model Prediction

Figure 3.3 shows the calculated values of E_1, E_{inst}, and E for CO_2 absorption in 0.4 M MEA/0.6 M PZ at 60°C. It is clear that E_1 dominates at low loading and E_{inst} plays an important role at high loading.

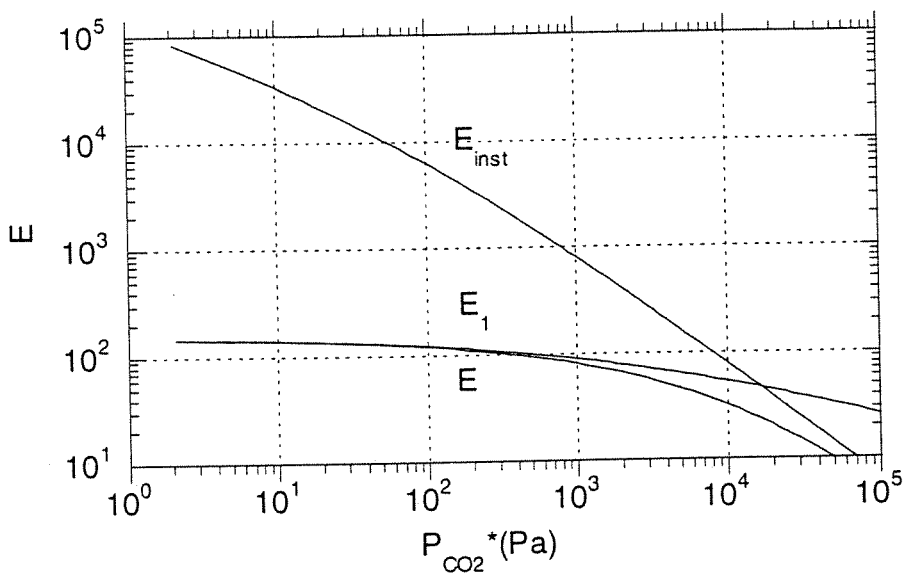

Figure 3.3. Predicted enhancement of CO_2 absorption in 0.4 M MEA/0.6 M PZ at 60°C, and k_l^o =1.6E-4.

If the PZ concentration is set to be zero, the rate model can be applied to $CO_2/MEA/H_2O$. Figures 3.4 to 3.7 are the rate model predictions for CO_2 absorption in different MEA and PZ concentrations at 60°C and 40°C. In these pictures, the solid diamonds are the specific values of enhancement factors at loading of 0.3 for MEA solution and MEA/PZ solution and the solid circles are those at the loading of 0.5 for each case. All the figures show that the addition of PZ to MEA solution can increase the CO_2 absorption rate by a factor of 1.5-2.5 compared to the MEA solution with the same total amine concentration. The larger the fraction of PZ, the significant the improvement. Furthermore, the enhancement of CO_2 absorption by PZ is more obvious at high loading (0.5) that at medium CO_2 loading (0.3).

In figures 3.4 to 3.7, the instantaneous enhancement factor is shown by a dashed line for each case. At high loading, the instantaneous enhancement becomes more important and even dominant for these cases.

In figure 3.5, two lines are shown for the enhancement of 1.9 M MEA/0.6 M PZ. The solid line is calculated with the value of k_{PZCOO^-} equal to $0.25k_{PZ}$. The dashed line is calculated with the value of k_{PCZOO^-} equal to $0.1k_{PZ}$. There is almost no significant difference between these two lines at low loading and the little difference shown at high loading is because the $PZCOO^-$ becomes an important species at high loading.

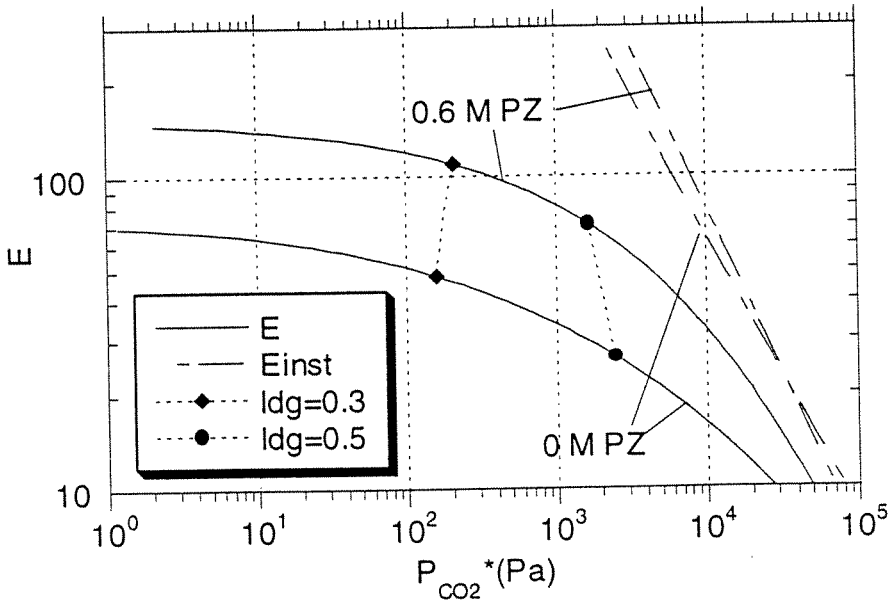

Figure 3.4. Enhancement of CO_2 absorption in 1.0 M MEA/PZ at 60°C.

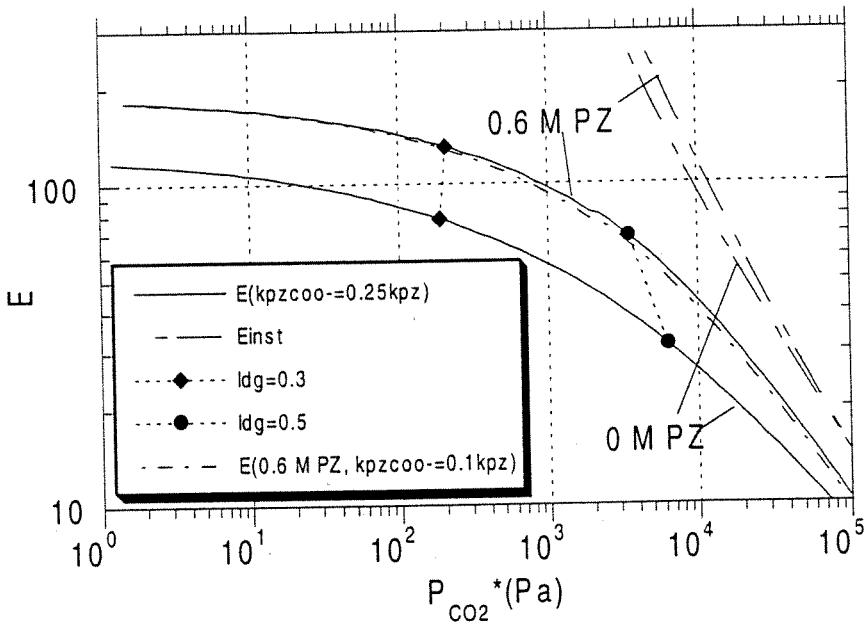

Figure 3.5. Enhancement of CO_2 absorption in 2.5 M MEA/PZ at 60°C.

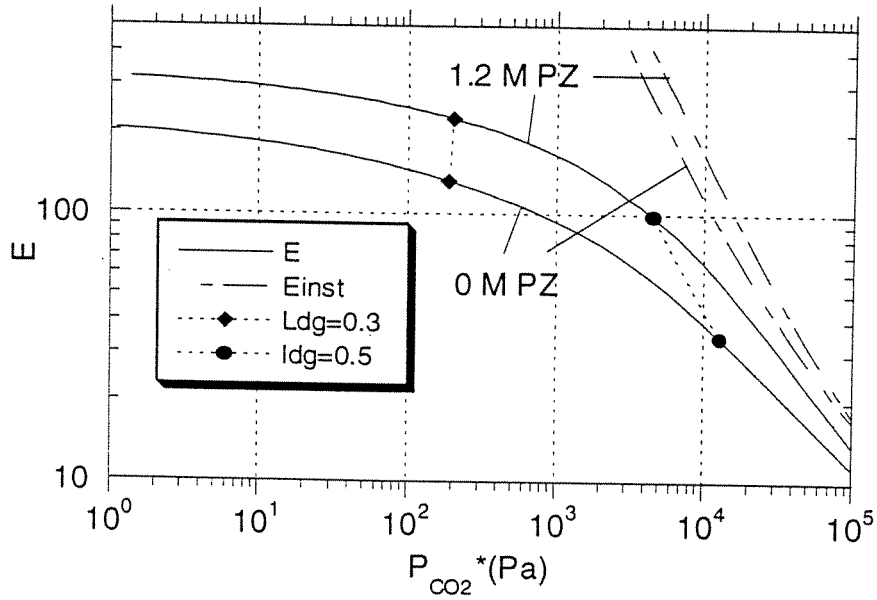

Figure 3.6. Enhancement of CO_2 absorption in 5.0 M MEA/PZ at 60°C.

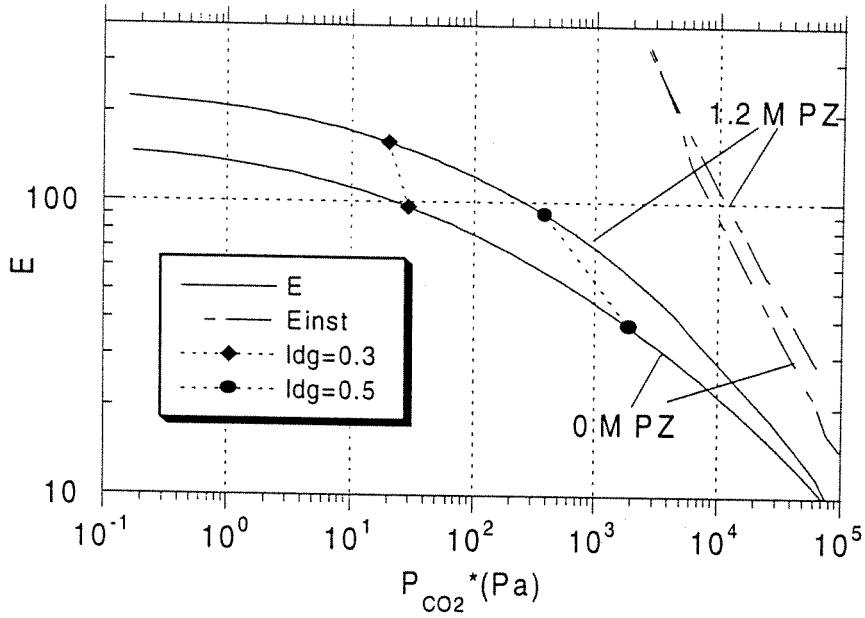

Figure 3.7. Enhancement of CO_2 absorption in 5.0 M MEA/PZ at 40°C.

Figure 3.8 compares the model predictions of CO_2 absorption rates in 3.8 M MEA/1.2 M PZ and 5.0 M MEA aqueous solutions at 40°C and 60°C respectively. The model predictions indicate that replacing 24% of the MEA by PZ can increase the absorption rate by a factor of 2.

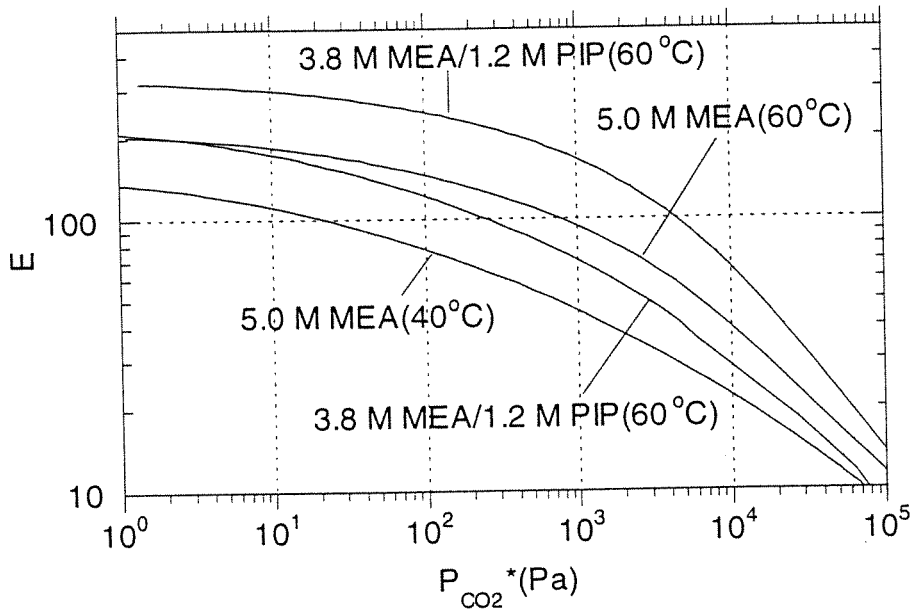

Figure 3.8. Enhancement of CO_2 absorption in 5.0 M MEA/PZ at 60°C and 40°C.

Speciation is very important for CO_2 absorption rate in loaded amine solution. Figure 3.9 shows the contributions of three important species, MEA, PZ and $PZCOO^-$, to the total absorption rate of CO_2 into 3.8 M MEA/1.2 M PZ at 60°C. When the loading is lower than 0.5 mol CO_2/mol amine, PZ contributes more than 50% to the total absorption rate. When the loading is higher than 65%, $PZCOO^-$ contributes more than 50% to the total absorption rate. The contribution of MEA to

the total absorption rate is never more than 30% in this case. Appendix C discusses the contributions of MEA, PZ and $PZCOO^-$ to the total absorption rate for all the MEA/PZ blends studied in this work.

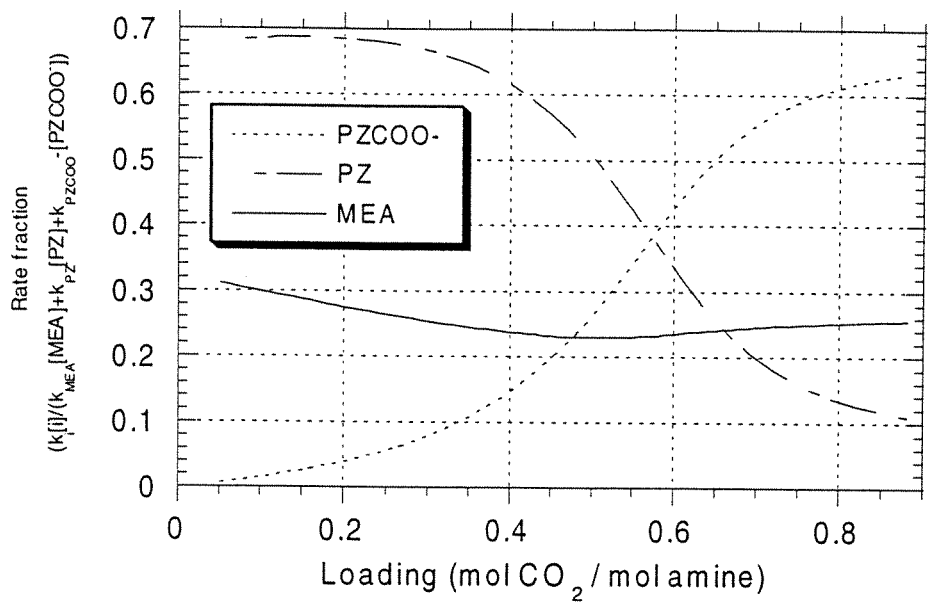

Figure 3.9. CO_2 absorption rate contribution of MEA, PZ and $PZCOO^-$ in 3.8 M MEA/1.2 M PZ at 60°C.

Chapter Four

Solubility and Absorption Rate of CO_2 in MEA/PZ/H_2O

Solubility and absorption rate of CO_2 in Monoethanolamine/Piperazine solution have been measured at 40°C and 60°C with a wetted wall column. The total amine concentration varied from 1.0 M to 5.0 M with 0 M, 0.6 M or 1.2 M PZ. The loading varied from about 0 to 0.7 mol CO_2 / mol amine.

4.1 Experimental Apparatus and Methods

Figure 4.1 shows the wetted wall column used in this work. The wetted wall column was constructed from a stainless steel tube with a well defined surface area (38.52 cm^2) and a characteristic liquid film mass transfer coefficient similar to that of a packed tower. The stainless steel tube is 9.1 cm long and had an outside diameter of 1.26 cm. Liquid passed up the inside of the stainless steel tube and overflowed to form a liquid film over the outer surface of the tube. Gas entered wetted wall column from the bottom and countercurrently contacted the liquid film.

Figure 4.2 shows the overall flow diagram of the apparatus used in this study to obtain rate of absorption and solubility data. The apparatus was originally built by Mshewa (1995) and modifications were made by Pacheco (Pacheco, 1998; Pacheco et al., 1999).

Flow from two gas cylinders was regulated by Brooks model 5850E mass flow

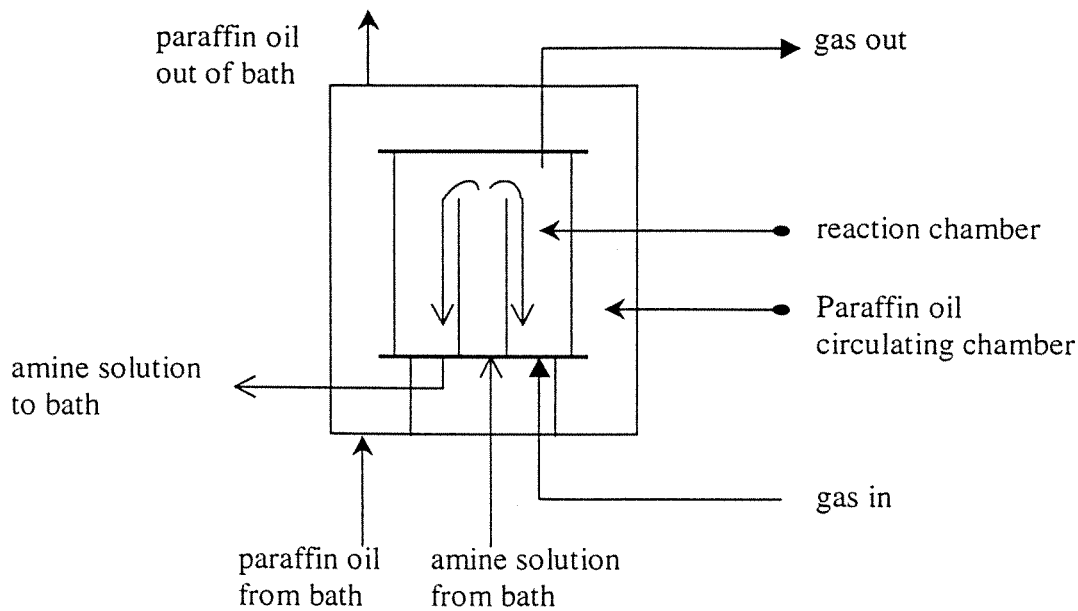

Figure 4.1. Detailed column diagram.

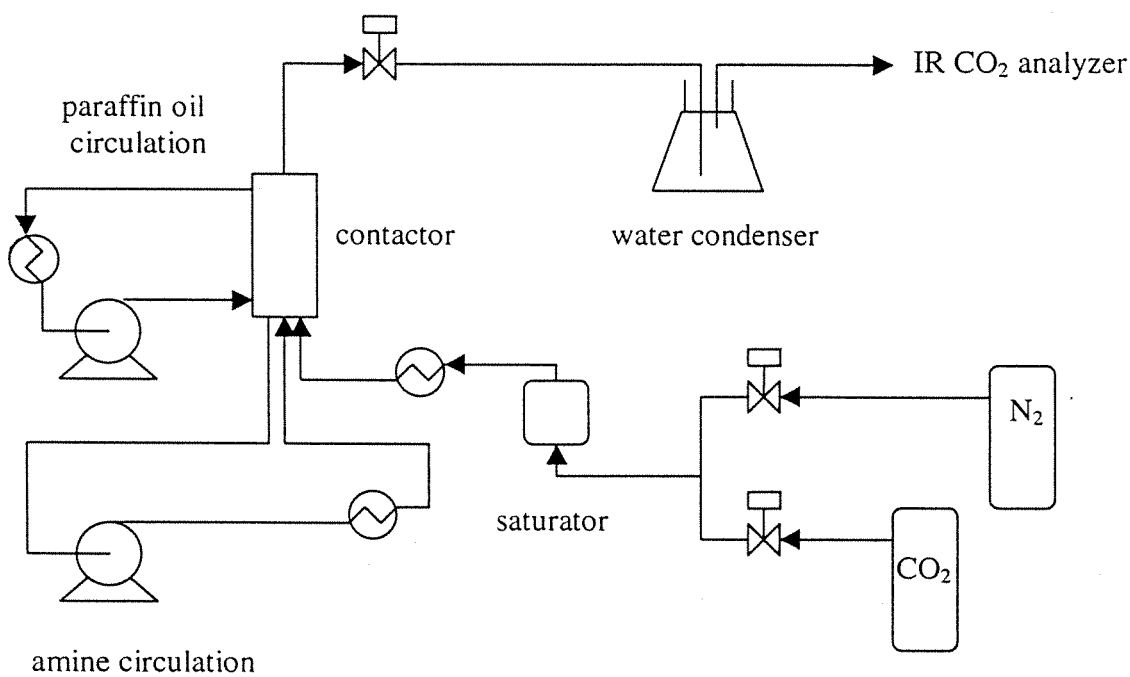

Figure 4.2. Overall experimental flowsheet

controllers. The accuracy was reported to be 1% of full scale. In this work, although CO_2 was used frequently, the mass flow controllers were calibrated by N_2 in the lab. The results of calibrations are listed in appendix D. A 20 SLPM flow controller was usually set at 25% (or a 15 SLPM flow controller was set at 34%) for nitrogen flow. A 1 SLPM flow controller was usually used for a blend mixture of 0.5 vol % CO_2 in nitrogen for low loading measurement. For experiments at medium or high loading and CO_2 partial pressures, pure CO_2 was used instead of the mixture gas, which was regulated by a 100 SCCM flow controller or a 1 SLPM flow controller respectively. The gas was sent to a water saturator that was kept at the same temperature as the wetted wall column. The saturator consisted of a 400 mL calorimeter bomb filled with water. The gas was sparged using an open stainless steel tube at the bottom of the bomb. After the water saturator, the gas was sent to the wetted wall column where it was contacted with the amine solution. Total pressure used in this work was around 4 to 5 atm. In the wetted wall, a portion of the carbon dioxide was transferred from the gas phase to the liquid phase.

The gas was sent from the column through a needle valve where the pressure was reduced to atmospheric. From the downstream side of the needle valve, the gas was sent to a condenser that consisted of an Erlenmeyer flask submerged in ice water. The gas was then passed on to a series of Horiba PIR 2000 carbon dioxide analyzers where the outlet carbon dioxide concentration was measured by infrared

spectroscopy. The PIR-2000 is a precise gas analyzer based on nondispersive infrared absorption for gas stream. The reading of the analyzer was usually monitored by means of a strip chart recorder, which had an accuracy of ±1% of full scale. The reading of the analyzer was also monitored by means of a digital voltmeter for more accuracy. Both readings gave consistent results. Two analyzers were used, each having a different concentration range (0-25% and 0-0.25%, volume basis). This series of analyzers allows the accurate measurement of carbon dioxide down to 100-200 ppm. The CO_2 flux into the liquid phase from the gas phase was determined by the difference of CO_2 concentrations in the gas stream into and out of the wetted wall column. Calibrations of these analyzers were performed by bypassing the reactor, varying the concentration of CO_2 in the gas to the analyzer and observing the analyzer reading at each CO_2 concentration. The calibration curve fits a straight line when the analyzer with a range of 0-25% was used and it was fitted a quadratic curve with the analyzer of range 0-0.25%. In other words, the high range analyzer had a linear response while the low range analyzer had a nonlinear response.

The amine solution was kept in a reservoir and passed through a coil submerged in a paraffin bath to heat it to the reactor temperature. Anhydrous piperazine flakes (CAS No. 110-85-0, 99.9% purity) were obtained from Aldrich Chemical and mixed with de-ionized water to make up the amine solution. A reservoir with a 2400 cm^3 holdup was used for the paraffin oil bath in this work. The flow of amine

solution was provided by a Cole-Parmer micropump and was measured by a liquid rotameter. The liquid flow rate used in this work was around 3 cm^3/s. The flow rate was assumed to be a function of solution viscosity and rotameter reading. The rotameter was calibrated by flowing solutions of MDEA through the rotameter and making tables of flow rate vs. rotameter reading. The results have been correlated using the following relationship (Bishnoi, 2000).

$$Q_L=Ax^2+Bx+C \tag{4.1}$$

where,

$$A=-1.5361E(-4)\mu^2+1.9243E(-2) \tag{4.2}$$

$$B=6.6596E(-3)\mu^2-9.3319E(-2)\mu+0.35810 \tag{4.3}$$

$$C=2.0916E(-3)\mu^2-2.55337E(-2)\mu+5.9803E(-2) \tag{4.4}$$

The paraffin oil in the bath was also circulated to the wetted wall column, keeping the entire apparatus at a uniform temperature. The temperature of the outlet and inlet liquid were measured by two heat sensors. The temperature in the wetted wall column was assumed equal to the average of these two.

Absorption or desorption of CO_2 was determined from the gas phase material balance using the measured inlet and outlet gas concentrations. Periodically, liquid samples were withdrawn from a sample port close to the reactor outlet and analyzed for total carbon dioxide loading using the same method as previous investigators (Bishnoi, 2000; Pacheco et al., 1999; Pacheco, 1998; Kaganoi, 1997; Mshewa, 1995). This was done by introducing the sample into a solution of

phosphoric acid, which reverses the amine/carbon dioxide reaction and liberates all the carbon dioxide as gas. This gas was swept with nitrogen carrier gas to an IR analyzer where the total carbon dioxide was determined. For data points at low loading, 150μL of solution from the reactor was combined with 3 mL of DI H_2O to form a sample vial. For higher loading samples, 100 μL of solution from the reactor was combined with 3 mL of DL H_2O. Usually samples of 20 to 150 μL from the sample vial were input into the analyzer. Calibration of the analyzer was achieved by introducing known amounts (between 10 μL and 500 μL) of 7mM Na_2CO_3 into the analyzer.

Small amount amine solution was added or withdrawn from the sample plot in order to keep the liquid level in the wetted wall column constant. If the liquid level is too high, there was no stable liquid film formed over the tube. If two low, some gas would go into liquid circulation.

Solubility was measured by bracketing equilibrium with both absorption and desorption measurements, which will be mentioned in the following sections. Absorption rate data was obtained in the same experiment as solubility measurement by adjusting the CO_2 partial pressure at least as high as 2 to 3 times of the equilibrium partial pressure at that loading. The measurement was done as fast as possible in order to keeping the solution loading approximately constant.

4.2 Data Analysis

In order to get solubility and absorption rate data of CO_2 in MEA/PZ solution, calculation must be done for physical properties and mass transfer coefficients. The following sections discuss the details of these calculations

4.2.1 Physical Properties

Density ρ, viscosity μ, Henry's law constant H, and diffusion coefficient D, are the most important properties in data analysis.

This work used Weiland's correlation (1998) to calculate ρ:

$$\rho = \frac{x_{Am}M_{Am} + x_{H_2O}M_{H_2O} + x_{CO_2}M_{CO_2}}{V} \tag{4.5}$$

Where, ρ is the solution density (g/mL), V is the volume of the solution (mL/mol), and x_i and M_i are the mole fractions and molecular weights of amine, water, and carbon dioxide, respectively. The molar volume of an ideal solution is the sum of the partial molar volumes of the components multiplied by their respective mole fractions. Loaded amine solutions are not ideal and have chemical reactions happening, so they certainly require additional terms to account for (amine + water and amine + carbon dioxide) interactions in addition to the use of the ideal terms:

$$V = X_{Am}V_{Am} + X_{H_2O}V_{H_2O} + X_{CO_2}V_{CO_2} + X_{Am}X_{H_2O}V^{*} + X_{Am}X_{CO_2}V^{**} \tag{4.6}$$

An expression for the molar volume of pure amine, V_{Am}, was developed using the pure component density data of Al-Ghawas et al (1989) and DeGuillo et al (1992) and is given by eq. 4.7:

$$V_{Am} = \frac{M_{Am}}{aT^2 + bT + C} \tag{4.7}$$

The molar volume associated with the interaction between carbon dioxide and the amine, V** is given by equation 4.8:

$$V^{**} = d + ex_{Am} \tag{4.8}$$

where, a=-5.351E(-7), b=-4.514E(-4), c=1.194, d=0, e=0, V*=-1.8218, and V_{CO2}=0.04747, for CO_2/MEA/H_2O system (Weiland et al., 1998). The result of the correlation was used to approximate the density of CO_2 loaded MEA and PZ mixture solution with the same total amine concentration as MEA.

This work used Weiland's correlations (1998) to calculate μ:

$$\frac{\mu}{\mu_{H_2O}} = \exp\frac{[(a\Omega + b)T + (c\Omega + d)][\alpha(e\Omega + fT + g) + 1]\Omega}{T^2} \tag{4.9}$$

where, μ and μ_{H2O} are the viscosities of the amine solution and water, respectively (mPa·s), Ω is the mass percent of amine, T is the temperature (K), and α is the CO_2 loading. Coefficients a=0, b=0, c=21.186, d=2373, e=0.01015, f=0.0093, g=-2.2589. μ_{H2O} was calculated by the following correlation:

$$\mu_{H2O}=\exp(-24.71+4209/T+0.04527T-0.00003376T^2) \quad (4.10)$$

The result of the correlation was used to approximate the viscosity of CO_2 loaded MEA and PZ mixture solution with the same total amine concentration as MEA.

The Henry's law constant correlation of CO_2 in MEA (Licht and Weiland, 1989) was used directly rather than using the N_2O analogy:

$$H_{CO_2,MEA}(atm/mole \cdot l) = R \cdot \exp[(\frac{-2625}{T(K)}) + 12.2] \quad (4.11)$$

$$R = \exp[(\frac{A}{T(K)} + B)X_I + hI] \quad (4.12)$$

where, X_I is the mole fraction of amine in unloaded solution, h is the Van Krevelen constant, I is the ionic strength which is typically equal to concentration of CO_2 in solution, and the model parameters A=5076 and B =-16.699. This work simplified the correlation by ignoring the hI term. The result of the correlation was used to approximate the Henry's law constant of CO_2 in loaded mixture of MEA and PZ solution with the same total amine concentration as MEA.

The CO_2 diffusion coefficient in MEA solution was calculated by N_2O analogy in this work, namely,

$$(D_{CO2,MEA})=C_I(D_{N2O,MEA}) \quad (4.13)$$

with

$$C_I=D_{CO2,H2O}/D_{N2O,H2O} \quad (4.14)$$

where, $D_{i,MEA}$ is the diffusion coefficient of i in MEA solution, and $D_{i,H2O}$ is the diffusion coefficient of i in water. $D_{CO2,H2O}$ and $D_{N2O,H2O}$ were calculated by the following expressions (Versteeg and Van Swaaij, 1988):

$$D_{CO2,H2O} = 2.35 \times 10^{-6} \exp(-2119/T) \quad (4.15)$$

$$D_{N2O,H2O} = 5.07 \times 10^{-6} \exp(-2371/T) \quad (4.16)$$

T is in Kelvin, and D is in m^2/s. The diffusion coefficient of N_2O in MEA solution was then estimated according to the modified Stokes-Einstein relation:

$$(D_{N2O}\, \mu^{0.8})_{MEA} = (D_{N2O}\, \mu^{0.8})_{H2O} \quad (4.17)$$

The result of the correlation was used to approximate the diffusion coefficient of CO_2 in the mixture of MEA and PZ solution with the same total amine concentration as MEA.

4.2.2 Liquid Phase and Gas Phase Mass Transfer Coefficients

The liquid film mass transfer coefficient of the wetted wall column was approximated by Pigford's model (1941). This model relies on solving the momentum balance for a falling film to determine the film thickness (δ) and surface velocity (u_{surf}). The mass transfer coefficient is then given as a function of the parameter $\eta = D\tau/\delta^2$, where τ is the contact time and δ is the film thickness, using the following relationships:

$$\Theta = \frac{[A]_i^L - [A]_o^{L,out}}{[A]_i^L - [A]_o^{L,out}} = 0.7857\exp(-5.12\eta) + 0.1001\exp(-39.2\eta) + 0.036\exp(-105.6\eta) + 0.0181\exp(-204.7\eta) \quad ; \quad \text{for} \quad \eta > 0.01 \quad (4.18)$$

$$\Theta = \frac{[A]_i^L - [A]_o^{L,out}}{[A]_i^L - [A]_o^{L,out}} = 1 - 3\sqrt{\frac{\eta}{\pi}} \quad ; \quad \text{for} \quad \eta > 0.01 \tag{4.19}$$

$$k_{L,A}^{o} = \frac{Q_L}{a}(1-\Theta) \tag{4.20}$$

where Q_L is the liquid flow rate. The liquid film mass transfer coefficient of the wetted wall column was measured by Mshewa (1995) and Pacheco (1998) by carbon dioxide desorption from water and ethylene glycol mixtures. Pacheco found that the above model predicted the their experimental data within 15%.

Pacheco (1998) determined the gas phase mass transfer coefficient of the apparatus by absorption of carbon dioxide into aqueous MEA. The Pacheco correlation was confirmed by Bishnoi (2000) by the absorption of sulfur dioxide into sodium hydroxide solutions. The gas film mass transfer coefficient is given by:

$$Sh = 1.075\left(Re \cdot Sc \cdot \frac{d}{h}\right)^{0.85} \tag{4.21}$$

where, d is the hydraulic diameter of the annulus (0.44cm) and h is the length of the column (9.1 cm).

To minimize gas film resistance, the flow rate used in this work was approximately 5 to 6 SLPM compared to the work of Pacheco (1998) where the overall flow rates were no greater than 2 SLPM.

4.2.3 Calculation of Enhancement Factor

In the mass transfer process between the gas phase and the liquid phase, which is enhanced by chemical reactions, the following expression was used to describe the relation of gas phase, liquid phase, and total mass transfer resistances:

$$\frac{1}{k_g} + \frac{1}{k_G'} = \frac{1}{K_G} \tag{4.22}$$

where, kg and K_G are the gas phase mass transfer coefficient and the total mass transfer coefficient respectively.

K_G can be calculated by the following expression:

$$K_G = \frac{\text{Flux}}{P_{CO_2} - P^*_{CO_2}} \tag{4.23}$$

where, P_{CO2} is the operational partial pressure of CO_2 in the wetted wall column, which was calculated by the log mean average:

$$P_{CO_2} = \frac{P_{CO_2,in} - P_{CO_2,out}}{Ln\left(P_{CO_2,in} / P_{CO_2,out}\right)} \tag{4.24}$$

k_G' represents the liquid film resistance with chemical reactions or the normalized flux. It can be expressed as:

$$\frac{1}{k_G'} = \frac{H}{k_l^o E} \tag{4.25}$$

4.3. Experimental Results and Discussion

Table 4.1 summarizes the experimental conditions under which CO_2 solubility and absorption rate were measured.

Table 4.1. Experimental conditions in this work.

T(°C)	60		40	
Camine	0.4M MEA/0.6M PZ	-	-	-
	1.9M MEA/0.6M PZ	2.5M MEA	-	-
	3.8M MEA/1.2M PZ	5.0M MEA	3.8M MEA/1.2 M PZ	5.0M MEA
Loading (moles CO_2/mol amine)	High (0.4-0.5)		High (0.4-0.5)	
	Medium(0.2-0.3)		Medium(0.2-0.3)	

In addition to the conditions listed above, several experimental data at very high loading (0.69) or very low loading (around zero) were also obtained.

4.3.1 Solubility of CO_2 in MEA/PZ/H_2O

In this work, at any given loading for a particular amine solution, both absorption and desorption rates were measured by variation of CO_2 partial pressure around the equilibrium partial pressure. When the flux is equal to zero, the partial pressure of CO_2 at the interface, $P_{CO2,i}$ will be the equilibrium partial pressure of CO_2 at that loading. This point can be found by bracketing the absorption and desorption rates. This concept is illustrated by figure 4.3 with a loaded 5.0 M MEA

solution (loading=0.299). While inferring this value, only measurements close to equilibrium were considered.

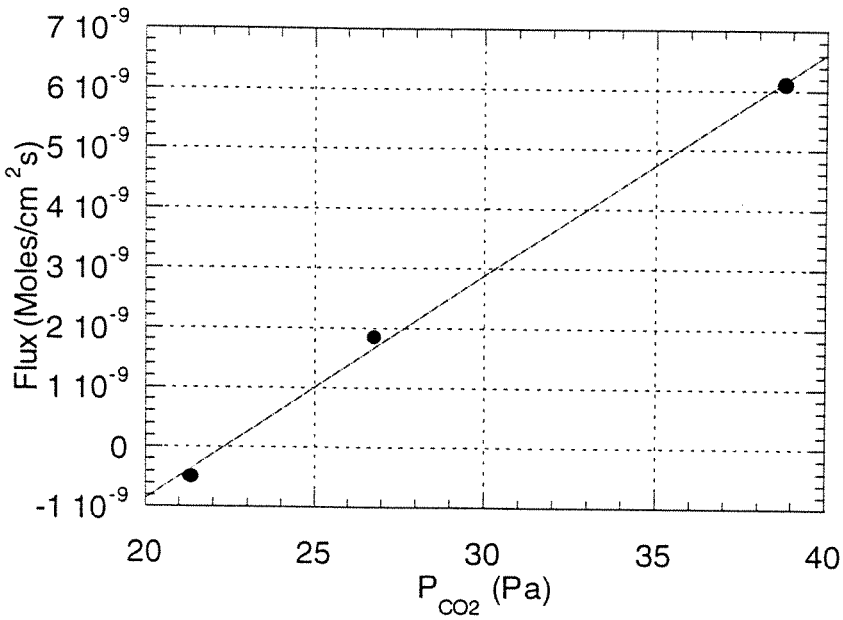

Figure 4.3. Extraction of CO_2 solubility in 5.0 M MEA at 40 °C, P_{CO2}*=22.1Pa, loading=0.299.

By applying the same concept to every loading, we achieved a series of solubility data for amine solutions with different concentrations at 40°C or 60°C. The solubility data obtained in this work is summarized in table 4.2 with the predicted values.

The measured CO_2 solubility in 5.0 M MEA blends with 0 or 1.2 M PZ at 40°C and 60°C is compared to the literature data (Jou et al., 1995) and the predicted

values in figure 4.4. Where, i represents model prediction, literature data, or the measured data in this work.

Table 4.2. Summary of CO_2 solubility in MEA/PZ/H_2O.

Amine (M)		40°C			60°C		
MEA	PZ	Loading	P_{CO2}* (Pa) (this work)	P_{CO2}* (Pa) (this model)	Loading	P_{CO2}* (Pa) (this work)	P_{CO2}* (Pa) (this model)
0.4	0.6	-	-	-	0.0557	18.2	1.5
		-	-	-	0.138	115	13
2.5	0	-	-	-	0.0912	27.6	4.6
		-	-	-	0.332	254	300
1.9	0.6	-	-	-	0.21	102	56.4
		-	-	-	0.443	2420	1500
5.0	0	0.299	22.1	29	0.27	224	116
		0.47	768	852	0.517	9550	20000
3.8	1.2	0.428	90.5	118	0.41	518	1003

At 40°C, the data from this work, model prediction, and literature match each other very well. At 60°C, experimental data matches the available literature data well, but the experimental data only fits the model prediction well at medium loading. The discrepancy might be because that the model itself doesn't fit the literature data well, which was used to fit the model parameters. At low or high loading, for example, the error may be more than 100%.

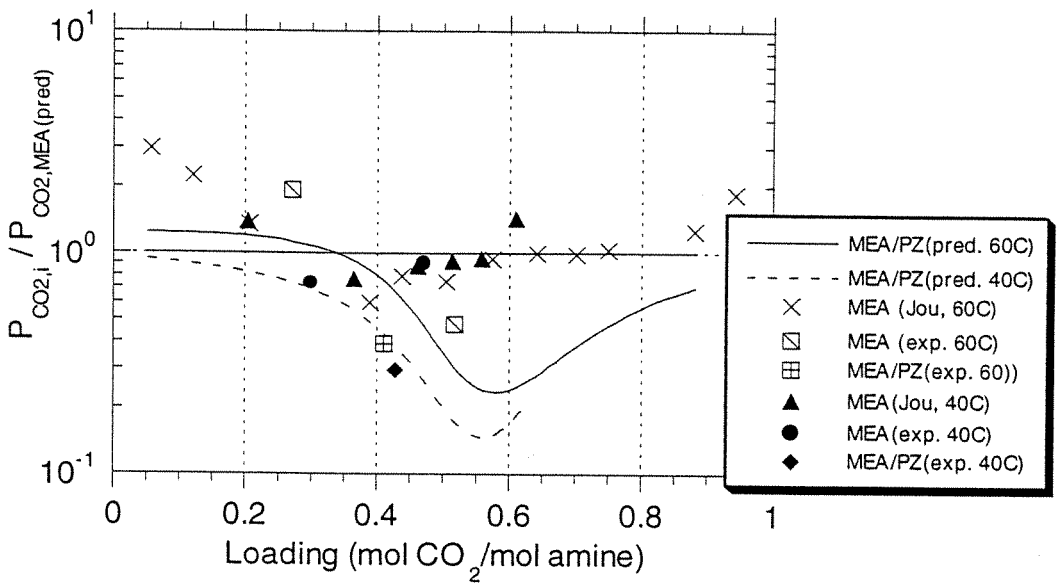

Figure 4.4. Comparison of predicted CO_2 solubility, literature data, and the experimental data of this work in 5.0 M MEA blends with 0 or 1.2 M PZ at 60°C and 40°C.

In figure 4.4, both model predictions and measured data indicate that the addition of PZ to MEA can decrease the CO_2 equilibrium partial pressure by a factor of 1.2-5 at medium and high loading, but has no significant effect at low loading.

Figures 4.5 and 4.6 are the comparisons of the predicted CO_2 solubility, literature data, and the experimental data of this work in 2.5 M MEA blends and 1.0 MEA blends with 0 or 0.6 M PZ at 60°C respectively. The model predictions

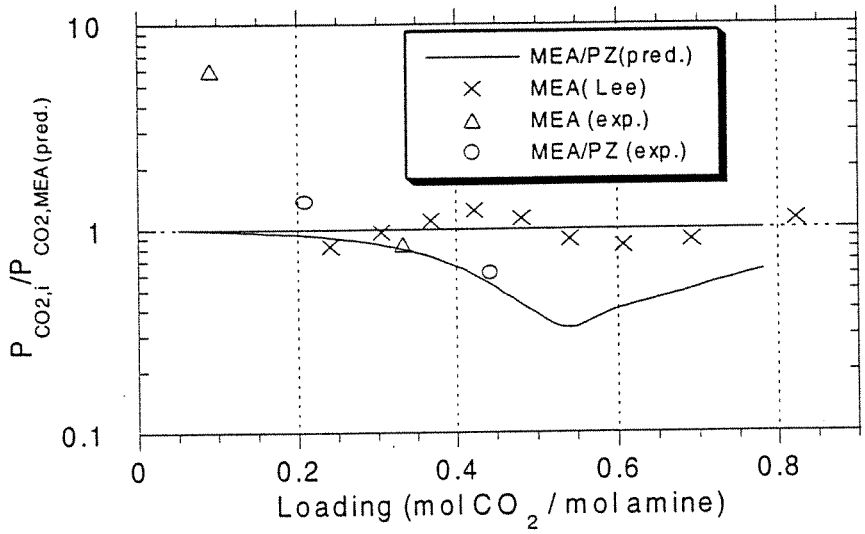

Figure 4.5. Comparison of predicted CO_2 solubility, literature data, and the experimental data of this work in 2.5 M MEA blends with 0 or 0.6 M PZ at 60°C.

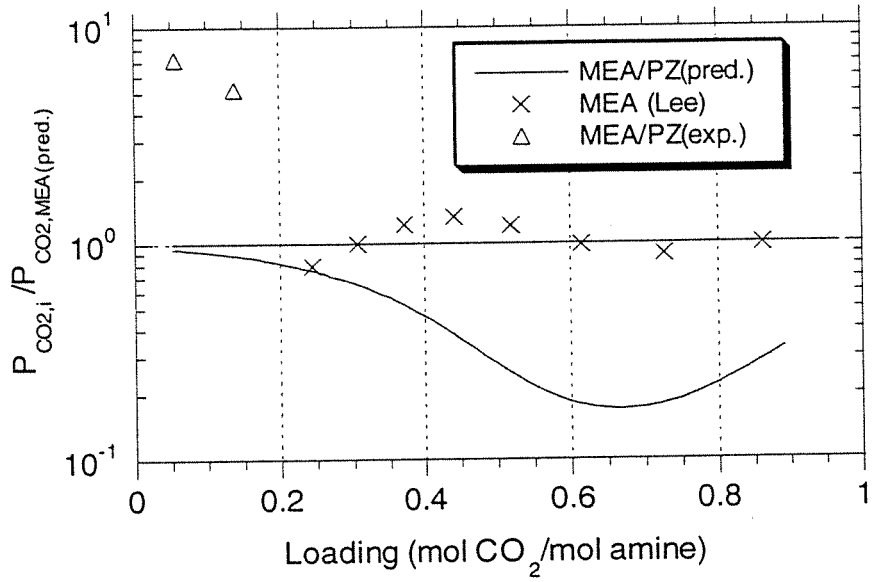

Figure 4.6. Comparison of predicted CO_2 solubility, literature data, and the experimental data of this work in 1.0 M MEA blends with 0 or 0.6 M PZ at 60°C.

and the literature data agree with each other well. The data of this work matches the model well at medium and high loading. At low loading, the measured data is much higher than the prediction. There is no literature data available from Lee et al., (1976) at this range.

4.3.2 Rate of CO_2 Absorption in MEA/PZ/H_2O

At each loading in a given amine concentration, the CO_2 partial pressure was varied to obtain a series of rate data. The enhancement factor derived from each series is reported in table 4.3. For each point, the equilibrium partial pressure of CO_2 was estimated from the actual measured CO_2 loading and the measured equilibrium pressure for the series. If the equilibrium of the following reaction was dominant in the system of CO_2/amine/H_2O,

$$NR + CO_2 \leftrightarrow NRH^+ + HCO_3^- \tag{4.26}$$

the equilibrium partial pressure of CO_2 would be proportional to the square of the loading:

$$\frac{P^*_{CO_2,1}}{P^*_{CO_2,2}} = \frac{(\text{Loading},_1)^2}{(\text{Loading},_2)^2} \tag{4.27}$$

Most of the data were converted by equation 4.27. Since at high loading, the dominant chemistry may not be the equation 4.26, equation 4.27 is no longer a good correction. So, according to the trend of the equilibrium solubility of CO_2 in

Table 4.3. Measured and predicted enhancement factors for CO_2 absorption in MEA/PZ/H_2O.

T [°C]	Amine[M] MEA	Amine[M] PZ	Loading [mol CO_2/mol amine]	P_{CO2}* [Pa]	$K_G' \cdot 10^{10}$ [mol/(cm^2·s·Pa)]	k_l^o [cm/s]	E_{exp}	E_{pred}	E_l	E_{inst}	k_G/k_g	P^*/P_i	Removal [%]
60	0.4	0.6	0.057	19.9	4.70	0.016	174	136	137	21910	0.68*	0.29	42.4
			0.14	121	2.88	0.016	107	117	120	5093	0.54	0.62*	39
	2.5	0	0.094	29.2	3.18	0.015	120	98.4	98.7	37945	0.56	0.25	38.7
			0.34	285	1.54	0.015	58.5	72	73	4015	0.31	0.14	25
			0.66	30701	0.54	0.015	20.4	16	28	38	0.19	0.74*	5.9*
	1.9	0.6	0.01	1	7.19	0.015	272	181	182	274989	0.73*	0.004	52.2
			0.21	105	3.14	0.014	127	144	145	12922	0.56	0.58*	53.9
			0.47	2705	1.46	0.013	64	74	87	482	0.39	0.55	31.1
	5.0	0	0.29	273	2.42	0.012	104	124	125	7314	0.48	0.30	32.5
			0.53	14084	0.44	0.011	20.6	33	55	84	0.14	0.39	8.4*
	3.8	1.2	0.43	852	2.96	0.011	140	172	183	2571	0.54	0.39	34.4
40	5.0	0	0.30	21.1	2.00	0.0085	92	101	101	76770	0.43	0.15	32.1
			0.51	3415	0.42	0.0078	20.8	32	36	279	0.14	0.10	11.5*
	3.8	1.2	0.44	97.0	2.04	0.0073	109	122	123	16622	0.44	0.51	24.3

k_l' (normalized flux)=flux/($P_{CO2,i}$-P_{CO2}*); k_l^o: liquid phase mass transfer coefficient; E_{exp}: measured enhancement factor; E_{pred}:predicted enhancement factor; E_l;predicted pseudo first order enhancement factor; E_{inst}: instantaneous enhancement factor.

* These parameters are indicative of potentially greater error in K_G'

MEA solution (Jou, et al., 1995): $Log_{10}P_{CO2}$=a+b*Loading, the rearranged correlation was used for the above situation:

$$P_2 = 10^{(\log_{10} P_1 + a)}\left(\frac{\text{loading}_1}{\text{loading}_2} - a\right) \qquad (4.28)$$

where, "a" is a constant that varies from 0-4. The reason for the variation of "a" is that equation 4.28 with constant value of "a", can not represent the relation between equilibrium partial pressure of CO_2 and CO_2 loading over the whole range of high loading. So we choose to adjust the value of "a" to get a good linear relation of flux versus ($P_{CO2,i}$ - P_{CO2}*), which is used to derive the measured enhancement factor. If applied, the values of "a" are listed in appendix E. Figure 4.7 is an example of the linear relation.

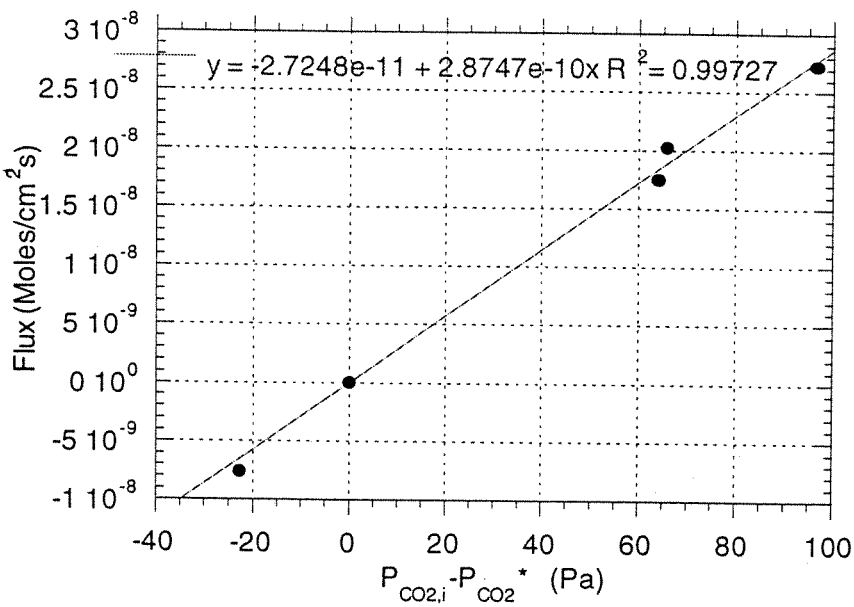

Figure 4.7. Linear relation between flux and ($P_{CO2,i}$ – P_{CO2}*) for CO_2 absorption in 0.4M MEA/0.6MPZ at loading of 0.138, 60°C.

The slope of the straight line in figure 4.7 is the normalized flux k_G'. By using eq. 4.25, E can be calculated. Table 4.3 summarizes the measured and predicted values of enhancement factor E with some important variables such as loading, $P_{CO2}*$, normalized flux and k_l^o, where the values of loading and $P_{CO2}*$ are the averages of each series rate data.

For data analysis, there are three important error parameters: gas film resistance, K_G/k_g; approach to equilibrium, $(P_{CO2,i}-P_{CO2}*)/P_{CO2,i}$; and removal of CO_2, $(P_{CO2,in} - P_{CO2,out})/P_{CO2,in}$. Gas film resistance determines the error of $P_{CO2,i}$. If it is higher than 70%, the error of calculated $P_{CO2,i}$ may be more than 30%. The parameter of approach to equilibrium determines the error of k_G' which is used to derive enhancement factor in this work. Rate data measured far away from equilibrium introduces less possible error to the k_G'. The removal of CO_2 indicates the error of measured flux. The more CO_2 removal is, the less error of the measured flux has. The detailed data and error analysis are in appendix E.

Figures 4.8 to 4.11 compare the experimental rate data with model predictions. The solid circles are the measurements of the CO_2 absorption rate in MEA solution and the solid diamonds are the measurements of the CO_2 absorption rate in the mixture of MEA and PZ. The curves are the rate model predictions with constants listed in the figures. The segment lines in figures 4.10 and 4.11 are used to connect the experimental data to the model predictions with the same CO_2 loading.

For CO_2 absorption in 1.0 M MEA blends with 0 or 0.6 M PZ (figure 4.8) and in 2.5 M MEA blends with 0 or 0.6 M PZ at 60°C (figure 4.9), most of the predictions are within 20 % of the measured enhancement factors.

The only measurement at very low loading (1 Pa CO_2 in 1.9 M MEA/ 0.6 M PZ) was about 80% greater than the model prediction. It is probable that MEA catalyzed the piperazine reaction with CO_2 by the zwitterion mechanism (Bishnoi, 2000). This effect is not seen at greater loading because most of the MEA is converted to products. This effect is not included in this model.

For CO_2 absorption in 5.0 M MEA blends with 0 or 1.2 M PZ at 60°C and 40°C (figures 4.10 and 4.11), the agreement of the model prediction and the experimental data is not as good. One of the possible reasons is the amine concentration.

Because of the definition of loading (mol CO_2/mol amine), the higher the amine concentration is , the higher the CO_2 equilibrium partial pressure is at the same CO_2 loading. The CO_2 partial pressure used for rate measurement in 5.0 M MEA blends is pretty high. At high CO_2 partial pressure, amine at the gas-liquid interface will be depleted by reacting with CO_2, which results in a significant amine concentration gradient in liquid film. So, the pseudo first order reaction assumption is no longer a good assumption for the rate model and the predicted values are higher that the measured ones.

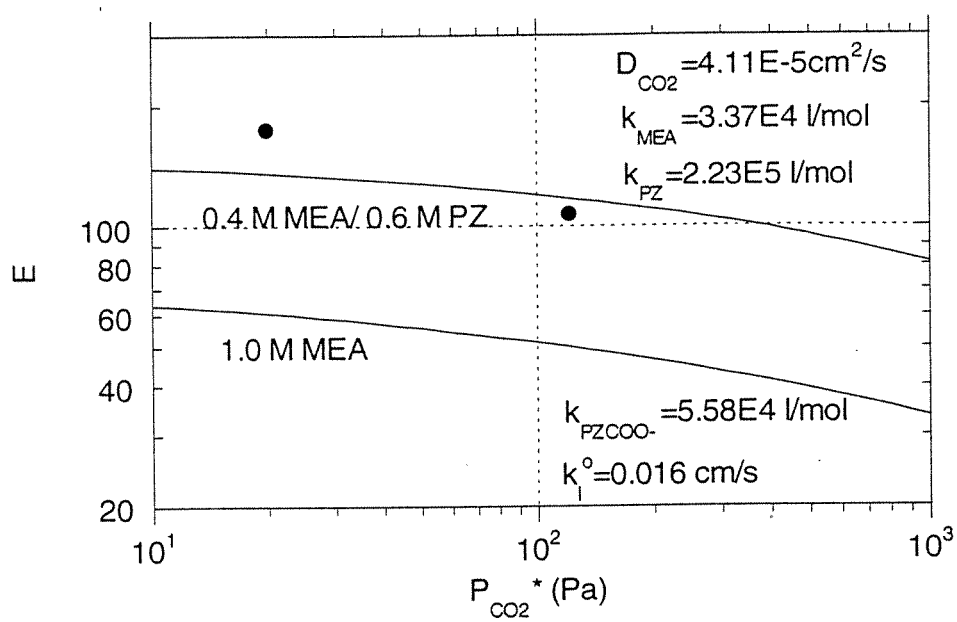

Figure 4.8. CO_2 absorption rate in 1.0 M MEA blends containing with 0 or 0.6M PZ at 60°C, curves predicted by the rate model with the listed constants.

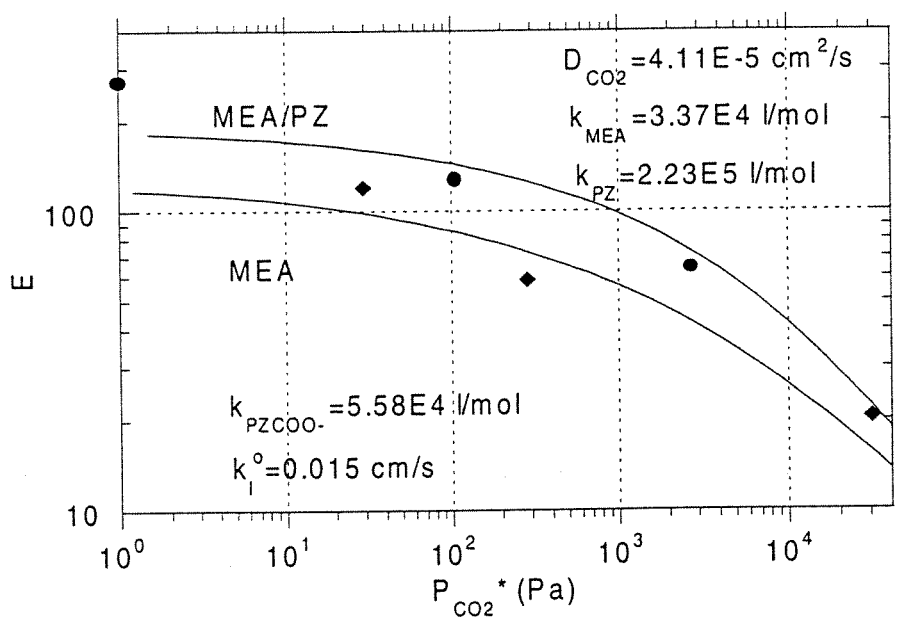

Figure 4.9. CO_2 absorption rate in 2.5 M MEA blends containing with 0 or 0.6M PZ at 60°C, curves predicted by the rate model with the listed constants.

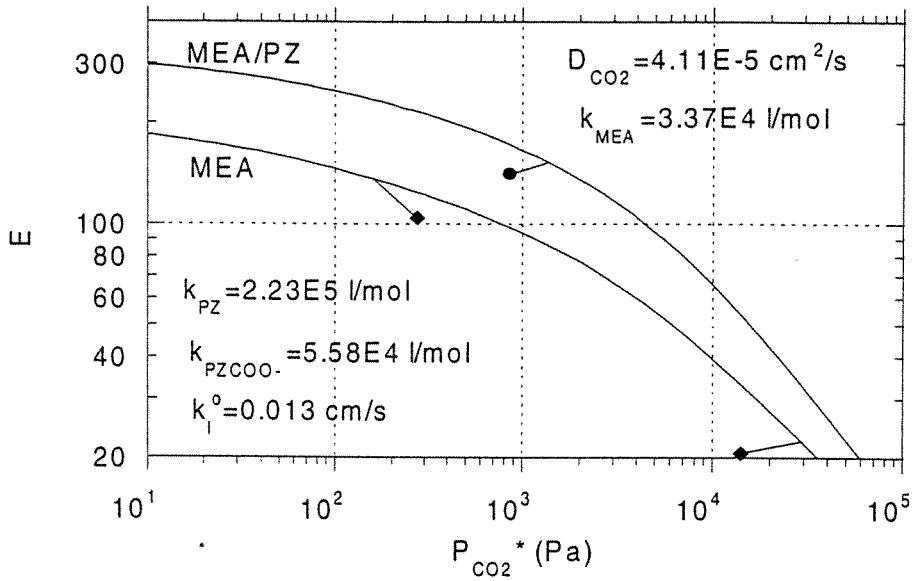

Figure 4.10. CO_2 absorption rate in 5.0 M MEA blends containing with 0 or 1.2 M PZ at 60°C, curves predicted by the rate model with the listed constants, line segments connect values of equal loading.

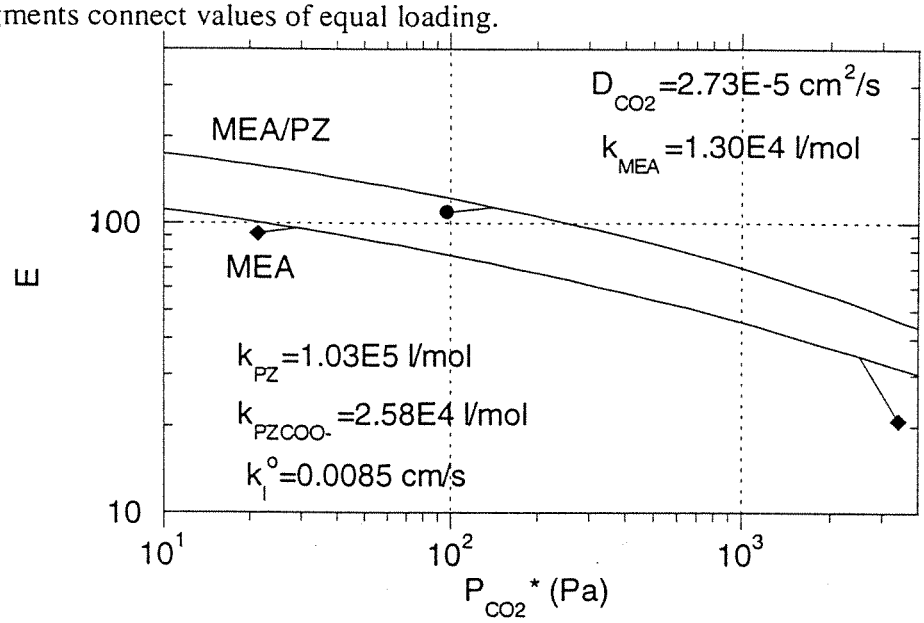

Figure 4.11. CO_2 absorption rate in 5.0 M MEA blends containing with 0 or 1.2 M PZ at 40°C, curves predicted by the rate model with the listed constants, line segments connected values of equal loading.

Overall, there are several reasons for the discrepancies between predictions and measurements. First, the pseudo first order assumption of the rate model has its limitation. At low loading, it is a good approximation because of the low equilibrium partial pressure of CO_2. While at high loading, the CO_2 partial pressure is very high which results in the depletion of amine at the interface. So there is a significant negative gradient of amine from the bulk liquid to the interface and the assumption of $[amine]_b=[amine]_i$ is not good under such situation. The instantaneous enhancement only accounts for the diffusion limitations of the mass transfer process and has no correction to the amine gradient in the liquid film. So at high loading, the measured absorption rates is systematically lower than the predicted values.

Second, the rate model depends on the speciation from the VLE model. At high loading, the VLE model does not agree well with the literature solubility data. The solution speciation has not been verified independent measurements, such as nuclear magnetic resonance. The prediction of the solution speciation is not guaranteed at high loading.

Chapter Five

Conclusions

5.1 Conclusions

The absorption rate of CO_2 in 0.4 M MEA/0.6 M PZ, 1.9 M MEA/0.6 M PZ, and 3.8 M MEA/1.2 M PZ is 1.5-2.5 times higher than that in 1.0 M MEA, 2.5 M MEA and 5.0 M MEA respectively, at 60°C and 40°C.

At loading lower than 0.4 mol CO_2/mol amine, PZ is the critical species which contributes more than 60% of the total absorption rate. At loading higher than 0.6, $PZCOO^-$ becomes important and accounts for more than 40% of total absorption rate. MEA accounts for less than 10% of the total absorption rate in 0.4 M MEA/0.6 M PZ at 60°C. For the other cases studied in this work, MEA has a 20% to 30% contribution to the total absorption rate over the whole range of loading. MEA is never dominates the total absorption rate in this work.

At loading higher than 0.4 – 0.5 mol CO_2/mol amine, the equilibrium partial pressure of CO_2 in 0.4 M MEA/0.6 M PZ, 1.9 M MEA/0.6 M PZ, and in 3.8 M MEA/1.2 M PZ is more than two times lower than that in 1.0 M MEA, 2.5 M MEA and 5.0 M MEA respectively, at 60°C and 40°C. At loading lower than 0.2 – 0.3, there is no significant effect of PZ on the equilibrium partial pressure of CO_2.

The result has been compared with the simple VLE and rate models of this work. The VLE model with two adjusted parameters fits the literature data well

except at very low and high loading. The VLE model fits the measured data of this work well at medium loading. At low and high loading, the fit is not as good as at medium loading. The rate model, which includes both pseudo first order enhancement and instantaneous enhancement, agrees well with the measured rate data of CO_2 absorption in 1.0 M MEA/PZ blend and 2.5 M MEA/PZ blend at 60°C. For CO_2 absorption in 5 M MEA/PZ blend at 60°C and 40°C, the prediction of the rate model is systematically higher than the measured data.

5.2 Recommendations

A more advanced thermodynamic model is necessary for the modeling of CO_2 absorption in the mixture of MEA and PZ solution not only because of the prediction of CO_2 solubility, but also because the VLE model is the basis of the rate model for the system. For example, the speciation of MEA, PZ and $PZCOO^-$ play very important roles in the pseudo-first order enhancement factor, and the CO_2 solubility dominates the instantaneous enhancement fact in the rate model. Therefore, improvement of the VLE model will definitely improve the quality of the rate model.

Either the AspenPlus rigorous VLE model or standalone electrolyte NRTL rigorous VLE model can accomplish this improvement. Such models for MEA are available. A wide range of VLE data for PZ and mixtures of MEA and PZ is needed to regress the model parameters in the rigorous MEA/PZ VLE model for this system.

VLE measurement of speciation of loaded amine solution with nuclear magnetic resonance is an effective method for verifying VLE models. Hydrogen NMR can be used for measurements of speciation of PZ/HPZ^+, $PZCOO^-/^+HPZCOO^-$, $PZCOO_2^=$, $MEA/MEAH^+$, and $MEACOO^-$. Carbon 13 NMR can be used for measurements of PZ/PZH^+, $HCO_3^-/CO_3^=$, $PZCOO^-/^+HPZCOO^-$, $PZCOO_2^=$, $MEA/MEAH^+$, and $MEACOO^-$.

More rigorous approaches are also needed for the rate model for CO_2 absorption in $MEA/PZ/H_2O$. One of them is the partial differential equation method based on penetration theory. Bishnoi and Rochelle (2000) have developed a PDE rate model for $MDEA/PZ/H_2O$ system. Similar work could be done for $MEA/PZ/H_2O$ in the future.

More rate data is needed at low loading with a range of temperature. More solubility data is needed in the medium and high loading in order to verify the significant decrease of CO_2 equilibrium partial pressure for the addition of PZ into MEA solution.

The experiments in this work include solubility measurement and absorption rate measurement. Usually, the solubility and absorption rate were measured at the same experiment. This has at least two disadvantages. First, good solubility data is the basis of rate data, and the quality of the solubility will be unknown until the sample analysis and raw data analysis have been done. So, continuos measurement will have more uncertainty about if the rate measurement is worth of doing or not at

that loading point. Second, rate measurement requires the absorption driving force big enough. If the solubility and absorption rate are measured in the same experiment, the range of the CO_2 analyzer will limit the increase of the absorption driving force, which may result in the rate data is not far enough from the equilibrium. Measuring solubility and absorption rate separately with different CO_2 analyzer ranges will solve this trouble.

Appendix A

Fortran Codes of VLE and Rate Models

A.1 VLE Model (3.8 M MEA/1.2 M PZ at 60°C)

```
      Program test
      real*8 temp,alpha,xmeat,xpzt,xdegt,pco2,par(10)
      read (*,*) par(7),par(8),par(9),par(10)
C
C     ENTER PARAMETER VALUES
C
      par(1)=1.000
      par(2)=1.000
      par(3)=1.000
      par(4)=1.000
      par(5)=-30.777
      temp=333.15
      alpha=0.05
      xmeat=0.09065
      xpzt=0.02863
      xdegt=0.0
      do 10 i=1,90
            call blendvle(temp,alpha,xmeat,xpzt,xdegt,par,pco2)
            xpzt=0.02863
            xmeat=0.09065
            xdegt=0.0
            open (unit=16, file='panda.txt',status='old')
            write (16,*) 'pco2=',pco2, 'alpha=',alpha
            alpha=alpha+0.01
10  continue
      end

CCCC
```

```
      implicit real*8 (a-h, o-z)
      real*8 k(14), x(14), f(14), j(14,14),xdx(14),fdx(14)
      real*8 p(14), s(14), hco2, temp, cco2, cpz, mw, par(10)
      integer n, ia, icount, lo(14)
      n=14
      ia=n
C
C
C     DICTIONARY OF VECTORS
C
C     X(1)  :X CO2
C     X(2)  :X H2O
C     X(3)  : X PZ
C     X(4)  :X MEA
C     X(5)  :X MEAH+
C     X(6)  :X PZH+
C     X(7)  :X H3O+
C     X(8)  :X HCO3-
C     X(9)  :X CO3=
C     X(10):X OH-
C     X(11):X PZCOO-
C     X(12):X H+PZCOO-
C     X(13):X -OOCPZCO-
C     X(14):X MEACOO-
C     F(N) : VECTOR OF EQUATIONS ALL=0 AT CONVERGENCE
C     J(N,N) : JACOBIAN MATRIX
C     ALPHA : LOADING OF SOLUTION
C     XCO2T : TOTAL CO2 CONCENTRATION
C     XMEAT : TOTAL MEA CONCENTRATION
C     XPZT : TOTAL PZ CONCENTRATION
C     XH2OT : TOTAL WATER CONCENTRATION
C
C     READ LOADING, AMINE STRENGTHS, AND EQM CONSTANTS
C


      icount=0
      k(1)=exp(231.465-12092.1/temp-36.7816*log(temp))
      k(2)=exp(216.049-12431.7/temp-35.4819*log(temp))
      k(3)=exp(par(7)+par(8)/temp)
      k(4)=exp(132.899-13445.9/temp-22.4773*log(temp))
      k(5)=exp(-11.91-4350.6/temp)
      k(6)=exp(-29.308*par(1)+5614.64*par(2)/temp)
      k(7)=exp(-8.212*par(3)-5285.94*par(4)/temp)
      k(8)=exp(par(5)+5614.64/temp)
      k(14)=exp(par(9)+par(10)/temp)
```

```
      hco2=2.95e8
C
C     RENORMALIZE MOLEFRACTIONS IN THE LOADED SOLN
C
      xamine=xpzt+xmeat
      xco2t=alpha*xamine
      xh2ot=1.0-xamine-xdegt
      totmol=xco2t+xh2ot+xamine+xdegt
      mw=(xco2t*44.01+xmeat*61.08+xpzt*86.13+xdegt*106.14+xh2ot*18.02)/
      totmol
      xco2t=xco2t/totmol
      xpzt=xpzt/totmol
      xmeat=xmeat/totmol
      xh2ot=xh2ot/totmol
      write (*,*) 'total initial molefrac:', (xh2ot+xmeat+xpzt+xco2t)
      write (*,*) 'co2,mea,pz,h2o,deg',xco2t,xmeat,xpzt,xh2ot,xdegt
C
C     ENTER INITIAL GUESSES FOR MOLEFRACTIONS
C

      x(1)=1.0e-8
      x(2)=xh2ot-1.0e-8-1.0e-5-1.0e-7-2.0e-8
      x(3)=(1.0-alpha)*xpzt
      x(4)=(1.0-2*alpha)*xmeat
      x(5)=alpha*xmeat
      x(6)=0.29*alpha*xpzt
      x(7)=1.0e-5
      x(8)=1e-4
      x(9)=1e-4
      x(10)=1.0e-7
      x(11)=0.3*alpha*xpzt
      x(12)=0.4*alpha*xpzt
      x(13)=0.01*alpha*xpzt
      x(14)=alpha*xmeat
1     continue
      icount=icount+1
      write (*,*) 'icount=',icount
C
C     EVALUATE FUNCTION VALUES
C
      call eq(n,x,xco2t,xmeat,xpzt,k,f)
C
C     CALCULATE THE JACOBIAN MATRIX
C
```

```
      do 30 i=1,n
            do 40 l=1,n
                  xdx(l)=x(l)
40          continue
            xdx(i)=1.04*x(i)
            call eq(n,xdx,xco2t,xmeat,xpzt,k,fdx)
            do 50 m=1,n
                  j(m,i)=(fdx(m)-f(m))/(xdx(i)-x(i))
50          continue
30    continue
C
C     USE GAUSSIAN ELIMINATION TO GET THE NEXT GUESS. FIRST
C     CALL
C     GAUSS FOR FORWARD ELIMINATION THEM CALL SOLVE FOR
C     BACK SUBSTITUTION
C

      call gauss(n,j,ia,lo,s)
      call solve(n,j,ia,lo,-f,p)
      do 60 i=1,n
            x(i)=x(i)+p(i)
60    continue
      do 70 i=1,n
            if (abs(p(i)/x(i)).gt.1.0e-8) then
                        goto 1
            else
                        continue
            endif
70    continue
      write (*,*) ' '
      write (*,*) ' '
      write (*,*) f(1),f(2),f(3)
      write (*,*) f(4),f(5),f(6)
      write (*,*) f(7),f(8),f(9)
      write (*,*) f(10),f(11),f(12)
      write (*,*) f(13),f(14)
      write (*,*) 'check material balances:'
      write (*,*) 'total molefractions'
      write (*,*) xco2t,xmeat,xpzt,xh2ot
      write (*,*) 'co2:',xco2t-x(1)-x(8)-x(9)-x(11)-x(12)-2*x(13)-x(14)
      write (*,*) 'MEA:',xmeat-x(4)-x(5)-x(14)
      write (*,*) 'pz:',xpzt-x(3)-x(6)-x(11)-x(12)-x(13)
```

```
      write (*,*) 'charge:',2*x(9)+x(8)+x(10)+x(11)-x(7)-x(5)-
      x(6)+2*x(13)+x(14)
      open (unit=18, file='fandx.txt',status='old')
      write (18,*) 'alpha=',alpha
      write (18,*) 'converged in',icount,'iterations.'
      tot=0.0
      do 10 i=1,n
                    write (18,*)'x(',i,')=',x(i),'F(',i,')=',f(i)
                    tot=tot+x(i)
10    continue
      cco2=x(1)/mw
      cpz=x(4)/mw
      cmea=x(3)/mw
      write (*,*) ' '
      write (*,*) 'temp(k)=',temp
      write (*,*) 'sum of molefractions=',tot
      pco2=x(1)*hco2
      write (*,*)'co2 partial pressure(pa)=',pco2
      open (unit=10, file='pred1.txt',status='old')
      open (unit=11, file='pred2.txt',status='old')
      open (unit=12, file='pred3.txt',status='old')
      open (unit=13, file='pred4.txt',status='old')
      open (unit=14, file='pred5.txt',status='old')
      open (unit=15, file='pred6.txt',status='old')
      write (10,*) pco2,alpha,x(1)
      write (11,*) x(2),x(3),x(4)
      write (12,*) x(5),x(6),x(7)
      write (13,*) x(8),x(9),x(10)

      write (14,*) x(11),x(12),x(13)
      write (15,*) x(14)
      return
      end
      subroutine eq(n,x,xco2t,xmeat,xpzt,k,f)
       real*8 k(14),x(n),f(n),xco2t,xmeat,xpzt
       f(1)=x(1)*x(2)*x(2)*k(1)-x(8)*x(7)
       f(2)=x(8)*x(2)*k(2)-x(9)*x(7)
       f(3)=x(5)*x(2)*k(3)-x(4)*x(7)
       f(4)=x(2)*x(2)*k(4)-x(7)*x(10)
       f(5)=x(6)*x(2)*k(5)-x(3)*x(7)
       f(6)=x(3)*x(1)*x(2)*k(6)-x(11)*x(7)
       f(7)=x(12)*x(2)*k(7)-x(7)*x(11)
```

```
      f(8)=x(11)*x(1)*x(2)*k(8)-x(13)*x(7)
      f(9)=x(1)+x(8)+x(9)+x(14)+x(11)+x(12)+2*x(13)-xco2t
      f(10)=x(4)+x(5)+x(14)-xmeat
      f(11)=x(3)+x(6)+x(11)+x(12)+x(13)-xpzt
      f(12)=x(1)+x(2)+x(3)+x(4)+x(5)+x(6)+x(7)+x(8)+x(9)+x(10)+x(11)+x(12)
      +x(13) +x(14)-1.0
      f(13)=2*x(9)+x(8)+x(10)+x(14)+x(11)+2*x(13)-x(7)-x(5)-x(6)
      f(14)=x(4)*x(1)*x(2)*k(14)-x(14)*x(7)
      return
      end
CCCCCCCCCCCCCCCCCCCCCCCCCCCCCCCCCCCCCCCCCCCCCCCCCCCC
C     THIS SUBROUTINE PERFORMS THE FORWARD ELIMINATION
C     PROCESS FOR GAUSSIAN ELIMINATION WITH SCALED PARTIAL
C     PIVOTING FOR N EQUATIONS. IT IS BASED ON THE BOOK
C     'NUMERICAL MATHEMATICS AND COMPUTING' BY CHENEY
C     AND
C     KINCAID. SECOND EDITION. CHAPTER 6 SEC 2
C

      subroutine gauss(n,a,ia,l,s)
      real*8 a(ia,n),s(n)
      integer i,j,k,l(n)
      do 3 i=1,n
                l(i)=i
                smax=0.0
                do 2 j=1,n
                        if (abs(a(i,j)).gt.smax) smax=abs(a(i,j))
2               continue
                s(i)=smax
3     continue
      do 7 k=1,n-1
            rmax=0.0
            do 4 i=k,n
                  r=abs(a(l(i),k))/s(l(i))
                  if (r.le.rmax) goto 4
                  j=i
                  rmax=r
4           continue
            lk=l(j)
            l(j)=l(k)
            l(k)=lk
            do 6 i=k+1,n
                  xmult=a(l(i),k)/a(lk,k)
```

```
                    do 5 j=k+1,n
                        a(l(i),j)=a(l(i),j)-xmult*a(lk,j)
5                   continue
                    a(l(i),k)=xmult
6           continue
7       continue
        return
        end
CCCCCCCCCCCCCCCCCCCCCCCCCCCCCCCCCCCCCCCCCCCC
C       THIS SUBROUTINE PERFORMS THE BACKWARD SUBSTITUTION
C       PROCESS FOR GAUSSIAN ELIMINATION WITH SCALED PARTIAL
C       PIVOTING FOR N EQUATIONS. IT IS BASED ON THE BOOK
C       'NUMERICAL MATHEMATICS AND COMPUTING' BY CHENEY
C       AND
C       KINCAID. SECOND EDITION. CHAPTER 6 SEC 2
C
        subroutine solve(n,a,ia,l,b,x)
        real*8 a(ia,n),b(n),x(n)
        integer n,l(n),i,k,j
        do 3 k=1,n-1
                do 2 i=k+1,n
                    b(l(i))=b(l(i))-a(l(i),k)*b(l(k))
2               continue
3       continue
        x(n)=b(l(n))/a(l(n),n)
        do 5 i=n-1,1,-1
                sum=b(l(i))
                do 4 j=i+1,n
                        sum=sum-a(l(i),j)*x(j)
4               continue
                x(i)=sum/a(l(i),i)
5       continue
        return
        end
```

A.2 Pseudo-First Order Enhancement Factor (3.8 M MEA/1.2 M PZ at 60°C)

```
real*8 cmea,xmea0,cpz,xpz0,cpzcoo,Emeapz,k2mea,k2pz,k2pzcoo,
      kl,dco2,temp
xmea0=0.09065
xpz0=0.02863
temp=333.15
k2mea=0.001*exp((10.99-2152/temp)*log(10.0))
k2pz=53.7*exp(-3.36e4*(1/temp-1/298.15)/8.3145)
k2pzcoo=k2pz/4
kl=0.012e-2
a=0.0
b=0.0
c=21.186
d=2373
e=0.01015
f=0.0093
g=-2.2589
o=0.3054
yhya=1/exp(((a*o+b)*temp+(c*o+d))*(alpha*(e*o+f*temp+g)+1)*o/(temp
      *temp))
dco2w=2.35e-6*exp(-2119/temp)
dco2=dco2w*yhya**0.8
do 10 i=1,90
      open (unit=1,file='cmea.txt',status='old')
      open (unit=2,file='alpha.txt',status='old')
      open (unit=3,file='pe.txt',status='old')
      open (unit=5,file='cpz.txt',status='old')
      open (unit=6,file='cpzcoo.txt',status='old')
      read (1,*)cmea
      read (2,*)alpha
      read (3,*)pe
      read (5,*)cpz
      read (6,*)cpzcoo
      cmea=cmea/((xmea0*61+xpz0*86+(1-xmea0-xpz0)*18
      +alpha*(xmea0+xpz0)*44)/(1+alpha*(xmea0+xpz0))/1000000)
      cpz=cpz/((xmea0*61+xpz0*86+(1-xmea0-xpz0)*18
      +alpha*(xmea0+xpz0)*44)/(1+alpha*(xmea0+xpz0))/1000000)
      cpzcoo=cpzcoo/((xmea0*61+xpz0*86+(1-xmea0-xpz0)*18
      +alpha*(xmea0+xpz0)*44)/(1+alpha*(xmea0+xpz0))/1000000)
      Emeapz=sqrt((k2mea*cmea+k2pz*cpz+k2pzcoo*cpzcoo)*dco2)/kl
      open (unit=4, file='rate.txt',status='old')
```

```
        write (*,*) alpha,cmea,cpz,Emeapz
        write (4,*) alpha,Emeapz
100     format(f5.3,f10.4,f10.3,f10.3)
10      continue
        end
```

A.3 Instantaneous Enhancement Factor (3.8 M MEA/1.2 M PZ at 60°C)

```
      temp=333.15
      hco2=51231
      hco2=hco2*1.01325e2
      cmea=5
      open (unit=1,file='pe.txt',status='old')
      open (unit=2,file='alpha.txt',status='old')
      read (1,*) pe1
      read (2,*) alpha1
      do 10 i=1,95
      read (1,*) pe2
      read (2,*) alpha2
      differencial=(alpha2-alpha1)/(pe2-pe1)
      Einst=cmea*hco2*differencial*sqrt(2.0)
      write(*,*) alpha1,Einst
      open (unit=3,file='Einst.txt',status='old')
      write(3,*)alpha1,Einst
      pe1=pe2
      alpha1=alpha2
10    continue
      end
```

Appendix B

CO_2 Equilibrium Partial Pressure and Speciation Of MEA, PZ and PZCOO$^-$

Table B.1 P_{CO2} and MEA speciation in CO_2/MEA/H_2O

Loading (moles CO_2 /mol amine)	1.0 M MEA (60°C)		2.5 M MEA (60°C)		5.0 M MEA(60°C)		5.0 M MEA (40°C)	
	P_{CO2} (Pa)	X_{MEA} (mole fraction)	P_{CO2} (Pa)	X_{MEA} (mole fraction)	P_{CO2} (Pa)	X_{MEA} (mole fraction)	P_{CO2} (Pa)	X_{MEA} (mole fraction)
5.0E-02	1.2E+00	1.7E-02	1.2E+00	4.5E-02	1.1E+00	1.0E-01	1.7E-01	1.0E-01
6.0E-02	1.8E+00	1.7E-02	1.8E+00	4.4E-02	1.6E+00	9.8E-02	2.5E-01	9.8E-02
7.0E-02	2.5E+00	1.6E-02	2.5E+00	4.3E-02	2.3E+00	9.6E-02	3.6E-01	9.6E-02
8.0E-02	3.4E+00	1.6E-02	3.5E+00	4.2E-02	3.2E+00	9.3E-02	5.0E-01	9.3E-02
9.0E-02	4.5E+00	1.6E-02	4.6E+00	4.1E-02	4.2E+00	9.1E-02	6.6E-01	9.1E-02
1.0E-01	5.8E+00	1.5E-02	5.9E+00	4.0E-02	5.5E+00	8.9E-02	8.6E-01	8.9E-02
1.1E-01	7.3E+00	1.5E-02	7.5E+00	3.9E-02	7.0E+00	8.6E-02	1.1E+00	8.6E-02
1.2E-01	9.1E+00	1.4E-02	9.4E+00	3.8E-02	8.7E+00	8.4E-02	1.4E+00	8.4E-02
1.3E-01	1.1E+01	1.4E-02	1.2E+01	3.7E-02	1.1E+01	8.2E-02	1.7E+00	8.2E-02
1.4E-01	1.4E+01	1.4E-02	1.4E+01	3.6E-02	1.3E+01	8.0E-02	2.1E+00	8.0E-02
1.5E-01	1.6E+01	1.3E-02	1.7E+01	3.5E-02	1.6E+01	7.7E-02	2.5E+00	7.7E-02
1.6E-01	2.0E+01	1.3E-02	2.1E+01	3.4E-02	1.9E+01	7.5E-02	3.0E+00	7.5E-02
1.7E-01	2.3E+01	1.3E-02	2.5E+01	3.3E-02	2.3E+01	7.3E-02	3.6E+00	7.3E-02
1.8E-01	2.7E+01	1.2E-02	2.9E+01	3.2E-02	2.7E+01	7.1E-02	4.3E+00	7.1E-02
1.9E-01	3.2E+01	1.2E-02	3.4E+01	3.1E-02	3.2E+01	6.8E-02	5.1E+00	6.8E-02
2.0E-01	3.8E+01	1.2E-02	4.1E+01	3.0E-02	3.8E+01	6.6E-02	6.0E+00	6.6E-02
2.1E-01	4.4E+01	1.1E-02	4.8E+01	2.9E-02	4.5E+01	6.4E-02	7.1E+00	6.4E-02
2.2E-01	5.1E+01	1.1E-02	5.6E+01	2.8E-02	5.3E+01	6.2E-02	8.3E+00	6.2E-02
2.3E-01	5.9E+01	1.1E-02	6.5E+01	2.8E-02	6.2E+01	6.0E-02	9.7E+00	6.0E-02
2.4E-01	6.8E+01	1.0E-02	7.6E+01	2.7E-02	7.2E+01	5.7E-02	1.1E+01	5.7E-02
2.5E-01	7.8E+01	1.0E-02	8.8E+01	2.6E-02	8.5E+01	5.5E-02	1.3E+01	5.5E-02
2.6E-01	9.0E+01	9.6E-03	1.0E+02	2.5E-02	9.9E+01	5.3E-02	1.6E+01	5.3E-02
2.7E-01	1.0E+02	9.3E-03	1.2E+02	2.4E-02	1.2E+02	5.1E-02	1.8E+01	5.1E-02
2.8E-01	1.2E+02	9.0E-03	1.4E+02	2.3E-02	1.4E+02	4.9E-02	2.1E+01	4.9E-02
2.9E-01	1.4E+02	8.7E-03	1.6E+02	2.2E-02	1.6E+02	4.7E-02	2.5E+01	4.7E-02
3.0E-01	1.6E+02	8.3E-03	1.9E+02	2.1E-02	1.9E+02	4.4E-02	2.9E+01	4.4E-02
3.1E-01	1.8E+02	8.0E-03	2.2E+02	2.0E-02	2.2E+02	4.2E-02	3.4E+01	4.2E-02
3.2E-01	2.1E+02	7.7E-03	2.5E+02	1.9E-02	2.6E+02	4.0E-02	4.0E+01	4.0E-02
3.3E-01	2.4E+02	7.4E-03	3.0E+02	1.8E-02	3.0E+02	3.8E-02	4.7E+01	3.8E-02
3.4E-01	2.7E+02	7.1E-03	3.5E+02	1.7E-02	3.6E+02	3.6E-02	5.6E+01	3.6E-02
3.5E-01	3.1E+02	6.8E-03	4.1E+02	1.6E-02	4.2E+02	3.4E-02	6.6E+01	3.4E-02
3.6E-01	3.5E+02	6.5E-03	4.8E+02	1.5E-02	5.0E+02	3.2E-02	7.9E+01	3.2E-02
3.7E-01	4.0E+02	6.2E-03	5.6E+02	1.5E-02	6.1E+02	3.0E-02	9.5E+01	3.0E-02
3.8E-01	4.6E+02	5.9E-03	6.6E+02	1.4E-02	7.3E+02	2.8E-02	1.1E+02	2.8E-02
3.9E-01	5.3E+02	5.7E-03	7.8E+02	1.3E-02	8.8E+02	2.6E-02	1.4E+02	2.6E-02
4.0E-01	6.1E+02	5.4E-03	9.3E+02	1.2E-02	1.1E+03	2.4E-02	1.7E+02	2.4E-02
4.1E-01	7.0E+02	5.1E-03	1.1E+03	1.1E-02	1.3E+03	2.2E-02	2.1E+02	2.2E-02
4.2E-01	8.0E+02	4.9E-03	1.3E+03	1.1E-02	1.7E+03	2.0E-02	2.6E+02	2.0E-02
4.3E-01	9.2E+02	4.6E-03	1.6E+03	9.8E-03	2.1E+03	1.8E-02	3.2E+02	1.9E-02
4.4E-01	1.1E+03	4.4E-03	1.9E+03	9.1E-03	2.6E+03	1.7E-02	4.0E+02	1.7E-02

Table B.1 continued

Loading (moles CO_2 /mol amine)	1.0 M MEA (60°C)		2.5 M MEA (60°C)		5.0 M MEA(60°C)		5.0 M MEA (40°C)	
	P_{CO2} (Pa)	X_{MEA} (mole fraction)	P_{CO2} (Pa)	X_{MEA} (mole fraction)	P_{CO2} (Pa)	X_{MEA} (mole fraction)	P_{CO2} (Pa)	X_{MEA} (mole fraction)
4.5E-01	1.2E+03	4.2E-03	2.3E+03	8.4E-03	3.3E+03	1.5E-02	5.1E+02	1.5E-02
4.6E-01	1.4E+03	3.9E-03	2.8E+03	7.7E-03	4.3E+03	1.3E-02	6.6E+02	1.4E-02
4.9E-01	2.1E+03	3.3E-03	5.1E+03	6.0E-03	9.7E+03	9.3E-03	1.5E+03	9.5E-03
5.0E-01	2.4E+03	3.1E-03	6.2E+03	5.5E-03	1.3E+04	8.1E-03	1.9E+03	8.3E-03
5.1E-01	2.8E+03	2.9E-03	7.6E+03	5.0E-03	1.7E+04	7.1E-03	2.5E+03	7.3E-03
5.2E-01	3.2E+03	2.8E-03	9.3E+03	4.5E-03	2.2E+04	6.3E-03	3.3E+03	6.4E-03
5.3E-01	3.7E+03	2.6E-03	1.1E+04	4.2E-03	2.9E+04	5.5E-03	4.3E+03	5.7E-03
5.4E-01	4.2E+03	2.5E-03	1.4E+04	3.8E-03	3.8E+04	4.9E-03	5.5E+03	5.0E-03
5.5E-01	4.8E+03	2.3E-03	1.6E+04	3.5E-03	4.8E+04	4.3E-03	7.1E+03	4.4E-03
5.6E-01	5.5E+03	2.2E-03	2.0E+04	3.2E-03	6.1E+04	3.8E-03	8.9E+03	4.0E-03
5.7E-01	6.3E+03	2.0E-03	2.4E+04	2.9E-03	7.6E+04	3.4E-03	1.1E+04	3.5E-03
5.8E-01	7.1E+03	1.9E-03	2.8E+04	2.7E-03	9.4E+04	3.1E-03	1.4E+04	3.2E-03
5.9E-01	8.1E+03	1.8E-03	3.3E+04	2.5E-03	1.1E+05	2.8E-03	1.7E+04	2.9E-03
6.0E-01	9.2E+03	1.7E-03	3.9E+04	2.3E-03	1.4E+05	2.5E-03	2.1E+04	2.6E-03
6.1E-01	1.0E+04	1.6E-03	4.6E+04	2.1E-03	1.7E+05	2.3E-03	2.5E+04	2.3E-03
6.2E-01	1.2E+04	1.5E-03	5.3E+04	1.9E-03	2.0E+05	2.1E-03	3.0E+04	2.1E-03
6.3E-01	1.3E+04	1.4E-03	6.2E+04	1.8E-03	2.3E+05	1.9E-03	3.6E+04	2.0E-03
6.4E-01	1.5E+04	1.3E-03	7.2E+04	1.7E-03	2.7E+05	1.8E-03	4.2E+04	1.8E-03
6.5E-01	1.7E+04	1.2E-03	8.2E+04	1.5E-03	3.1E+05	1.7E-03	4.9E+04	1.6E-03
6.6E-01	1.9E+04	1.2E-03	9.4E+04	1.4E-03	3.6E+05	1.5E-03	5.7E+04	1.5E-03
6.7E-01	2.1E+04	1.1E-03	1.1E+05	1.3E-03	4.1E+05	1.4E-03	6.7E+04	1.4E-03
6.8E-01	2.4E+04	1.0E-03	1.2E+05	1.2E-03	4.7E+05	1.3E-03	7.7E+04	1.3E-03
6.9E-01	2.7E+04	9.7E-04	1.4E+05	1.2E-03	5.3E+05	1.2E-03	8.9E+04	1.2E-03
7.0E-01	3.0E+04	9.1E-04	1.6E+05	1.1E-03	5.9E+05	1.2E-03	-	-
7.1E-01	3.4E+04	8.6E-04	1.8E+05	1.0E-03	6.7E+05	1.1E-03	-	-
7.2E-01	3.7E+04	8.1E-04	2.0E+05	9.5E-04	7.4E+05	1.0E-03	-	-
7.3E-01	4.2E+04	7.6E-04	2.2E+05	9.0E-04	8.2E+05	9.7E-04	-	-
7.4E-01	4.6E+04	7.1E-04	2.5E+05	8.4E-04	9.1E+05	9.1E-04	-	-
7.5E-01	5.2E+04	6.7E-04	2.7E+05	7.9E-04	1.0E+06	8.6E-04	-	-
7.6E-01	5.7E+04	6.3E-04	3.0E+05	7.4E-04	1.1E+06	8.2E-04	-	-
7.7E-01	6.3E+04	5.9E-04	3.3E+05	7.0E-04	1.2E+06	7.8E-04	-	-
7.8E-01	7.0E+04	5.6E-04	3.7E+05	6.6E-04	1.3E+06	7.4E-04	-	-
7.9E-01	7.8E+04	5.2E-04	4.1E+05	6.2E-04	1.4E+06	7.0E-04	-	-
8.0E-01	8.6E+04	4.9E-04	4.5E+05	5.9E-04	1.5E+06	6.7E-04	-	-
8.1E-01	9.5E+04	4.6E-04	4.9E+05	5.6E-04	1.7E+06	6.4E-04	-	-
8.2E-01	1.0E+05	4.3E-04	5.3E+05	5.2E-04	1.8E+06	6.1E-04	-	-
8.3E-01	1.2E+05	4.0E-04	5.8E+05	5.0E-04	1.9E+06	5.8E-04	-	-
8.4E-01	1.3E+05	3.8E-04	6.3E+05	4.7E-04	2.1E+06	5.6E-04	-	-
8.5E-01	1.4E+05	3.6E-04	6.9E+05	4.5E-04	2.2E+06	5.3E-04	-	-
8.6E-01	1.5E+05	3.3E-04	7.4E+05	4.2E-04	2.4E+06	5.1E-04	-	-
8.7E-01	1.7E+05	3.1E-04	8.0E+05	4.0E-04	2.5E+06	4.9E-04	-	-
8.8E-01	1.9E+05	2.9E-04	8.7E+05	3.8E-04	2.7E+06	4.7E-04	-	-
8.9E-01	2.0E+05	2.7E-04	9.3E+05	3.6E-04	2.8E+06	4.6E-04	-	-
9.0E-01	2.2E+05	2.6E-04	1.0E+06	3.5E-04	3.0E+06	4.4E-04	-	-
9.1E-01	2.4E+05	2.4E-04	1.1E+06	3.3E-04	3.2E+06	4.2E-04	-	-

Table B.2 P_{CO2} and speciation in 0.4 M MEA/0.6 M PZ/H_2O systems at 60°C

Loading (moles CO_2/mol amine)	P_{CO2} (Pa)	X_{MEA} (mole fraction)	X_{PZ} (mole fraction)	X_{PZCOO^-} (mole fraction)
5.0E-02	2.1E+00	6.6E-03	1.1E-02	3.7E-04
6.0E-02	3.1E+00	6.5E-03	1.0E-02	4.5E-04
7.0E-02	4.3E+00	6.3E-03	1.0E-02	5.3E-04
8.0E-02	5.8E+00	6.1E-03	1.0E-02	6.2E-04
9.0E-02	7.6E+00	6.0E-03	9.9E-03	7.0E-04
1.0E-01	9.8E+00	5.8E-03	9.7E-03	7.9E-04
1.1E-01	1.2E+01	5.6E-03	9.5E-03	8.7E-04
1.2E-01	1.5E+01	5.5E-03	9.3E-03	9.5E-04
1.3E-01	1.9E+01	5.3E-03	9.1E-03	1.0E-03
1.4E-01	2.2E+01	5.2E-03	8.9E-03	1.1E-03
1.5E-01	2.7E+01	5.0E-03	8.8E-03	1.2E-03
1.6E-01	3.2E+01	4.9E-03	8.6E-03	1.3E-03
1.7E-01	3.7E+01	4.7E-03	8.4E-03	1.4E-03
1.8E-01	4.4E+01	4.6E-03	8.2E-03	1.4E-03
1.9E-01	5.1E+01	4.4E-03	8.0E-03	1.5E-03
2.0E-01	5.9E+01	4.3E-03	7.8E-03	1.6E-03
2.1E-01	6.7E+01	4.2E-03	7.6E-03	1.7E-03
2.2E-01	7.7E+01	4.0E-03	7.4E-03	1.7E-03
2.3E-01	8.8E+01	3.9E-03	7.3E-03	1.8E-03
2.4E-01	1.0E+02	3.8E-03	7.1E-03	1.9E-03
2.5E-01	1.1E+02	3.7E-03	6.9E-03	1.9E-03
2.6E-01	1.3E+02	3.5E-03	6.7E-03	2.0E-03
2.7E-01	1.5E+02	3.4E-03	6.5E-03	2.0E-03
2.8E-01	1.6E+02	3.3E-03	6.3E-03	2.1E-03
2.9E-01	1.8E+02	3.2E-03	6.2E-03	2.2E-03
3.0E-01	2.1E+02	3.1E-03	6.0E-03	2.2E-03
3.1E-01	2.3E+02	3.0E-03	5.8E-03	2.3E-03
3.2E-01	2.6E+02	2.9E-03	5.6E-03	2.3E-03
3.3E-01	2.9E+02	2.8E-03	5.4E-03	2.3E-03
3.4E-01	3.2E+02	2.7E-03	5.3E-03	2.4E-03
3.5E-01	3.6E+02	2.6E-03	5.1E-03	2.4E-03
3.6E-01	4.0E+02	2.5E-03	4.9E-03	2.5E-03
3.7E-01	4.4E+02	2.4E-03	4.7E-03	2.5E-03
3.8E-01	4.9E+02	2.3E-03	4.6E-03	2.5E-03
3.9E-01	5.4E+02	2.2E-03	4.4E-03	2.5E-03
4.0E-01	6.0E+02	2.2E-03	4.3E-03	2.6E-03
4.1E-01	6.7E+02	2.1E-03	4.1E-03	2.6E-03
4.2E-01	7.4E+02	2.0E-03	3.9E-03	2.6E-03
4.3E-01	8.2E+02	1.9E-03	3.8E-03	2.6E-03
4.4E-01	9.0E+02	1.8E-03	3.6E-03	2.6E-03
4.5E-01	1.0E+03	1.8E-03	3.5E-03	2.6E-03
4.6E-01	1.1E+03	1.7E-03	3.3E-03	2.6E-03
4.7E-01	1.2E+03	1.6E-03	3.2E-03	2.6E-03
4.8E-01	1.3E+03	1.6E-03	3.1E-03	2.6E-03
4.9E-01	1.5E+03	1.5E-03	2.9E-03	2.6E-03

Table B.2 continued

Loading (moles CO_2/mol amine)	P_{CO2} (Pa)	X_{MEA} (mole fraction)	X_{PZ} (mole fraction)	X_{PZCOO^-} (mole fraction)
5.0E-01	1.6E+03	1.4E-03	2.8E-03	2.6E-03
5.1E-01	1.8E+03	1.4E-03	2.7E-03	2.6E-03
5.2E-01	2.0E+03	1.3E-03	2.5E-03	2.6E-03
5.3E-01	2.2E+03	1.3E-03	2.4E-03	2.5E-03
5.4E-01	2.4E+03	1.2E-03	2.3E-03	2.5E-03
5.5E-01	2.7E+03	1.2E-03	2.2E-03	2.5E-03
5.6E-01	2.9E+03	1.1E-03	2.1E-03	2.5E-03
5.7E-01	3.3E+03	1.1E-03	2.0E-03	2.4E-03
5.8E-01	3.6E+03	1.0E-03	1.9E-03	2.4E-03
5.9E-01	4.0E+03	9.6E-04	1.8E-03	2.3E-03
6.0E-01	4.4E+03	9.2E-04	1.7E-03	2.3E-03
6.1E-01	4.8E+03	8.7E-04	1.6E-03	2.3E-03
6.2E-01	5.3E+03	8.3E-04	1.5E-03	2.2E-03
6.3E-01	5.9E+03	7.9E-04	1.4E-03	2.2E-03
6.4E-01	6.5E+03	7.5E-04	1.3E-03	2.1E-03
6.5E-01	7.2E+03	7.1E-04	1.3E-03	2.1E-03
6.6E-01	7.9E+03	6.8E-04	1.2E-03	2.0E-03
6.7E-01	8.7E+03	6.4E-04	1.1E-03	2.0E-03
6.8E-01	9.7E+03	6.1E-04	1.0E-03	1.9E-03
6.9E-01	1.1E+04	5.8E-04	9.7E-04	1.8E-03
7.0E-01	1.2E+04	5.5E-04	9.1E-04	1.8E-03
7.1E-01	1.3E+04	5.2E-04	8.5E-04	1.7E-03
7.2E-01	1.5E+04	4.9E-04	7.9E-04	1.7E-03
7.3E-01	1.6E+04	4.6E-04	7.4E-04	1.6E-03
7.4E-01	1.8E+04	4.3E-04	6.8E-04	1.5E-03
7.5E-01	2.0E+04	4.1E-04	6.4E-04	1.5E-03
7.6E-01	2.2E+04	3.8E-04	5.9E-04	1.4E-03
7.7E-01	2.4E+04	3.6E-04	5.5E-04	1.4E-03
7.8E-01	2.7E+04	3.4E-04	5.1E-04	1.3E-03
7.9E-01	3.0E+04	3.2E-04	4.7E-04	1.2E-03
8.0E-01	3.4E+04	3.0E-04	4.3E-04	1.2E-03
8.1E-01	3.7E+04	2.8E-04	4.0E-04	1.1E-03
8.2E-01	4.2E+04	2.6E-04	3.7E-04	1.1E-03
8.3E-01	4.7E+04	2.4E-04	3.4E-04	9.9E-04
8.4E-01	5.2E+04	2.2E-04	3.1E-04	9.3E-04
8.5E-01	5.8E+04	2.1E-04	2.8E-04	8.8E-04
8.6E-01	6.5E+04	1.9E-04	2.6E-04	8.2E-04
8.7E-01	7.3E+04	1.8E-04	2.3E-04	7.7E-04
8.8E-01	8.2E+04	1.6E-04	2.1E-04	7.2E-04
8.9E-01	9.2E+04	1.5E-04	1.9E-04	6.7E-04

Table B.3 P_{CO2} and speciation in 1.9 M MEA/0.6 M PZ/H_2O systems at 60°C

Loading (moles CO_2/mol amine)	P_{CO2} (Pa)	X_{MEA} (mole fraction)	X_{PZ} (mole fraction)	X_{PZCOO^-} (mole fraction)
5.0E-02	1.5E+00	3.5E-02	1.1E-02	4.1E-04
6.0E-02	2.2E+00	3.4E-02	1.1E-02	5.1E-04
7.0E-02	3.1E+00	3.3E-02	1.1E-02	6.0E-04
8.0E-02	4.3E+00	3.2E-02	1.1E-02	6.9E-04
9.0E-02	5.6E+00	3.1E-02	1.1E-02	7.9E-04
1.0E-01	7.3E+00	3.0E-02	1.1E-02	8.8E-04
1.1E-01	9.2E+00	3.0E-02	1.0E-02	9.8E-04
1.2E-01	1.1E+01	2.9E-02	1.0E-02	1.1E-03
1.3E-01	1.4E+01	2.8E-02	1.0E-02	1.2E-03
1.4E-01	1.7E+01	2.7E-02	9.8E-03	1.3E-03
1.5E-01	2.1E+01	2.6E-02	9.6E-03	1.4E-03
1.6E-01	2.5E+01	2.6E-02	9.4E-03	1.5E-03
1.7E-01	3.0E+01	2.5E-02	9.2E-03	1.6E-03
1.8E-01	3.5E+01	2.4E-02	9.0E-03	1.7E-03
1.9E-01	4.1E+01	2.3E-02	8.7E-03	1.8E-03
2.0E-01	4.8E+01	2.3E-02	8.5E-03	1.9E-03
2.1E-01	5.6E+01	2.2E-02	8.3E-03	2.0E-03
2.2E-01	6.6E+01	2.1E-02	8.1E-03	2.0E-03
2.3E-01	7.6E+01	2.0E-02	7.9E-03	2.1E-03
2.4E-01	8.8E+01	2.0E-02	7.6E-03	2.2E-03
2.5E-01	1.0E+02	1.9E-02	7.4E-03	2.3E-03
2.6E-01	1.2E+02	1.8E-02	7.2E-03	2.4E-03
2.7E-01	1.4E+02	1.8E-02	6.9E-03	2.5E-03
2.8E-01	1.6E+02	1.7E-02	6.7E-03	2.6E-03
2.9E-01	1.8E+02	1.6E-02	6.5E-03	2.7E-03
3.0E-01	2.0E+02	1.6E-02	6.2E-03	2.8E-03
3.1E-01	2.3E+02	1.5E-02	6.0E-03	2.8E-03
3.2E-01	2.7E+02	1.4E-02	5.8E-03	2.9E-03
3.3E-01	3.1E+02	1.4E-02	5.5E-03	3.0E-03
3.4E-01	3.5E+02	1.3E-02	5.3E-03	3.0E-03
3.5E-01	4.1E+02	1.3E-02	5.1E-03	3.1E-03
3.6E-01	4.6E+02	1.2E-02	4.8E-03	3.2E-03
3.7E-01	5.3E+02	1.1E-02	4.6E-03	3.2E-03
3.8E-01	6.1E+02	1.1E-02	4.4E-03	3.3E-03
3.9E-01	7.0E+02	1.0E-02	4.1E-03	3.3E-03
4.0E-01	8.1E+02	9.8E-03	3.9E-03	3.3E-03
4.1E-01	9.3E+02	9.3E-03	3.7E-03	3.3E-03
4.2E-01	1.1E+03	8.8E-03	3.5E-03	3.4E-03
4.3E-01	1.2E+03	8.3E-03	3.3E-03	3.4E-03
4.4E-01	1.4E+03	7.9E-03	3.0E-03	3.4E-03
4.5E-01	1.7E+03	7.4E-03	2.8E-03	3.4E-03
4.6E-01	1.9E+03	7.0E-03	2.6E-03	3.3E-03
4.6E-01	1.9E+03	7.0E-03	2.6E-03	3.3E-03
4.7E-01	2.2E+03	6.6E-03	2.5E-03	3.3E-03
4.8E-01	2.6E+03	6.1E-03	2.3E-03	3.3E-03

Table B.3 continued

Loading (moles CO_2/mol amine)	P_{CO2} (Pa)	X_{MEA} (mole fraction)	X_{PZ} (mole fraction)	X_{PZCOO^-} (mole fraction)
4.9E-01	3.0E+03	5.8E-03	2.1E-03	3.2E-03
5.0E-01	3.5E+03	5.4E-03	1.9E-03	3.2E-03
5.1E-01	4.0E+03	5.0E-03	1.8E-03	3.1E-03
5.2E-01	4.7E+03	4.7E-03	1.6E-03	3.1E-03
5.3E-01	5.5E+03	4.4E-03	1.5E-03	3.0E-03
5.4E-01	6.4E+03	4.1E-03	1.3E-03	2.9E-03
5.5E-01	7.5E+03	3.8E-03	1.2E-03	2.8E-03
5.6E-01	8.8E+03	3.5E-03	1.1E-03	2.7E-03
5.7E-01	1.0E+04	3.3E-03	1.0E-03	2.6E-03
5.8E-01	1.2E+04	3.0E-03	9.0E-04	2.6E-03
5.9E-01	1.4E+04	2.8E-03	8.1E-04	2.5E-03
6.0E-01	1.6E+04	2.6E-03	7.3E-04	2.3E-03
6.1E-01	1.9E+04	2.4E-03	6.5E-04	2.2E-03
6.2E-01	2.2E+04	2.2E-03	5.8E-04	2.1E-03
6.3E-01	2.6E+04	2.1E-03	5.2E-04	2.0E-03
6.4E-01	3.0E+04	1.9E-03	4.7E-04	1.9E-03
6.5E-01	3.5E+04	1.8E-03	4.2E-04	1.8E-03
6.6E-01	4.1E+04	1.6E-03	3.7E-04	1.7E-03
6.7E-01	4.7E+04	1.5E-03	3.3E-04	1.7E-03
6.8E-01	5.4E+04	1.4E-03	3.0E-04	1.6E-03
6.9E-01	6.3E+04	1.3E-03	2.7E-04	1.5E-03
7.0E-01	7.2E+04	1.2E-03	2.4E-04	1.4E-03
7.1E-01	8.2E+04	1.1E-03	2.2E-04	1.3E-03
7.2E-01	9.4E+04	1.0E-03	1.9E-04	1.2E-03
7.3E-01	1.1E+05	9.7E-04	1.7E-04	1.2E-03
7.4E-01	1.2E+05	9.0E-04	1.6E-04	1.1E-03
7.5E-01	1.4E+05	8.4E-04	1.4E-04	1.0E-03
7.6E-01	1.6E+05	7.8E-04	1.3E-04	9.7E-04
7.7E-01	1.8E+05	7.3E-04	1.2E-04	9.1E-04
7.8E-01	2.0E+05	6.8E-04	1.0E-04	8.6E-04
7.9E-01	2.3E+05	6.3E-04	9.5E-05	8.0E-04
8.0E-01	2.5E+05	5.9E-04	8.6E-05	7.6E-04
8.1E-01	2.8E+05	5.5E-04	7.8E-05	7.1E-04
8.2E-01	3.2E+05	5.1E-04	7.1E-05	6.7E-04
8.3E-01	3.5E+05	4.8E-04	6.5E-05	6.3E-04
8.4E-01	3.9E+05	4.5E-04	5.9E-05	5.9E-04
8.5E-01	4.3E+05	4.2E-04	5.4E-05	5.5E-04
8.6E-01	4.8E+05	3.9E-04	4.9E-05	5.2E-04
8.7E-01	5.3E+05	3.7E-04	4.5E-05	4.9E-04
8.8E-01	5.8E+05	3.5E-04	4.2E-05	4.6E-04
8.9E-01	6.4E+05	3.2E-04	3.8E-05	4.3E-04

Table B.4 P_{CO2} and speciation in 3.8 M MEA/1.2 M PZ/H_2O systems at 60°C

Loading (moles CO_2/mol amine)	P_{CO2} (Pa)	X_{MEA} (mole fraction)	X_{PZ} (mole fraction)	X_{PZCOO^-} (mole fraction)
5.00E-02	1.35E+00	8.02E-02	2.66E-02	1.03E-03
6.00E-02	2.03E+00	7.82E-02	2.61E-02	1.25E-03
7.00E-02	2.88E+00	7.62E-02	2.57E-02	1.47E-03
8.00E-02	3.93E+00	7.42E-02	2.52E-02	1.69E-03
9.00E-02	5.21E+00	7.22E-02	2.48E-02	1.92E-03
1.00E-01	6.73E+00	7.02E-02	2.43E-02	2.14E-03
1.10E-01	8.55E+00	6.83E-02	2.39E-02	2.37E-03
1.20E-01	1.07E+01	6.64E-02	2.34E-02	2.60E-03
1.30E-01	1.32E+01	6.44E-02	2.29E-02	2.83E-03
1.40E-01	1.61E+01	6.25E-02	2.24E-02	3.06E-03
1.50E-01	1.94E+01	6.07E-02	2.19E-02	3.29E-03
1.60E-01	2.33E+01	5.88E-02	2.14E-02	3.53E-03
1.70E-01	2.78E+01	5.70E-02	2.09E-02	3.76E-03
1.80E-01	3.30E+01	5.51E-02	2.04E-02	3.99E-03
1.90E-01	3.89E+01	5.33E-02	1.99E-02	4.22E-03
2.00E-01	4.56E+01	5.16E-02	1.94E-02	4.45E-03
2.10E-01	5.34E+01	4.98E-02	1.89E-02	4.68E-03
2.20E-01	6.23E+01	4.81E-02	1.83E-02	4.90E-03
2.30E-01	7.25E+01	4.63E-02	1.78E-02	5.13E-03
2.40E-01	8.42E+01	4.46E-02	1.72E-02	5.35E-03
2.50E-01	9.75E+01	4.30E-02	1.67E-02	5.56E-03
2.60E-01	1.13E+02	4.13E-02	1.61E-02	5.78E-03
2.70E-01	1.30E+02	3.97E-02	1.56E-02	5.99E-03
2.80E-01	1.50E+02	3.81E-02	1.50E-02	6.19E-03
2.90E-01	1.74E+02	3.65E-02	1.44E-02	6.39E-03
3.00E-01	2.00E+02	3.50E-02	1.39E-02	6.58E-03
3.10E-01	2.31E+02	3.34E-02	1.33E-02	6.76E-03
3.20E-01	2.66E+02	3.19E-02	1.27E-02	6.93E-03
3.30E-01	3.07E+02	3.05E-02	1.22E-02	7.09E-03
3.40E-01	3.55E+02	2.90E-02	1.16E-02	7.24E-03
3.50E-01	4.10E+02	2.76E-02	1.10E-02	7.38E-03
3.60E-01	4.74E+02	2.62E-02	1.05E-02	7.51E-03
3.70E-01	5.49E+02	2.49E-02	9.89E-03	7.62E-03
3.80E-01	6.36E+02	2.35E-02	9.33E-03	7.71E-03
3.90E-01	7.39E+02	2.22E-02	8.78E-03	7.79E-03
4.00E-01	8.60E+02	2.10E-02	8.23E-03	7.85E-03
4.10E-01	1.00E+03	1.98E-02	7.69E-03	7.89E-03
4.20E-01	1.17E+03	1.86E-02	7.16E-03	7.91E-03
4.30E-01	1.37E+03	1.74E-02	6.64E-03	7.91E-03
4.40E-01	1.61E+03	1.63E-02	6.14E-03	7.88E-03
4.50E-01	1.90E+03	1.52E-02	5.64E-03	7.83E-03
4.60E-01	2.25E+03	1.42E-02	5.17E-03	7.75E-03
4.70E-01	2.67E+03	1.32E-02	4.71E-03	7.65E-03
4.80E-01	3.17E+03	1.22E-02	4.27E-03	7.52E-03
4.90E-01	3.79E+03	1.13E-02	3.86E-03	7.37E-03

Table B.4 continued

Loading (moles CO_2/mol amine)	P_{CO2} (Pa)	X_{MEA} (mole fraction)	X_{PZ} (mole fraction)	X_{PZCOO^-} (mole fraction)
5.00E-01	4.54E+03	1.04E-02	3.46E-03	7.19E-03
5.10E-01	5.47E+03	9.56E-03	3.09E-03	6.99E-03
5.20E-01	6.61E+03	8.76E-03	2.74E-03	6.76E-03
5.30E-01	8.01E+03	8.01E-03	2.42E-03	6.51E-03
5.40E-01	9.75E+03	7.31E-03	2.12E-03	6.24E-03
5.50E-01	1.19E+04	6.65E-03	1.85E-03	5.96E-03
5.60E-01	1.46E+04	6.04E-03	1.60E-03	5.66E-03
5.70E-01	1.79E+04	5.47E-03	1.39E-03	5.36E-03
5.80E-01	2.20E+04	4.94E-03	1.19E-03	5.05E-03
5.90E-01	2.71E+04	4.47E-03	1.02E-03	4.73E-03
6.00E-01	3.33E+04	4.03E-03	8.71E-04	4.43E-03
6.10E-01	4.10E+04	3.63E-03	7.42E-04	4.12E-03
6.20E-01	5.03E+04	3.28E-03	6.31E-04	3.83E-03
6.30E-01	6.16E+04	2.96E-03	5.37E-04	3.55E-03
6.40E-01	7.51E+04	2.67E-03	4.57E-04	3.29E-03
6.50E-01	9.13E+04	2.41E-03	3.90E-04	3.04E-03
6.60E-01	1.10E+05	2.19E-03	3.33E-04	2.81E-03
6.70E-01	1.33E+05	1.99E-03	2.85E-04	2.60E-03
6.80E-01	1.59E+05	1.81E-03	2.45E-04	2.40E-03
6.90E-01	1.89E+05	1.65E-03	2.12E-04	2.22E-03
7.00E-01	2.23E+05	1.50E-03	1.84E-04	2.05E-03
7.10E-01	2.62E+05	1.38E-03	1.60E-04	1.90E-03
7.20E-01	3.06E+05	1.27E-03	1.40E-04	1.76E-03
7.30E-01	3.56E+05	1.16E-03	1.23E-04	1.64E-03
7.40E-01	4.11E+05	1.07E-03	1.08E-04	1.52E-03
7.50E-01	4.72E+05	9.94E-04	9.58E-05	1.42E-03
7.60E-01	5.39E+05	9.21E-04	8.53E-05	1.32E-03
7.70E-01	6.12E+05	8.56E-04	7.62E-05	1.24E-03
7.80E-01	6.91E+05	7.97E-04	6.83E-05	1.16E-03
7.90E-01	7.78E+05	7.44E-04	6.15E-05	1.08E-03
8.00E-01	8.71E+05	6.95E-04	5.56E-05	1.02E-03
8.20E-01	1.08E+06	6.11E-04	4.60E-05	9.00E-04
8.30E-01	1.19E+06	5.75E-04	4.20E-05	8.49E-04
8.40E-01	1.31E+06	5.42E-04	3.85E-05	8.01E-04
8.50E-01	1.44E+06	5.11E-04	3.54E-05	7.58E-04
8.60E-01	1.57E+06	4.83E-04	3.27E-05	7.18E-04
8.70E-01	1.71E+06	4.58E-04	3.02E-05	6.81E-04
8.80E-01	1.86E+06	4.34E-04	2.80E-05	6.47E-04

Table B.5 P_{CO2} and speciation in 3.8 M MEA/1.2 M PZ/H_2O systems at 40°C

Loading (moles CO_2 /mol amine)	P_{CO2} (Pa)	X_{MEA} (mole fraction)	X_{PZ} (mole fraction)	X_{PZCOO^-} (mole fraction)	X_{MEA} (mole fraction)	X_{PZCOO^-} (mole fraction)
5.0E-02	1.6E-01	8.1E-02	2.6E-02	2.2E-03	6.2E-03	1.7E-05
6.0E-02	2.4E-01	7.9E-02	2.5E-02	2.6E-03	7.3E-03	2.4E-05
7.0E-02	3.4E-01	7.7E-02	2.5E-02	3.1E-03	8.4E-03	3.3E-05
8.0E-02	4.6E-01	7.5E-02	2.4E-02	3.5E-03	9.5E-03	4.4E-05
9.0E-02	6.0E-01	7.4E-02	2.3E-02	4.0E-03	1.1E-02	5.7E-05
1.0E-01	7.8E-01	7.2E-02	2.3E-02	4.4E-03	1.2E-02	7.1E-05
1.1E-01	9.8E-01	7.0E-02	2.2E-02	4.8E-03	1.3E-02	8.8E-05
1.2E-01	1.2E+00	6.8E-02	2.2E-02	5.3E-03	1.4E-02	1.1E-04
1.3E-01	1.5E+00	6.6E-02	2.1E-02	5.7E-03	1.5E-02	1.3E-04
1.4E-01	1.8E+00	6.5E-02	2.0E-02	6.1E-03	1.6E-02	1.5E-04
1.5E-01	2.2E+00	6.3E-02	2.0E-02	6.5E-03	1.7E-02	1.7E-04
1.6E-01	2.6E+00	6.1E-02	1.9E-02	6.9E-03	1.8E-02	2.0E-04
1.7E-01	3.1E+00	6.0E-02	1.9E-02	7.2E-03	1.9E-02	2.3E-04
1.8E-01	3.6E+00	5.8E-02	1.8E-02	7.6E-03	2.0E-02	2.6E-04
1.9E-01	4.3E+00	5.6E-02	1.8E-02	8.0E-03	2.1E-02	3.0E-04
2.0E-01	5.0E+00	5.5E-02	1.7E-02	8.3E-03	2.2E-02	3.4E-04
2.1E-01	5.8E+00	5.3E-02	1.6E-02	8.6E-03	2.3E-02	3.8E-04
2.2E-01	6.7E+00	5.1E-02	1.6E-02	9.0E-03	2.4E-02	4.2E-04
2.3E-01	7.7E+00	5.0E-02	1.5E-02	9.3E-03	2.5E-02	4.7E-04
2.4E-01	8.9E+00	4.8E-02	1.5E-02	9.6E-03	2.6E-02	5.2E-04
2.5E-01	1.0E+01	4.6E-02	1.4E-02	9.8E-03	2.7E-02	5.8E-04
2.6E-01	1.2E+01	4.5E-02	1.4E-02	1.0E-02	2.8E-02	6.4E-04
2.7E-01	1.3E+01	4.3E-02	1.3E-02	1.0E-02	2.9E-02	7.0E-04
2.8E-01	1.5E+01	4.2E-02	1.2E-02	1.1E-02	3.0E-02	7.7E-04
2.9E-01	1.8E+01	4.0E-02	1.2E-02	1.1E-02	3.1E-02	8.4E-04
3.0E-01	2.0E+01	3.9E-02	1.1E-02	1.1E-02	3.2E-02	9.1E-04
3.1E-01	2.3E+01	3.7E-02	1.1E-02	1.1E-02	3.3E-02	1.0E-03
3.2E-01	2.6E+01	3.6E-02	1.0E-02	1.1E-02	3.4E-02	1.1E-03
3.3E-01	3.0E+01	3.4E-02	9.8E-03	1.1E-02	3.5E-02	1.2E-03
3.4E-01	3.4E+01	3.3E-02	9.3E-03	1.2E-02	3.6E-02	1.3E-03
3.5E-01	3.9E+01	3.1E-02	8.8E-03	1.2E-02	3.7E-02	1.4E-03
3.6E-01	4.5E+01	3.0E-02	8.3E-03	1.2E-02	3.8E-02	1.5E-03
3.7E-01	5.1E+01	2.9E-02	7.8E-03	1.2E-02	3.9E-02	1.6E-03
3.8E-01	5.9E+01	2.7E-02	7.3E-03	1.2E-02	4.0E-02	1.7E-03
3.9E-01	6.7E+01	2.6E-02	6.9E-03	1.2E-02	4.1E-02	1.9E-03
4.0E-01	7.8E+01	2.5E-02	6.4E-03	1.2E-02	4.2E-02	2.0E-03
4.1E-01	9.0E+01	2.3E-02	5.9E-03	1.2E-02	4.3E-02	2.1E-03
4.2E-01	1.0E+02	2.2E-02	5.5E-03	1.2E-02	4.4E-02	2.3E-03
4.3E-01	1.2E+02	2.1E-02	5.1E-03	1.1E-02	4.5E-02	2.5E-03
4.4E-01	1.4E+02	2.0E-02	4.7E-03	1.1E-02	4.6E-02	2.6E-03
4.5E-01	1.6E+02	1.8E-02	4.3E-03	1.1E-02	4.7E-02	2.8E-03
4.6E-01	1.9E+02	1.7E-02	3.9E-03	1.1E-02	4.7E-02	3.0E-03
4.7E-01	2.3E+02	1.6E-02	3.5E-03	1.1E-02	4.8E-02	3.2E-03
4.8E-01	2.7E+02	1.5E-02	3.2E-03	1.0E-02	4.9E-02	3.4E-03
4.9E-01	3.2E+02	1.4E-02	2.8E-03	1.0E-02	5.0E-02	3.6E-03

Table B.5 continued

Loading (moles CO_2 /mol amine)	P_{CO2} (Pa)	X_{MEA} (mole fraction)	X_{PZ} (mole fraction)	X_{PZCOO^-} (mole fraction)	X_{MEA} (mole fraction)	X_{PZCOO^-} (mole fraction)
5.0E-01	3.8E+02	1.3E-02	2.5E-03	9.8E-03	5.1E-02	3.9E-03
5.1E-01	4.6E+02	1.2E-02	2.2E-03	9.4E-03	5.2E-02	4.1E-03
5.2E-01	5.6E+02	1.1E-02	2.0E-03	9.1E-03	5.3E-02	4.4E-03
5.3E-01	6.8E+02	9.8E-03	1.7E-03	8.6E-03	5.3E-02	4.7E-03
5.4E-01	8.4E+02	8.9E-03	1.5E-03	8.2E-03	5.4E-02	4.9E-03
5.5E-01	1.0E+03	8.1E-03	1.2E-03	7.7E-03	5.5E-02	5.2E-03
5.6E-01	1.3E+03	7.2E-03	1.1E-03	7.2E-03	5.6E-02	5.5E-03
5.7E-01	1.7E+03	6.5E-03	8.8E-04	6.7E-03	5.7E-02	5.9E-03
5.8E-01	2.1E+03	5.7E-03	7.3E-04	6.2E-03	5.8E-02	6.2E-03
5.9E-01	2.7E+03	5.1E-03	6.0E-04	5.7E-03	5.8E-02	6.5E-03
6.0E-01	3.5E+03	4.5E-03	4.9E-04	5.2E-03	5.9E-02	6.9E-03
6.1E-01	4.6E+03	3.9E-03	3.9E-04	4.7E-03	6.0E-02	7.2E-03
6.2E-01	6.0E+03	3.4E-03	3.2E-04	4.3E-03	6.1E-02	7.6E-03
6.8E-01	2.7E+04	1.5E-03	8.9E-05	2.3E-03	6.5E-02	9.7E-03
6.9E-01	3.4E+04	1.4E-03	7.4E-05	2.1E-03	6.6E-02	1.0E-02
7.0E-01	4.2E+04	1.2E-03	6.1E-05	1.9E-03	6.6E-02	1.0E-02
7.1E-01	5.2E+04	1.1E-03	5.2E-05	1.7E-03	6.7E-02	1.1E-02
7.2E-01	6.3E+04	9.5E-04	4.4E-05	1.6E-03	6.7E-02	1.1E-02
7.3E-01	7.7E+04	8.5E-04	3.7E-05	1.4E-03	6.8E-02	1.1E-02
7.5E-01	1.1E+05	6.9E-04	2.7E-05	1.2E-03	6.9E-02	1.2E-02
7.6E-01	1.3E+05	6.2E-04	2.4E-05	1.1E-03	7.0E-02	1.3E-02
7.7E-01	1.5E+05	5.6E-04	2.1E-05	1.0E-03	7.0E-02	1.3E-02
8.0E-01	2.5E+05	4.2E-04	1.4E-05	8.2E-04	7.2E-02	1.4E-02

Appendix C

Contributions of Important Species to CO_2 Total Absorption Rate

Speciation of amine solution plays a very important role in CO_2 absorption rate. This section compares the contributions of three important species in MEA/PZ blends, (MEA, PZ, and $PZCOO^-$), to the total absorption rate. The rate fraction of each species is calculated as:

$$\text{rate fraction of species } i = k_i[i]/(k_{MEA}[MEA]+k_{PZ}[PZ]+k_{PZCOO^-}[PZCOO^-])$$

where, as before, k_{MEA}=3.37E4 L/mol, k_{PZ}=2.23E5 L/mol at 60°C and k_{MEA}=1.30E4 L/mol, k_{PZ}=1.03E5 L/mol at 40°C. k_{PZCOO^-} is equal to one fourth of k_{PZ} at each temperature. [i] is the concentration of each species in M or mole fraction, which is based on the speciation predicted by the VLE model of this work.

Figure C.1 shows the rate fractions of MEA, PZ, and $PZCOO^-$ in 0.4 M MEA/0.6 M PZ at 60°C. Because PZ accounts for 60% of total amine and its rate constant is much higher than the other two, PZ dominates the absorption rate over the loading from 0 to 0.9 mol CO_2/mol amine. MEA has no significant contribution to the total rate. Figures C.2 to C.4 show the rate fractions of MEA, PZ, and $PZCOO^-$ in MEA blends with 24 % PZ at 60°C and 40°C respectively. At loading lower than 0.5, PZ dominates the absorption rate and at loading higher than 0.6, $PZCOO^-$ becomes dominant. MEA has significant contribution to the rate, but never the most important one.

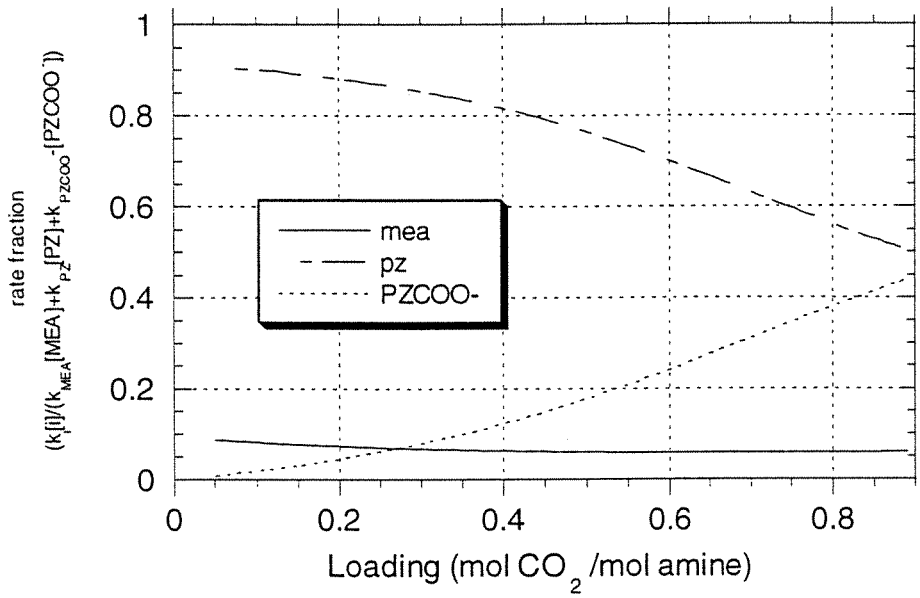

Figure C.1. CO_2 absorption rate contribution of MEA, PZ and $PZCOO^-$ in 0.4 M MEA/0.6 M PZ at 60°C.

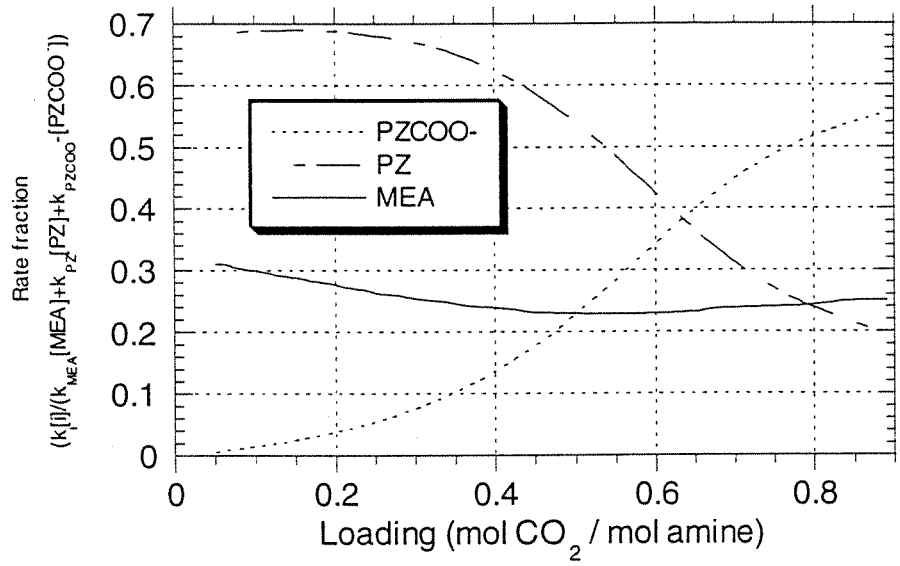

Figure C.2. CO_2 absorption rate contribution of MEA, PZ and $PZCOO^-$ in 1.9 M MEA/0.6 M PZ at 60°C.

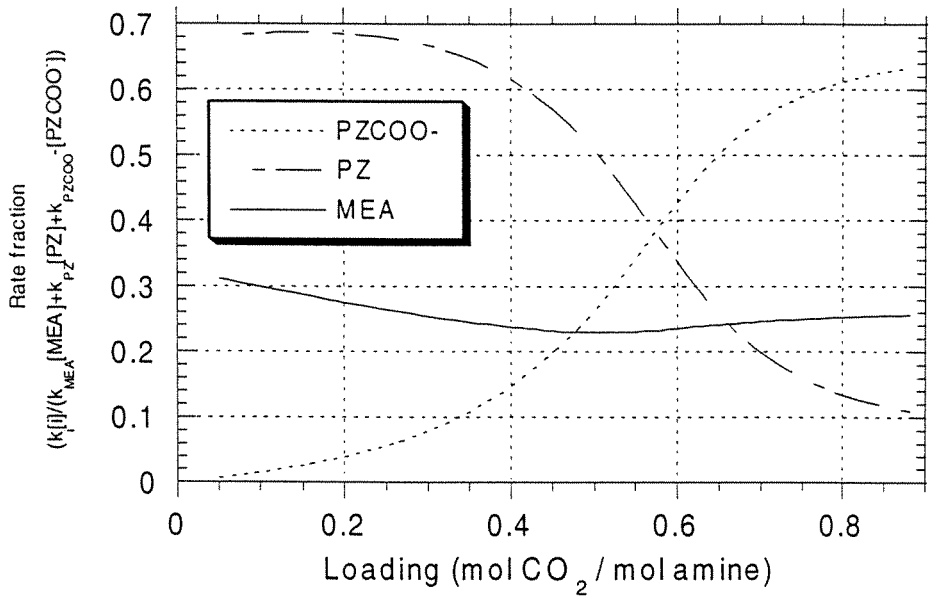

Figure C.3. CO_2 absorption rate contribution of MEA, PZ and $PZCOO^-$ in 3.8 M MEA/1.2 M PZ at 60°C.

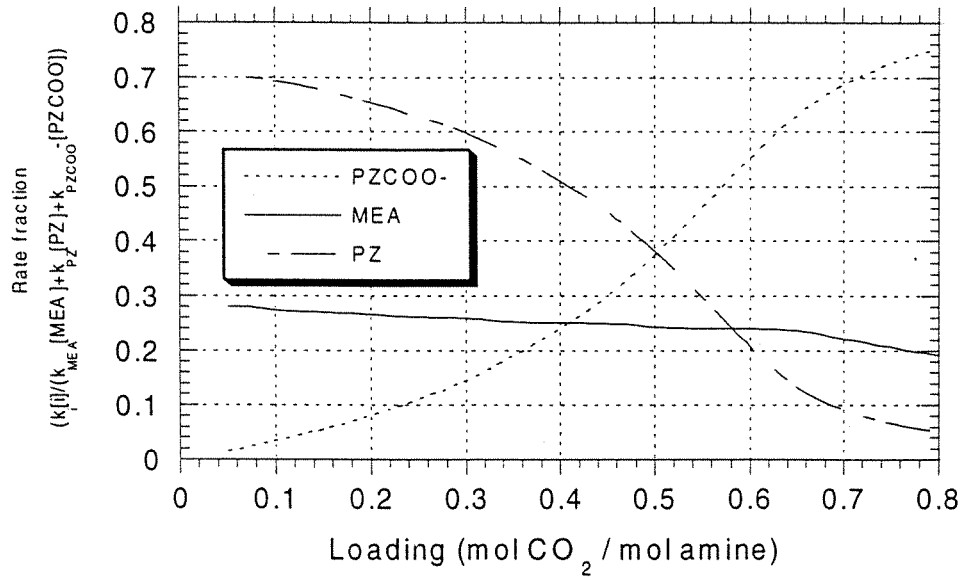

Figure C.4. CO_2 absorption rate contribution of MEA, PZ and $PZCOO^-$ in 3.8 M MEA/1.2 M PZ at 40°C.

Appendix D

Calibrations of Mass Flow Rate Controllers

Table D. Calibrations of mass flow rate controllers

Size	Series Number	Calibration Gas	Relationship Y, flow rate/(mole/s) X, opening percentage*100
20L	8708HCO33980	N_2	Y=1.4694E(-4)X + 1.4880E(-4)
15L	9310HCO38402	N_2	Y=1.3839E(-4) X– 3.4551E(-4)
1L	8707HCO3315	N_2	Y=7.5509E(-6)X – 5.8661E(-7)
100cc	8507HCO27519	N_2	Y=5.3381E(-7)X – 9.8241E(-7)

Appendix E

Detailed Experimental Results

This section tabulates the detailed experimental data. They consist of CO_2 solubility, absorption rate, and other important variables, such as percentage absorption of CO_2, gas film resistance, and approach to equilibrium.

In these tables, the first two or three points were measured near equilibrium to get CO_2 solubility data. The others are the raw data for absorption rate. In each series of rate data, flux was plotted versus liquid driving force to form a straight line. The normalized flux k_G' is equal to the slope of the straight line. By using eq. 4.25, E can be calculated and has been listed in table 4.3.

During the rate measurement, CO_2 loading and its equilibrium partial pressure change from the measured solubility data. Generally, eq. 4.27 was used to calculate P_{CO2}*. There are five series of rate data whose P_{CO2}* are calculated by eq. 4.28. The parameter "a" in that equation is listed in the corresponding tables.

In the tables, $(P_{CO2}-P_{CO2,i}) / (P_{CO2}-P_{CO2}*)$ is the gas film resistance. Where, P_{CO2} is the log mean CO_2 partial pressure in the gas phase, $P_{CO2,i}$ is the CO_2 partial pressure at the liquid-gas interface, and the P_{CO2}* is the equilibrium partial pressure of CO_2 at specific CO_2 loading. The gas film resistance can also be expressed as $k_G/k_g=(P_{CO2}-P_{CO2,i})/(P_{CO2}-P_{CO2}*)$, which is useful for the calculation of $P_{CO2,i}$. In the work, the range of the gas film resistance is from 14%-73%. For example, for the

CO_2 absorption in 2.5 M MEA at 60°C (table E.8), the percentage of gas film resistance is about 20%. If assuming the measurement has 5% error, the calculated $P_{CO2,i}$ will have a maximum error of 10%. While, if the gas film resistance is about 70% (table E.1, CO_2 absorption in 0.4 M MEA/0.6 M PZ, 60°C), the calculated $P_{CO2,i}$ will have a maximum error of 35%. When the gas film resistance is very high, it is the diffusion of CO_2 in the gas film that dominates the absorption rate, and CO_2 absorption rate with chemical reactions cannot be derived by the experimental data correctly.

$P_{CO2}^*/P_{CO2,i}$ is a variable that can be used to indicate the approach to equilibrium. When it is equal to zero, it means the absorption is far away from the equilibrium. When it is equal to one, the absorption is at equilibrium and the data cannot be used as rate data. In this work, $P_{CO2}^*/P_{CO2,i}$ ranges from 0.004 to 0.74. For example, in the experiment of CO_2 absorption in 2.5 M MEA at loading of 0.66 and 60°C (table E.8), $P_{CO2}^*/P_{CO2,i}$ is equal to 0.74. If assuming 5% error for $P_{CO2,i}$, and P_{CO2}^*, the maximum error of k_G' will be 60%.

$(P_{CO2,in}-P_{CO2,out}) / P_{CO2,in}$ is the fraction of absorbed CO_2 over the input CO_2. Where, "in" and "out" means input and output of the wetted wall column. It indicates the possible error in the flux measurement. In this work the percentage removal of CO_2 is from 5.9% to 53.9%. For example, in the experiment of CO_2 absorption in 2.5 M MEA at loading of 0.66 and 60°C(table E.8), the percentage removal of CO_2 is only 5.9%. One of the reasons is that the absorption is not far

away from equilibrium. As mentioned above, $P_{CO2}*/P_{CO2,i}$ is equal to 0.74 in this case. This will lead to maximum error of 150% of the measured flux.

Table E.1. CO_2 in 0.4 M MEA/0.6 M PZ at 60°C.

	E.1-1*	E.1-2*	E.1-3*	E.1-4	E.1-5	E.1-6	E.1-7	E.1-8
flux (mol/(cm^{2}s))	3.53E-10	-9.61E-10	-1.35E-09	3.07E-09	1.54E-08	2.21E-08	3.15E-08	3.67E-08
k_g (mol/(atm cm^2 s))	2.39E-05	2.39E-05	2.38E-05	2.41E-05	2.40E-05	2.38E-05	2.35E-05	2.78E-05
k_l^o (cm/sec)	1.59E-02	1.59E-02	1.59E-02	1.59E-02	1.60E-02	1.60E-02	1.60E-02	1.59E-02
H_{CO2}(atm cm^3/mol)	5.91E+04	5.93E+04	5.93E+04	5.93E+04	5.94E+04	5.98E+04	5.95E+04	5.95E+04
D(cm/s^2)	4.07E-05	4.08E-05	4.08E-05	4.08E-05	4.09E-05	4.12E-05	4.10E-05	4.10E-05
μ(cP)	5.69E-01	5.67E-01	5.67E-01	5.67E-01	5.66E-01	5.62E-01	5.65E-01	5.65E-01
gas rate (cm^3/s)	2.33E+01	2.33E+01	2.33E+01	2.33E+01	2.33E+01	2.33E+01	2.33E+01	2.33E+01
liquid rate (cm^3/s)	3.25E+00	3.25E+00	3.25E+00	3.25E+00	3.25E+00	3.26E+00	3.25E+00	3.23E+00
loading (mol CO_2/mol amine)	5.62E-02	5.57E-02	5.62E-02	5.55E-02	5.59E-02	5.59E-02	5.79E-02	5.97E-02
P_{CO2} (atm)	2.01E-04	1.23E-04	1.00E-04	3.47E-04	1.10E-03	1.58E-03	2.22E-03	2.29E-03
P^*_{CO2} (atm)	1.77E-04	1.74E-04	1.77E-04	1.72E-04	1.79E-04	1.79E-04	1.93E-04	2.04E-04
$(P_{CO2,in}-P_{CO2,out})/P_{CO2,in}$ (%)	7.32E+00	-4.05E+01	-8.00E+01	3.16E+01	4.52E+01	4.52E+01	4.59E+01	4.40E+01
P interface (atm)	1.86E-04	1.63E-04	1.57E-04	2.20E-04	4.54E-04	6.48E-04	8.73E-04	9.72E-04
$(P_{CO2,i}-P_{CO2}^*)$ (atm)	9.53E-06	-1.05E-05	-2.02E-05	4.73E-05	2.75E-04	4.69E-04	6.80E-04	7.68E-04
driving force (atm)	2.43E-05	-5.08E-05	-7.68E-05	1.75E-04	9.19E-04	1.40E-03	2.02E-03	2.09E-03
$(P_{CO2}-P_{CO2,i}) / (P_{CO2}-P_{CO2}^*)$ (%)	6.07E+01	7.93E+01	7.37E+01	7.29E+01	7.01E+01	6.64E+01	6.64E+01	6.32E+01
K_G (atm mol / (cm^{2}s))	1.45E-05	1.89E-05	1.76E-05	1.76E-05	1.68E-05	1.58E-05	1.56E-05	1.76E-05
E	1.38E+02	3.40E+02	2.49E+02	2.41E+02	2.09E+02	1.76E+02	1.72E+02	1.78E+02
flux/$(P_{CO2,i}-P_{CO2}^*)$ (mol/(atm cm^{2}s))	3.70E-05	9.14E-05	6.70E-05	6.49E-05	5.62E-05	4.71E-05	4.63E-05	4.77E-05
k_2 (mol/(cm^{3}s))	1.17E+08	7.15E+08	3.84E+08	3.61E+08	2.71E+08	1.92E+08	1.84E+08	1.96E+08

E=174; *, solubility data.

Table E.2. CO_2 in 0.4 M MEA/0.6 M PZ at 60°C.

	E.2-1	E.2-2	E.2-3	E.2-4*	E.2-5*	E.2-6*	E.2-7
flux (mol/(cm^{2}s))	2.02E-08	2.73E-08	1.74E-08	4.03E-09	4.04E-10	-3.52E-09	-7.64E-09
k_g (mol/(atm cm^2 s))	2.59E-05	2.62E-05	2.61E-05	2.65E-05	2.52E-05	2.57E-05	2.53E-05
k_l^o (cm/sec)	1.56E-02	1.57E-02	1.58E-02	1.56E-02	1.56E-02	1.55E-02	1.56E-02
H_{CO2}(atm cm^3/mol)	5.89E+04	5.88E+04	5.87E+04	5.85E+04	5.84E+04	5.84E+04	5.87E+04
D(cm/s^2)	4.02E-05	4.01E-05	4.00E-05	3.99E-05	3.98E-05	3.98E-05	4.00E-05
μ(cP)	5.78E-01	5.79E-01	5.80E-01	5.82E-01	5.83E-01	5.82E-01	5.80E-01
gas rate (cm^3/s)	2.59E+01	2.59E+01	2.59E+01	2.59E+01	2.59E+01	2.59E+01	2.59E+01
liquid rate (cm^3/s)	3.13E+00	3.16E+00	3.25E+00	3.16E+00	3.16E+00	3.13E+00	3.16E+00
loading (mol CO_2/mol amine)	1.43E-01	1.43E-01	1.42E-01	1.41E-01	1.39E-01	1.38E-01	1.34E-01
P_{CO2} (atm)	2.64E-03	3.20E-03	2.49E-03	1.43E-03	1.19E-03	8.52E-04	5.39E-04
$(P_{CO2,in}-P_{CO2,out})/P_{CO2,in}$ (%)	2.57E+01	2.78E+01	2.37E+01	1.03E+01	1.38E+00	-1.80E+01	-7.86E+01
P^*_{CO2} (atm)	1.21E-03	1.20E-03	1.19E-03	1.18E-03	1.14E-03	1.12E-03	1.07E-03
P interface (atm)	1.86E-03	2.16E-03	1.82E-03	1.28E-03	1.17E-03	9.90E-04	8.41E-04
$(P_{CO2,i}-P_{CO2}^*)$ (atm)	6.50E-04	9.53E-04	6.33E-04	9.65E-05	2.99E-05	-1.31E-04	-2.25E-04
driving force (atm)	1.43E-03	1.99E-03	1.30E-03	2.49E-04	4.59E-05	-2.68E-04	-5.27E-04
$(P_{CO2}-P_{CO2,i}) / (P_{CO2}-P_{CO2}^*)$ (%)	5.45E+01	5.22E+01	5.13E+01	6.12E+01	3.49E+01	5.11E+01	5.74E+01
K_G (atm mol / (cm^{2}s))	1.41E-05	1.37E-05	1.34E-05	1.62E-05	8.80E-06	1.31E-05	1.45E-05
E	1.17E+02	1.07E+02	1.02E+02	1.57E+02	5.06E+01	1.01E+02	1.28E+02
flux/$(P_{CO2,i}-P_{CO2}^*)$ (mol/(atm cm^{2}s))	3.10E-05	2.86E-05	2.75E-05	4.18E-05	1.35E-05	2.68E-05	3.40E-05
k_2 (mol/(cm^{3}s))	8.20E+07	6.96E+07	6.43E+07	1.48E+08	1.54E+07	6.08E+07	9.82E+07

E=107; *, solubility data.

Table E.3. CO_2 in 1.9 M MEA/0.6 M PZ at 60°C.

	E.3-1*	E.3-2*	E.3-3	E.3-4	E.3-5
flux (mol/(cm^{2}s))	5.29E-09	2.10E-08	3.10E-08	4.11E-08	5.05E-08
k_g (mol/(atm cm^2 s))	2.34E-05	2.41E-05	2.56E-05	2.70E-05	2.79E-05
k_l^o (cm/sec)	1.51E-02	1.50E-02	1.51E-02	1.50E-02	1.50E-02
H_{CO2}(atm cm^3/mol)	5.68E+04	5.65E+04	5.66E+04	5.65E+04	5.62E+04
D(cm/s^2)	4.13E-05	4.09E-05	4.10E-05	4.09E-05	4.07E-05
μ(cP)	7.10E-01	7.15E-01	7.13E-01	7.16E-01	7.19E-01
gas rate (cm^3/s)	2.29E+01	2.29E+01	2.29E+01	2.29E+01	2.29E+01
liquid rate (cm^3/s)	3.05E+00	3.07E+00	3.07E+00	3.07E+00	3.10E+00
loading (mol CO_2/mol amine)	2.60E-03	3.88E-03	4.48E-03	6.04E-03	7.82E-03
P_{CO2} (atm)	2.98E-04	1.16E-03	1.64E-03	2.08E-03	2.51E-03
$(P_{CO2,in}-P_{CO2,out})/P_{CO2,in}$ (%)	5.44E+01	5.36E+01	5.28E+01	5.24E+01	5.15E+01
P^*_{CO2} (atm)	3.99E-07	8.91E-07	1.19E-06	2.16E-06	3.62E-06
P interface (atm)	7.21E-05	2.91E-04	4.28E-04	5.64E-04	6.96E-04
$(P_{CO2,i}-P_{CO2}^*)$ (atm)	7.17E-05	2.90E-04	4.27E-04	5.61E-04	6.92E-04
driving force (atm)	2.97E-04	1.16E-03	1.64E-03	2.08E-03	2.50E-03
$(P_{CO2}-P_{CO2,i}) / (P_{CO2}-P_{CO2}^*)$ (%)	7.59E+01	7.50E+01	7.39E+01	7.30E+01	7.23E+01
K_G (atm mol / (cm^{2}s))	1.78E-05	1.81E-05	1.89E-05	1.97E-05	2.02E-05
E	2.78E+02	2.72E+02	2.73E+02	2.75E+02	2.73E+02
flux/$(P_{CO2,i}-P_{CO2}^*)$ (mol/(atm cm^{2}s))	7.38E-05	7.23E-05	7.26E-05	7.31E-05	7.29E-05
k_2 (mol/(cm^{3}s))	1.70E+08	1.63E+08	1.65E+08	1.67E+08	1.65E+08

E=272; *, solubility data.

Table E.4. CO_2 in 1.9 M MEA/0.6 M PZ at 60°C.

	E.4-1*	E.4-2*	E.4-3	E.4-4	E.4-5
flux (mol/(cm^{2}s))	7.63E-10	-2.22E-09	2.57E-08	-6.69E-09	-1.39E-08
k_g (mol/(atm cm^2 s))	2.39E-05	2.34E-05	2.66E-05	2.44E-05	2.41E-05
k_l^o (cm/sec)	1.43E-02	1.42E-02	1.44E-02	1.40E-02	1.42E-02
H_{CO2}(atm cm^3/mol)	5.54E+04	5.57E+04	5.57E+04	5.57E+04	5.59E+04
D(cm/s^2)	3.86E-05	3.89E-05	3.88E-05	3.88E-05	3.90E-05
μ(cP)	7.96E-01	7.91E-01	7.92E-01	7.93E-01	7.90E-01
gas rate (cm^3/s)	2.34E+01	2.34E+01	2.34E+01	2.34E+01	2.34E+01
liquid rate (cm^3/s)	3.11E+00	3.00E+00	3.11E+00	2.89E+00	3.00E+00
loading (mol CO_2/mol amine)	2.13E-01	2.14E-01	2.14E-01	2.14E-01	2.15E-01
P_{CO2} (atm)	1.04E-03	9.09E-04	2.82E-03	5.47E-04	4.50E-05
$(P_{CO2,in}-P_{CO2,out})/P_{CO2,in}$ (%)	3.12E+00	-1.14E+01	2.91E+01	-6.88E+01	-6.38E+07
P^*_{CO2} (atm)	1.03E-03	1.03E-03	1.04E-03	1.04E-03	1.05E-03
P interface (atm)	1.00E-03	1.00E-03	1.85E-03	8.22E-04	6.23E-04
$(P_{CO2,i}-P_{CO2}^*)$ (atm)	-2.25E-05	-2.98E-05	8.13E-04	-2.17E-04	-4.23E-04
driving force (atm)	9.44E-06	-1.25E-04	1.78E-03	-4.91E-04	-1.00E-03
$(P_{CO2}-P_{CO2,i}) / (P_{CO2}-P_{CO2}^*)$ (%)	3.38E+02	7.61E+01	5.43E+01	5.59E+01	5.77E+01
K_G (atm mol / (cm^{2}s))	8.08E-05	1.78E-05	1.44E-05	1.36E-05	1.39E-05
E	-1.31E+02	2.93E+02	1.22E+02	1.23E+02	1.29E+02
flux/$(P_{CO2,i}-P_{CO2}^*)$ (mol/(atm cm^{2}s))	-3.40E-05	7.46E-05	3.16E-05	3.09E-05	3.29E-05
k_2 (mol/(cm^{3}s))	3.71E+07	1.80E+08	3.22E+07	3.08E+07	3.52E+07

E=127; *, solubility data.

Table E.5 CO_2 in 1.9 M MEA/0.6 M PZ at 60°C.

	E.5-1*	E.5-2*	E.5-3*	E.5-4	E.5-5	E.5-6	E.5-7
flux (mol/(cm^{2}s))	-9.20E-08	-7.13E-08	1.31E-07	1.67E-07	2.00E-07	2.08E-07	-1.40E-07
k_g (mol/(atm cm^2 s))	2.31E-05	2.28E-05	2.36E-05	2.52E-05	2.44E-05	2.33E-05	2.31E-05
k_l^o (cm/sec)	1.35E-02	1.35E-02	1.35E-02	1.35E-02	1.34E-02	1.34E-02	1.35E-02
H_{CO2}(atm cm^3/mol)	5.57E+04	5.59E+04	5.59E+04	5.60E+04	5.59E+04	5.61E+04	5.59E+04
D(cm/s^2)	3.62E-05	3.64E-05	3.63E-05	3.63E-05	3.62E-05	3.62E-05	3.61E-05
μ(cP)	8.71E-01	8.67E-01	8.70E-01	8.72E-01	8.75E-01	8.77E-01	8.78E-01
gas rate (cm^3/s)	2.25E+01	2.25E+01	2.25E+01	2.25E+01	2.25E+01	2.25E+01	2.25E+01
liquid rate (cm^3/s)	2.95E+00	2.92E+00	2.92E+00	2.92E+00	2.92E+00	2.92E+00	2.95E+00
loading (mol CO_2/mol amine)	4.41E-01	4.42E-01	4.48E-01	4.59E-01	4.65E-01	4.78E-01	4.72E-01
P_{CO2} (atm)	1.32E-02	1.62E-02	3.85E-02	4.10E-02	4.75E-02	5.26E-02	1.10E-02
$(P_{CO2,in}-P_{CO2,out})/P_{CO2,in}$ (%)	-3.66E+01	-2.22E+01	1.39E+01	1.54E+01	1.64E+01	1.61E+01	-7.66E+01
P^*_{CO2} (atm)	2.37E-02	2.38E-02	2.45E-02	2.56E-02	2.63E-02	2.78E-02	2.71E-02
P interface (atm)	1.72E-02	1.93E-02	3.30E-02	3.44E-02	3.93E-02	4.36E-02	1.70E-02
$(P_{CO2,i}-P_{CO2}^*)$ (atm)	-6.46E-03	-4.55E-03	8.49E-03	8.76E-03	1.30E-02	1.58E-02	-1.01E-02
driving force (atm)	-1.04E-02	-7.68E-03	1.40E-02	1.54E-02	2.12E-02	2.47E-02	-1.61E-02
$(P_{CO2}-P_{CO2,i}) / (P_{CO2}-P_{CO2}^*)$ (%)	3.81E+01	4.07E+01	3.95E+01	4.31E+01	3.88E+01	3.61E+01	3.74E+01
K_G (atm mol / (cm^{2}s))	8.81E-06	9.29E-06	9.33E-06	1.09E-05	9.46E-06	8.43E-06	8.66E-06
E	5.87E+01	6.49E+01	6.39E+01	7.93E+01	6.43E+01	5.51E+01	5.75E+01
flux/$(P_{CO2,i}-P_{CO2}^*)$ (mol/(atm cm^{2}s))	1.42E-05	1.57E-05	1.54E-05	1.91E-05	1.54E-05	1.32E-05	1.38E-05
k_2 (mol/(cm^{3}s))	6.94E+06	8.43E+06	8.17E+06	1.26E+07	8.25E+06	6.06E+06	6.63E+06

E=64; *, solubility data.

Table E.6. CO_2 in 2.5 M MEA at 60°C.

	E.6-1*	E.6-2*	E.6-3*	E.6-4	E.6-5	E.6-6	E.6-7
flux (mol/(cm^{2}s))	1.70E-09	-1.25E-09	4.45E-09	2.28E-08	2.64E-08	3.05E-08	3.39E-08
k_g (mol/(atm cm^2 s))	2.46E-05	2.44E-05	2.47E-05	2.60E-05	2.64E-05	2.59E-05	2.59E-05
k_l^o (cm/sec)	1.52E-02	1.53E-02	1.52E-02	1.52E-02	1.52E-02	1.52E-02	1.52E-02
H_{CO2}(atm cm^3/mol)	5.73E+04	5.74E+04	5.71E+04	5.69E+04	5.70E+04	5.70E+04	5.71E+04
D(cm/s^2)	4.10E-05	4.10E-05	4.08E-05	4.06E-05	4.06E-05	4.06E-05	4.07E-05
μ(cP)	6.97E-01	6.97E-01	7.00E-01	7.03E-01	7.02E-01	7.03E-01	7.01E-01
gas rate (cm^3/s)	2.39E+01	2.39E+01	2.39E+01	2.39E+01	2.39E+01	2.39E+01	2.39E+01
liquid rate (cm^3/s)	3.06E+00	3.06E+00	3.05E+00	3.05E+00	3.05E+00	3.05E+00	3.05E+00
loading (mol CO_2/mol amine)	9.12E-02	9.11E-02	9.18E-02	9.27E-02	9.31E-02	9.46E-02	9.48E-02
P_{CO2} (atm)	3.73E-04	2.00E-04	5.12E-04	1.81E-03	2.08E-03	2.40E-03	2.71E-03
$(P_{CO2,in}-P_{CO2,out})/P_{CO2,in}$ (%)	1.74E+01	-3.06E+01	3.05E+01	3.88E+01	3.85E+01	3.89E+01	3.85E+01
P^*_{CO2} (atm)	2.72E-04	2.71E-04	2.75E-04	2.81E-04	2.84E-04	2.93E-04	2.94E-04
P interface (atm)	3.04E-04	2.51E-04	3.32E-04	9.36E-04	1.08E-03	1.23E-03	1.40E-03
$(P_{CO2,i}-P_{CO2}^*)$ (atm)	3.17E-05	-1.98E-05	5.63E-05	6.55E-04	8.00E-04	9.36E-04	1.11E-03
driving force (atm)	1.01E-04	-7.12E-05	2.36E-04	1.53E-03	1.80E-03	2.11E-03	2.42E-03
$(P_{CO2}-P_{CO2,i}) / (P_{CO2}-P_{CO2}^*)$ (%)	6.85E+01	7.22E+01	7.62E+01	5.72E+01	5.55E+01	5.57E+01	5.42E+01
K_G (atm mol / (cm^{2}s))	1.68E-05	1.76E-05	1.89E-05	1.49E-05	1.46E-05	1.44E-05	1.40E-05
E	2.01E+02	2.38E+02	2.97E+02	1.31E+02	1.24E+02	1.22E+02	1.15E+02
flux/$(P_{CO2,i}-P_{CO2}^*)$ (mol/(atm cm^{2}s))	5.36E-05	6.32E-05	7.92E-05	3.48E-05	3.29E-05	3.26E-05	3.07E-05
k_2 (mol/(cm^{3}s))	9.04E+07	1.26E+08	1.97E+08	3.80E+07	3.40E+07	3.33E+07	2.96E+07

E=120; *, solubility data.

Table E.7. CO_2 in 2.5 M MEA at 60°C.

	E.7-1*	E.7-2*	E.7-3*	E.7-4	E.7-5	E.7-6	E.7-7	E.7-8
flux (mol/(cm^{2}s))	9.03E-09	-1.32E-08	3.06E-08	2.08E-07	2.40E-07	2.74E-07	3.01E-07	3.16E-07
k_g (mol/(atm cm^2 s))	3.52E-05	3.52E-05	3.52E-05	3.54E-05	3.55E-05	3.55E-05	3.55E-05	3.56E-05
k_l^o (cm/sec)	1.46E-02	1.46E-02	1.46E-02	1.48E-02	1.48E-02	1.48E-02	1.48E-02	1.49E-02
H_{CO2}(atm cm^3/mol)	5.57E+04	5.57E+04	5.53E+04	5.60E+04	5.60E+04	5.60E+04	5.60E+04	5.63E+04
D(cm/s^2)	3.76E-05	3.76E-05	3.73E-05	3.78E-05	3.78E-05	3.77E-05	3.76E-05	3.79E-05
μ(cP)	7.83E-01	7.83E-01	7.90E-01	7.80E-01	7.81E-01	7.83E-01	7.87E-01	7.82E-01
gas rate (cm^3/s)	3.36E+01	3.36E+01	3.36E+01	3.36E+01	3.36E+01	3.36E+01	3.36E+01	3.36E+01
liquid rate (cm^3/s)	3.00E+00	3.00E+00	3.06E+00	3.06E+00	3.09E+00	3.09E+00	3.08E+00	3.09E+00
loading (mol CO_2/mol amine)	3.24E-01	3.19E-01	3.25E-01	3.26E-01	3.33E-01	3.37E-01	3.53E-01	3.53E-01
P_{CO2} (atm)	3.19E-03	1.47E-03	4.93E-03	2.03E-02	2.38E-02	2.73E-02	3.09E-02	3.38E-02
$(P_{CO2,in}-P_{CO2,out})/P_{CO2,in}$ (%)	7.98E+00	-3.03E+01	1.67E+01	2.58E+01	2.54E+01	2.53E+01	2.46E+01	2.37E+01
P^*_{CO2} (atm)	2.53E-03	2.45E-03	2.55E-03	2.57E-03	2.67E-03	2.74E-03	3.00E-03	3.00E-03
P interface (atm)	2.93E-03	1.85E-03	4.06E-03	1.44E-02	1.71E-02	1.96E-02	2.24E-02	2.49E-02
$(P_{CO2,i}-P_{CO2}^*)$ (atm)	4.00E-04	-6.01E-04	1.52E-03	1.19E-02	1.44E-02	1.69E-02	1.94E-02	2.19E-02
driving force (atm)	6.56E-04	-9.77E-04	2.39E-03	1.77E-02	2.12E-02	2.46E-02	2.79E-02	3.08E-02
$(P_{CO2}-P_{CO2,i}) / (P_{CO2}-P_{CO2}^*)$ (%)	3.90E+01	3.85E+01	3.65E+01	3.31E+01	3.20E+01	3.13E+01	3.04E+01	2.88E+01
K_G (atm mol / (cm^{2}s))	1.38E-05	1.36E-05	1.28E-05	1.17E-05	1.13E-05	1.11E-05	1.08E-05	1.03E-05
E	8.60E+01	8.40E+01	7.65E+01	6.65E+01	6.31E+01	6.13E+01	5.87E+01	5.47E+01
flux/$(P_{CO2,i}-P_{CO2}^*)$ (mol/(atm cm^{2}s))	2.26E-05	2.21E-05	2.02E-05	1.75E-05	1.67E-05	1.62E-05	1.55E-05	1.44E-05
k_2 (mol/(cm^{3}s))	1.57E+07	1.50E+07	1.25E+07	9.52E+06	8.62E+06	8.11E+06	7.42E+06	6.46E+06

E=58.5; *, solubility data.

Table E.8. CO_2 in 2.5 M MEA at 60°C.

	E.8-1*	E.8-2*	E.8-3*	E.8-4	E.8-5	E.8-6	E.8-7
flux (mol/(cm^{2}s))	2.97E-07	4.32E-08	-1.88E-07	8.29E-07	6.94E-07	3.87E-07	4.31E-07
k_g (mol/(atm cm^2 s))	2.25E-05	2.24E-05	2.26E-05	2.23E-05	2.22E-05	2.22E-05	2.22E-05
k_l^o (cm/sec)	1.47E-02	1.48E-02	1.47E-02	1.45E-02	1.46E-02	1.45E-02	1.46E-02
H_{CO2}(atm cm^3/mol)	5.74E+04	5.70E+04	5.67E+04	5.67E+04	5.67E+04	5.67E+04	5.67E+04
D(cm/s^2)	3.63E-05	3.60E-05	3.58E-05	3.55E-05	3.54E-05	3.53E-05	3.52E-05
m(cP)	8.44E-01	8.52E-01	8.55E-01	8.66E-01	8.70E-01	8.74E-01	8.74E-01
gas rate (cm^3/s)	2.33E+01	2.33E+01	2.33E+01	2.33E+01	2.33E+01	2.33E+01	2.33E+01
liquid rate (cm^3/s)	3.02E+00	3.10E+00	3.07E+00	3.01E+00	3.03E+00	3.03E+00	3.06E+00
loading (mol CO_2/mol amine)	6.11E-01	6.15E-01	6.07E-01	6.46E-01	6.57E-01	6.70E-01	6.72E-01
P_{CO2} (atm)	1.22E-01	8.46E-02	4.62E-02	3.68E-01	4.16E-01	4.65E-01	5.06E-01
$(P_{CO2,in}-P_{CO2,out})/P_{CO2,in}$ (%)	1.02E+01	2.22E+00	-1.95E+01	9.42E+00	7.09E+00	3.59E+00	3.67E+00
P^*_{CO2} (atm)	7.07E-02	7.94E-02	6.30E-02	1.92E-01	2.58E-01	3.70E-01	3.93E-01
P interface (atm)	1.09E-01	8.27E-02	5.46E-02	3.31E-01	3.84E-01	4.47E-01	4.87E-01
$(P_{CO2,i}-P_{CO2}^*)$ (atm)	3.79E-02	3.30E-03	-8.38E-03	1.39E-01	1.26E-01	7.69E-02	9.33E-02
driving force (atm)	5.12E-02	5.22E-03	-1.67E-02	1.77E-01	1.58E-01	9.43E-02	1.13E-01
$(P_{CO2}-P_{CO2,i}) / (P_{CO2}-P_{CO2}^*)$ (%)	2.59E+01	3.69E+01	4.99E+01	2.11E+01	1.99E+01	1.85E+01	1.72E+01
K_G (atm mol / (cm^{2}s))	5.81E-06	8.27E-06	1.13E-05	4.70E-06	4.40E-06	4.10E-06	3.82E-06
E	3.06E+01	5.06E+01	8.69E+01	2.32E+01	2.14E+01	1.96E+01	1.79E+01
flux/$(P_{CO2,i}-P_{CO2}^*)$ (mol/(atm cm^{2}s))	7.84E-06	1.31E-05	2.25E-05	5.95E-06	5.49E-06	5.03E-06	4.62E-06
k_2 (mol/(cm^{3}s))	1.94E+06	5.38E+06	1.58E+07	1.11E+06	9.42E+05	7.92E+05	6.66E+05

E=20.41; a=3.7; *, solubility data.

Table E.9. CO_2 in 3.8 M MEA/1.2 PZ at 40°C.

	E.9-1*	E.9-2*	E.9-3*	E.9-4	E.9-5	E.9-6	E.9-7
flux (mol/(cm^{2}s))	-5.87E-09	-1.13E-09	2.48E-09	1.29E-08	1.59E-08	2.28E-08	2.57E-08
k_g (mol/(atm cm^2 s))	2.57E-05	2.58E-05	2.58E-05	2.58E-05	2.58E-05	2.54E-05	2.53E-05
k_l^o (cm/sec)	7.41E-03	7.40E-03	7.37E-03	7.33E-03	7.32E-03	7.32E-03	7.34E-03
H_{CO2}(atm cm^3/mol)	3.90E+04	3.88E+04	3.87E+04	3.86E+04	3.86E+04	3.86E+04	3.87E+04
D(cm/s^2)	2.25E-05	2.24E-05	2.24E-05	2.23E-05	2.22E-05	2.22E-05	2.23E-05
μ(cP)	2.98E+00	2.98E+00	2.99E+00	3.02E+00	3.02E+00	3.02E+00	3.01E+00
gas rate (cm^3/s)	2.47E+01	2.47E+01	2.47E+01	2.47E+01	2.47E+01	2.47E+01	2.47E+01
liquid rate (cm^3/s)	1.85E+00	1.85E+00	1.85E+00	1.84E+00	1.83E+00	1.83E+00	1.84E+00
loading (mol CO_2/mol amine)	4.34E-01	4.27E-01	4.29E-01	4.34E-01	4.35E-01	4.35E-01	4.35E-01
P_{CO2} (atm)	4.90E-04	7.84E-04	1.09E-03	2.00E-03	2.32E-03	2.96E-03	3.27E-03
$(P_{CO2,in}-P_{CO2,out})/P_{CO2,in}$ (%)	-6.04E+01	-5.81E+00	8.45E+00	2.20E+01	2.31E+01	2.59E+01	2.63E+01
P^*_{CO2} (atm)	9.52E-04	9.22E-04	9.34E-04	9.52E-04	9.58E-04	9.58E-04	9.58E-04
P interface (atm)	7.18E-04	8.28E-04	9.98E-04	1.50E-03	1.70E-03	2.06E-03	2.26E-03
$(P_{CO2,i}-P_{CO2}^*)$ (atm)	-2.34E-04	-9.40E-05	6.37E-05	5.47E-04	7.42E-04	1.10E-03	1.30E-03
driving force (atm)	-4.63E-04	-1.38E-04	1.60E-04	1.05E-03	1.36E-03	2.00E-03	2.32E-03
$(P_{CO2}-P_{CO2,i}) / (P_{CO2}-P_{CO2}^*)$ (%)	4.94E+01	3.18E+01	6.01E+01	4.78E+01	4.53E+01	4.49E+01	4.39E+01
K_G (atm mol / (cm^{2}s))	1.27E-05	8.22E-06	1.55E-05	1.23E-05	1.17E-05	1.14E-05	1.11E-05
E	1.32E+02	6.32E+01	2.04E+02	1.25E+02	1.13E+02	1.09E+02	1.04E+02
flux/$(P_{CO2,i}-P_{CO2}^*)$ (mol/(atm cm^{2}s))	2.51E-05	1.21E-05	3.89E-05	2.37E-05	2.14E-05	2.07E-05	1.98E-05
k_2 (mol/(cm^{3}s))	1.50E+07	3.40E+06	3.55E+07	1.33E+07	1.08E+07	1.02E+07	9.34E+06

E=109; *, solubility data.

Table E.1.0 CO_2 in 3.8 M MEA/1.2 PZ at 40°C.

	E.10-1*	E.10-2*	E.10-3*	E.10-4	E.10-5	E.10-6	E.10-7
flux (mol/(cm^{2}s))	-2.81E-09	2.93E-08	5.66E-08	1.85E-07	2.15E-07	2.29E-07	1.40E-07
k_g (mol/(atm cm^2 s))	2.50E-05	2.50E-05	2.50E-05	2.49E-05	2.49E-05	2.47E-05	2.47E-05
k_l^o (cm/sec)	6.24E-03	6.15E-03	6.14E-03	6.09E-03	6.07E-03	6.03E-03	5.96E-03
H_{CO2}(atm cm^3/mol)	3.92E+04	3.90E+04	3.90E+04	3.90E+04	3.92E+04	3.91E+04	3.90E+04
D(cm/s^2)	2.01E-05	1.99E-05	1.98E-05	1.98E-05	1.98E-05	1.97E-05	1.95E-05
μ(cP)	3.88E+00	3.95E+00	3.96E+00	3.99E+00	4.01E+00	4.04E+00	4.10E+00
gas rate (cm^3/s)	2.40E+01	2.40E+01	2.40E+01	2.40E+01	2.40E+01	2.40E+01	2.40E+01
liquid rate (cm^3/s)	1.50E+00	1.47E+00	1.47E+00	1.44E+00	1.43E+00	1.42E+00	1.40E+00
loading (mol CO_2/mol amine)	6.93E-01	7.04E-01	7.06E-01	7.14E-01	7.25E-01	7.30E-01	7.41E-01
P_{CO2} (atm)	4.66E-03	9.62E-03	1.47E-02	3.45E-02	3.95E-02	4.23E-02	3.01E-02
$(P_{CO2,in}-P_{CO2,out})/P_{CO2,in}$ (%)	-2.49E+00	1.16E+01	1.45E+01	1.96E+01	1.98E+01	1.99E+01	1.73E+01
P^*_{CO2} (atm)	5.20E-03	6.16E-03	6.37E-03	7.30E-03	8.67E-03	9.29E-03	1.11E-02
P interface (atm)	4.77E-03	8.44E-03	1.24E-02	2.71E-02	3.09E-02	3.31E-02	2.45E-02
$(P_{CO2,i}-P_{CO2}^*)$ (atm)	-4.31E-04	2.28E-03	6.02E-03	1.98E-02	2.22E-02	2.38E-02	1.34E-02
driving force (atm)	-5.43E-04	3.46E-03	8.28E-03	2.72E-02	3.08E-02	3.30E-02	1.91E-02
$(P_{CO2}-P_{CO2,i}) / (P_{CO2}-P_{CO2}^*)$ (%)	2.08E+01	3.39E+01	2.74E+01	2.73E+01	2.80E+01	2.80E+01	2.97E+01
K_G (atm mol / (cm^{2}s))	5.18E-06	8.47E-06	6.84E-06	6.79E-06	6.97E-06	6.93E-06	7.32E-06
E	4.10E+01	8.13E+01	5.98E+01	5.99E+01	6.25E+01	6.24E+01	6.82E+01
flux/$(P_{CO2,i}-P_{CO2}^*)$ (mol/(atm cm^{2}s))	6.53E-06	1.28E-05	9.41E-06	9.34E-06	9.67E-06	9.63E-06	1.04E-05
k_2 (mol/(cm^{3}s))	2.12E+06	8.50E+06	4.61E+06	4.70E+06	5.28E+06	5.33E+06	6.52E+06

E=61; a=2; *, solubility data.

Table E.11. CO_2 in 3.8 M MEA/1.2 PZ at 60°C.

	E.11-1*	E.11-2*	E.11-3*	E.11-4	E.11-5	E.11-6	E.11-7
flux (mol/(cm^{2}s))	4.57E-08	-5.96E-09	1.03E-07	3.28E-07	3.69E-07	4.17E-07	4.69E-07
k_g (mol/(atm cm^2 s))	2.62E-05	2.62E-05	2.62E-05	2.59E-05	2.59E-05	2.59E-05	2.60E-05
k_l^o (cm/sec)	1.06E-02	1.06E-02	1.07E-02	1.06E-02	1.06E-02	1.05E-02	1.06E-02
H_{CO2}(atm cm^3/mol)	5.15E+04	5.15E+04	5.14E+04	5.15E+04	5.15E+04	5.14E+04	5.17E+04
D(cm/s^2)	3.40E-05	3.39E-05	3.39E-05	3.38E-05	3.37E-05	3.35E-05	3.38E-05
m(cP)	1.89E+00	1.89E+00	1.88E+00	1.91E+00	1.92E+00	1.94E+00	1.93E+00
gas rate (cm^3/s)	2.59E+01	2.59E+01	2.59E+01	2.59E+01	2.59E+01	2.59E+01	2.59E+01
liquid rate (cm^3/s)	2.35E+00	2.37E+00	2.38E+00	2.37E+00	2.36E+00	2.37E+00	2.38E+00
loading (mol CO_2/mol amine)	4.10E-01	4.13E-01	4.07E-01	4.20E-01	4.27E-01	4.32E-01	4.35E-01
P_{CO2} (atm)	8.87E-03	4.57E-03	1.31E-02	3.02E-02	3.48E-02	3.92E-02	4.34E-02
$(P_{CO2,in}-P_{CO2,out})/P_{CO2,in}$ (%)	1.82E+01	-5.21E+00	2.62E+01	3.47E+01	3.40E+01	3.42E+01	3.45E+01
P^*_{CO2} (atm)	5.13E-03	5.52E-03	4.78E-03	6.61E-03	7.94E-03	9.20E-03	9.90E-03
P interface (atm)	7.12E-03	4.80E-03	9.21E-03	1.75E-02	2.05E-02	2.31E-02	2.53E-02
$(P_{CO2,i}-P_{CO2}^*)$ (atm)	1.99E-03	-7.20E-04	4.44E-03	1.09E-02	1.26E-02	1.39E-02	1.54E-02
driving force (atm)	3.73E-03	-9.48E-04	8.35E-03	2.36E-02	2.68E-02	3.00E-02	3.35E-02
$(P_{CO2}-P_{CO2,i}) / (P_{CO2}-P_{CO2}^*)$ (%)	4.68E+01	2.40E+01	4.69E+01	5.37E+01	5.30E+01	5.38E+01	5.39E+01
K_G (atm mol / (cm^{2}s))	1.22E-05	6.29E-06	1.23E-05	1.39E-05	1.37E-05	1.39E-05	1.40E-05
E	1.12E+02	4.00E+01	1.11E+02	1.46E+02	1.43E+02	1.47E+02	1.48E+02
flux/$(P_{CO2,i}-P_{CO2}^*)$ (mol/(atm cm^{2}s))	2.30E-05	8.28E-06	2.31E-05	3.00E-05	2.92E-05	3.01E-05	3.04E-05
k_2 (mol/(cm^{3}s))	1.40E+07	1.82E+06	1.40E+07	2.43E+07	2.34E+07	2.52E+07	2.58E+07

E=140.7; a=2; *, solubility data.

Table E.12. CO_2 in 5.0 M MEA at 40°C.

	E.12-1*	E.12-2*	E.12-3*	E.12-4	E.12-5	E.12-6	E.12-7
flux (mol/(cm^{2}s))	6.10E-09	-4.92E-10	1.85E-09	1.88E-08	2.16E-08	2.55E-08	2.84E-08
k_g (mol/(atm cm^2 s))	2.67E-05	2.65E-05	2.63E-05	2.64E-05	2.64E-05	2.63E-05	2.67E-05
k_l^o (cm/sec)	9.03E-03	8.48E-03	8.53E-03	8.46E-03	8.46E-03	8.50E-03	8.50E-03
H_{CO2}(atm cm^3/mol)	3.84E+04	3.87E+04	3.86E+04	3.86E+04	3.86E+04	3.86E+04	3.86E+04
D(cm/s^2)	2.38E-05	2.40E-05	2.39E-05	2.39E-05	2.39E-05	2.39E-05	2.39E-05
μ(cP)	2.26E+00	2.24E+00	2.24E+00	2.24E+00	2.24E+00	2.24E+00	2.24E+00
gas rate (cm^3/s)	2.59E+01	2.59E+01	2.59E+01	2.59E+01	2.59E+01	2.59E+01	2.59E+01
liquid rate (cm^3/s)	2.65E+00	2.15E+00	2.20E+00	2.15E+00	2.15E+00	2.17E+00	2.17E+00
loading (mol CO_2/mol amine)	2.98E-01	3.00E-01	2.97E-01	2.97E-01	2.97E-01	2.97E-01	2.97E-01
P_{CO2} (atm)	6.12E-04	1.92E-04	3.35E-04	1.82E-03	2.13E-03	2.41E-03	2.68E-03
$(P_{CO2,in}-P_{CO2,out})/P_{CO2,in}$ (%)	3.13E+01	-1.02E+01	1.90E+01	3.20E+01	3.15E+01	3.26E+01	3.22E+01
P^*_{CO2} (atm)	2.10E-04	2.12E-04	2.08E-04	2.08E-04	2.08E-04	2.08E-04	2.08E-04
P interface (atm)	3.83E-04	2.11E-04	2.64E-04	1.11E-03	1.31E-03	1.44E-03	1.62E-03
$(P_{CO2,i}-P_{CO2}^*)$ (atm)	1.73E-04	-1.65E-06	5.60E-05	9.02E-04	1.10E-03	1.24E-03	1.41E-03
driving force (atm)	4.02E-04	-2.02E-05	1.26E-04	1.61E-03	1.92E-03	2.21E-03	2.47E-03
$(P_{CO2}-P_{CO2,i}) / (P_{CO2}-P_{CO2}^*)$ (%)	5.70E+01	9.18E+01	5.57E+01	4.40E+01	4.26E+01	4.39E+01	4.31E+01
K_G (atm mol / (cm^{2}s))	1.52E-05	2.44E-05	1.46E-05	1.16E-05	1.13E-05	1.16E-05	1.15E-05
E	1.50E+02	1.36E+03	1.50E+02	9.49E+01	8.94E+01	9.38E+01	9.16E+01
flux/$(P_{CO2,i}-P_{CO2}^*)$ (mol/(atm cm^{2}s))	3.53E-05	2.99E-04	3.30E-05	2.08E-05	1.96E-05	2.07E-05	2.02E-05
k_2 (mol/(cm^{3}s))	2.20E+07	1.59E+09	1.93E+07	7.67E+06	6.81E+06	7.55E+06	7.21E+06

E=92; *, solubility data.

Table E.13. CO_2 in 5.0 M MEA at 40°C.

	E.13-1*	E.13-2*	E.13-3*	E.13-4	E.13-5	E.13-6	E.13-7
flux (mol/(cm^{2}s))	2.14E-07	4.84E-07	7.52E-07	1.50E-06	1.35E-06	1.07E-06	8.71E-07
k_g (mol/(atm cm^2 s))	2.61E-05	2.63E-05	2.64E-05	2.63E-05	2.62E-05	2.60E-05	2.59E-05
k_l^o (cm/sec)	7.92E-03	7.89E-03	7.88E-03	7.77E-03	7.80E-03	7.80E-03	7.69E-03
H_{CO2}(atm cm^3/mol)	3.87E+04	3.88E+04	3.87E+04	3.88E+04	3.89E+04	3.89E+04	3.88E+04
D(cm/s^2)	2.23E-05	2.23E-05	2.22E-05	2.20E-05	2.20E-05	2.20E-05	2.19E-05
μ(cP)	2.61E+00	2.62E+00	2.64E+00	2.69E+00	2.69E+00	2.69E+00	2.72E+00
gas rate (cm^3/s)	2.53E+01	2.53E+01	2.53E+01	2.53E+01	2.53E+01	2.53E+01	2.53E+01
liquid rate (cm^3/s)	2.10E+00	2.10E+00	2.11E+00	2.06E+00	2.08E+00	2.08E+00	2.03E+00
loading (mol CO_2/mol amine)	4.69E-01	4.77E-01	4.83E-01	5.09E-01	5.12E-01	5.14E-01	5.21E-01
P_{CO2} (atm)	3.29E-02	6.47E-02	9.61E-02	4.13E-01	3.82E-01	3.52E-01	3.21E-01
$(P_{CO2,in}-P_{CO2,out})/P_{CO2,in}$ (%)	2.22E+01	2.49E+01	2.57E+01	1.28E+01	1.25E+01	1.09E+01	9.89E+00
P^*_{CO2} (atm)	7.43E-03	9.55E-03	1.17E-02	2.81E-02	3.12E-02	3.30E-02	4.26E-02
P interface (atm)	2.47E-02	4.63E-02	6.77E-02	3.55E-01	3.30E-01	3.11E-01	2.87E-01
$(P_{CO2,i}-P_{CO2}^*)$ (atm)	1.73E-02	3.67E-02	5.60E-02	3.27E-01	2.99E-01	2.78E-01	2.45E-01
driving force (atm)	2.55E-02	5.52E-02	8.44E-02	3.85E-01	3.50E-01	3.19E-01	2.79E-01
$(P_{CO2}-P_{CO2,i}) / (P_{CO2}-P_{CO2}^*)$ (%)	3.22E+01	3.34E+01	3.37E+01	1.49E+01	1.47E+01	1.28E+01	1.21E+01
K_G (atm mol / (cm^{2}s))	8.41E-06	8.77E-06	8.91E-06	3.91E-06	3.84E-06	3.34E-06	3.13E-06
E	6.07E+01	6.47E+01	6.60E+01	2.29E+01	2.24E+01	1.91E+01	1.80E+01
flux/$(P_{CO2,i}-P_{CO2}^*)$ (mol/(atm cm^{2}s))	1.24E-05	1.32E-05	1.34E-05	4.59E-06	4.50E-06	3.83E-06	3.56E-06
k_2 (mol/(cm^{3}s))	3.90E+06	4.47E+06	4.71E+06	5.88E+05	5.69E+05	4.13E+05	3.64E+05

E=20.8; a=4; *, solubility data.

Table E.14. CO_2 in 5.0 M MEA at 60°C.

	E.14-1*	E.14-2*	E.14-3*	E.14-4	E.14-5	E.14-6
flux (mol/(cm^{2}s))	6.63E-09	1.25E-09	9.72E-08	1.23E-07	1.50E-07	1.76E-07
k_g (mol/(atm cm^2 s))	2.79E-05	2.76E-05	2.65E-05	2.65E-05	2.66E-05	2.66E-05
k_l^o (cm/sec)	1.23E-02	1.24E-02	1.23E-02	1.24E-02	1.23E-02	1.23E-02
H_{CO2}(atm cm^3/mol)	5.24E+04	5.26E+04	5.25E+04	5.24E+04	5.24E+04	5.24E+04
D(cm/s^2)	3.76E-05	3.77E-05	3.75E-05	3.73E-05	3.73E-05	3.72E-05
μ(cP)	1.37E+00	1.37E+00	1.38E+00	1.39E+00	1.40E+00	1.40E+00
gas rate (cm^3/s)	2.85E+01	2.85E+01	2.85E+01	2.85E+01	2.85E+01	2.85E+01
liquid rate (cm^3/s)	2.66E+00	2.66E+00	2.65E+00	2.72E+00	2.72E+00	2.72E+00
loading (mol CO_2/mol amine)	2.69E-01	2.74E-01	2.80E-01	2.87E-01	2.91E-01	2.92E-01
P_{CO2} (atm)	2.48E-03	2.26E-03	1.03E-02	1.24E-02	1.44E-02	1.65E-02
$(P_{CO2,in}-P_{CO2,out})/P_{CO2,in}$ (%)	9.03E+00	1.96E+00	3.03E+01	3.15E+01	3.27E+01	3.34E+01
P^*_{CO2} (atm)	2.36E-03	2.44E-03	2.55E-03	2.68E-03	2.75E-03	2.77E-03
P interface (atm)	2.24E-03	2.22E-03	6.60E-03	7.76E-03	8.79E-03	9.90E-03
$(P_{CO2,i}-P_{CO2}^*)$ (atm)	-1.18E-04	-2.19E-04	4.05E-03	5.07E-03	6.04E-03	7.13E-03
driving force (atm)	1.20E-04	-1.74E-04	7.71E-03	9.70E-03	1.17E-02	1.38E-02
$(P_{CO2}-P_{CO2,i}) / (P_{CO2}-P_{CO2}^*)$ (%)	1.98E+02	-2.60E+01	4.75E+01	4.77E+01	4.83E+01	4.82E+01
K_G (atm mol / (cm^{2}s))	5.53E-05	-7.17E-06	1.26E-05	1.27E-05	1.28E-05	1.28E-05
E	-2.39E+02	-2.42E+01	1.02E+02	1.03E+02	1.05E+02	1.05E+02
flux/$(P_{CO2,i}-P_{CO2}^*)$ (mol/(atm cm^{2}s))	-5.63E-05	-5.69E-06	2.40E-05	2.42E-05	2.48E-05	2.48E-05
k_2 (mol/(cm^{3}s))	6.34E+07	6.54E+05	1.17E+07	1.21E+07	1.28E+07	1.28E+07

E=104; *, solubility data.

Table E.15. CO_2 in 5.0 M MEA at 60°C.

	E.15-1*	E.15-2*	E.15-3*	E.15-4	E.15-5	E.15-6
flux (mol/(cm^{2}s))	-1.26E-07	7.39E-08	-3.52E-07	9.28E-07	9.51E-07	6.10E-07
k_g (mol/(atm cm^2 s))	2.73E-05	2.75E-05	2.71E-05	2.70E-05	2.71E-05	2.72E-05
k_l^o (cm/sec)	1.10E-02	1.10E-02	1.09E-02	1.11E-02	1.10E-02	1.10E-02
H_{CO2}(atm cm^3/mol)	5.24E+04	5.26E+04	5.23E+04	5.24E+04	5.22E+04	5.23E+04
D(cm/s^2)	3.40E-05	3.39E-05	3.36E-05	3.36E-05	3.34E-05	3.34E-05
m(cP)	1.72E+00	1.73E+00	1.74E+00	1.75E+00	1.77E+00	1.77E+00
gas rate (cm^3/s)	2.73E+01	2.73E+01	2.73E+01	2.73E+01	2.73E+01	2.73E+01
liquid rate (cm^3/s)	2.47E+00	2.46E+00	2.45E+00	2.59E+00	2.56E+00	2.56E+00
loading (mol CO_2/mol amine)	5.06E-01	5.17E-01	5.17E-01	5.29E-01	5.31E-01	5.36E-01
P_{CO2} (atm)	7.42E-02	1.06E-01	4.21E-02	3.44E-01	3.77E-01	3.12E-01
$(P_{CO2,in}-P_{CO2,out})/P_{CO2,in}$ (%)	-6.47E+00	2.52E+00	-3.64E+01	9.48E+00	8.83E+00	6.92E+00
P^*_{CO2} (atm)	7.78E-02	9.49E-02	9.49E-02	1.16E-01	1.20E-01	1.33E-01
P interface (atm)	7.88E-02	1.03E-01	5.51E-02	3.10E-01	3.42E-01	2.89E-01
$(P_{CO2,i}-P_{CO2}^*)$ (atm)	9.93E-04	8.31E-03	-3.98E-02	1.94E-01	2.22E-01	1.56E-01
driving force (atm)	-3.62E-03	1.10E-02	-5.27E-02	2.28E-01	2.57E-01	1.79E-01
$(P_{CO2}-P_{CO2,i}) / (P_{CO2}-P_{CO2}^*)$ (%)	1.27E+02	2.45E+01	2.46E+01	1.51E+01	1.36E+01	1.25E+01
K_G (atm mol / (cm^{2}s))	3.48E-05	6.72E-06	6.67E-06	4.06E-06	3.69E-06	3.41E-06
E	-6.02E+02	4.25E+01	4.23E+01	2.26E+01	2.03E+01	1.85E+01
flux/$(P_{CO2,i}-P_{CO2}^*)$ (mol/(atm cm^{2}s))	-1.27E-04	8.89E-06	8.84E-06	4.79E-06	4.28E-06	3.90E-06
k_2 (mol/(cm^{3}s))	5.26E+08	2.67E+06	2.63E+06	7.95E+05	6.36E+05	5.37E+05

E=20.6; a=0; *, solubility data.

Nomenclature

a	interfacial area of wetted wall column, (m^2)
C	concentration, (mol/m^3)
d	hydraulic diameter of the wetted wall column, (m)
D	diffusion coefficient, (m^2/s)
E	enhancement factor
h	height of the wetted wall column, (m)
H	Henry's law constant, (Pa^{-1})
I	ionic strength
k	rate constant, ($m^3/mol\ s$)
k_g	gas film mass transfer coefficient, ($mol/(Pa \cdot cm^2 \cdot s)$)
k_G	Mass transfer coefficient based on gas phase, (m/s)
k_l^o	liquid film mass transfer coefficient, ($mol/(Pa \cdot cm^2 \cdot s)$)
K	Equilibrium constant
M	molecular weight
P_x	Partial pressure of x, (Pa)
Q_L	flow rate, (m^3/s)
Re	Reynolds number
Sc	Schmidt number
Sh	Sherwood number
T	Temperature, (K)
V	volume of solution, (m^3)
X	mole fraction
α	CO_2 loading, (mol CO_2/mol amine)
η	parameter to calculate mass transfer coefficient

Θ	parameter to calculate mass transfer coefficient
δ	film thickness, (m)
τ	contact time, (s)
μ	viscosity, (Pa·s)
ρ	density, (kg/m^3)
Ω	mass percent of amine

* Units are as above without specific definition

References

Al-Ghawas, H. A., Hagewieache, D. P., Ruiz-Ibanez, Sandall, O. C., "Physicochemical Properties Important for Carbon Dioxide Absorption in Aqueous Methyldiethanolamine", *J. Chem. Eng. Data.* **1989**, 34, 385.

Appl, M., Wagner, U., Henrici, H. J., Kuessner, K., Volkamer, K., Fuerst, E., "Removal of CO_2 and/or H_2S and/or COS from gases containing these constituents", *Canadian Patent No. 1,090,098.* **1980**.

Appl, M., Wagner, U., Henrici, H. J., Kuessner, K., Volkamer, F., Ernst Neust, U., "Removal of CO_2 and/or H_2S and/or COS From Gases Containing These Constituents", *U.S. Patent No. 4,336,233.* **1982**.

Atadan, E. M., Ph.D Dissertation, University of Tennessee, 1954.

Austgen, D. M., Rochelle, G. T., Chen, C-C., "A Model of Vapor-Liquid Equilibria for Aqueous Acid Gas-Alkanolamine System. 2. Representation of H_2S and CO_2 Solubility in Aqueous Mixture of MDEA with MEA and DEA.", *Ind. Eng. Chem. Res.* **1991**, 30, 543.

Austgen, D. M., Rochelle, G. T., Peng, X., Chen, C-C., "Model of Vapor-Liquid Equilibria for Aqueous Acid Gas-Alkanolamine System Using the Electrolyte-NRTL Equation", *Am. Chem. Soc.* **1989**, 28, 1060.

Bartholome, E., Schmidt, H. W., Friebe, J., "Process for Removing Carbon Dioxide from Gas Mixtures", *U.S. Patent 3,622,267.* **1971**.

Beutier, D., Renon, H., "Representation of NH_3-H_2S-H_2O, NH_3-CO_2-H_2O, and NH_3-SO_2-H_2O Vapor-Liquid Equilibriua", *Ind. Eng. Chem. Process Des. Dev.* **1978**, 17(3), 220.

Bishnoi, S., Gary. T. G., "Absorption of Carbon Dioxide into Aqueous Piperazine: Reaction Kinetics, Mass Transfer and Solubility", *Submitted to Chem. Eng. Science*, December 16, **1999**.

Bishnoi, S., Ph.D Dissertation, The University of Texas at Austin, December, 2000.

Bottoms, R. R., "Organic Bases for Gas Purification", *Ind. Eng. Chem.* **1931**, 23(5), 501.

Cadours, R., Bouallou, C., "Rigorous Simulation of Gas Absorption into Aqueous Solution", *Ind. Eng. Chem. Res.* **1998**, 37, 1063.

Cornelisse, R., Beenackers, A. A. C. M., van Beckum, F. P. H., van Swaaij, W. P. M., "Numerical Calculation of Simultaneous Mass Transfer of Two Gases Accompanied by Complex Reversible Reactions", *Chem. Eng. Sci.* **1980**, 35, 1245.

DeGuillo, R. M., Lee, R. J., Schaeffer, S. T., Brasher, L. L., Teja, A. S., "Densities and Viscosities of the Ethanolamines", *J. Chem. Eng. Data.* **1992**, 37, 239.

Deshmukh, R. D., Mather, A. E., "A Mathematical Model for Equilibrium Solubility of Hydrocarbon Sulfide and Carbon Dioxide in Aqueous Alkanolamine Solutions", *Chem. Eng. Sci.* **1981**, 36, 355.

Edwards, T. J., Mauer, G., Newman, J., Prausnitz, J. M., "Vapor-Liquid Equilibria in Multicomponent Aqueous Solution of Volatile Weak Electrolytes", *AIChE J.* **1978**, 24(6), 996.

Edwards, T. J., Newman, J., Prausnitz, J. M., "Thermodynamics of Aqueous Solutions Containing Volatile Weak Electrolytes". *AIChE J.* **1975**, 21(2), 248.

Fürst, W., Renon, H., "Representation of Excess Properties of Electrolyte Solutions Using a New Equation of State", *AIChE J.* **1993**, 39, 335.

Glasscock, D. A., Rochelle, G. T., "Numerical Simulation of Theories for Gas Absorption with Chemical Reaction", *AIChE J.* **1989**, 35, 1271.

Hagewiesche, D. P., Ashour, S. S., Al-Ghawas, H. A., Sandall, O. R., "Absorption of Carbon Dioxide into Aqueous Blends of Monoethanolamine and *N*-Methyldiethanolamine", *Chem. Eng. Sci.* **1995**, 50, 1071.

Hikita, H., Asai, S., Ishikawa, H., Honda, M., "The Kinetics of Reactions of Carbon Dioxide with Monoethanolamine, Diethanolamine and Triethanolamine by a Rapid Mixing Method", *Chem. Eng. J.* **1977**, 13, 7

Isaacs, E. E., Otto, F. D., Mather, A. E., "Solubility of Mixtures of H2S and CO2 in a Monoethanolamine solution at Low Partial Pressures", *J. Chem. Eng. Data.* **1980**, 25, 118.

Jones, J. H., Froning, H. R., Claytor, E. E., "Solubility of Acidic Gases in Aqueous Monoethanolamine", *J. Chem. Eng. Data.* **1959**, 4(1), 85.

Jou, F-Y., Mather, A. E., Otto, F. D., "The Solubility of CO_2 in a 30 Mass Percent Monoethanolamine Solution", *Can. J. Chem. Eng.* **1995**, 73, 140.

Kaganoi, S., " Carbon Dioxide Absorption in Methyldiethanolamine with Piperazine or Diethanolamine: Thermodynamics and Rate Measurements", M.S. Thesis, The University of Texas at Austin, **1997**.

Kent, R., Eisenberg, B., "Better Data for Amine treating", *Hydrocarbon Process.* **1976**, 55(2), 87.

Kohl, A. L., Nielsen, R. B., "Gas Purification", 5th Edition, Houston, **1997**.

Kuranov, G., Rumpf, B., Maurer, G., Smirnova, N., "VLE Modeling for Aqueous Systems Containing Methyldiethanolamine, Carbon Dioxide and Hydrogen Sulfide", *Fluid Phase Equilibria.* **1997**, 136, 147.

Lawson, J. D., Garst, A. W., "Gas Sweeting Data: Equilibrium Solubility of Hydrogen Sulfide and Carbon Dioxide in Aqueous Monoethanolamine and Aqueous Diethanolamine Solutions", *J. Chem. Eng. Data.* **1976**, 21(1), 20.

Lee, J. I., Otto, F. D., Mather, A. E., "Equilibrium Between Carbon Dioxide and Aqueous Monoethamolamine Solutions", *Appl. Chem. Biotechnol.* **1976**, 26, 541

Lee, J. I., Otto, F. D., Mather, A. E., "The Solubility of H2S and CO2 in Aqueous Monoethanolamine Solutions", *Can. J. Chem. Eng.* **1974**, 52, 803.

Lee, L., "Thermodynamic Models for Natural Gas Sweeting Units", Gas Research Institute 1992 Annual Report, Contract 5091-260-2288.

Lee, L., "Thermodynamic Models for Natural Gas Sweeting Units", Gas Research Institute 1994 Annual Report, Contract 5091-260-2288.

Licht, S. E., Weiland, R. H., "Density and Physical Solubility of Carbon Dioxide in Partial-Loaded Solution of MEA, DEA, and MDEA and Their Blends", Presented at the Spring National Meeting, American Institute of Chemical Engineers, Houston, Texas, April 2-6, **1989**.

Little, R. J., Filmer, B., Versteeg, G. F., van Swaaij, W. P. M., "Modelingof Simultaneous Absorption of H2S and CO2 in Alkanolamine Solutions: the

Influence of Parallel and Consecutive Reversible Reactions and the Coupled Diffusion of Ionic Species", *Chem, Eng, Sci.* **1991**, 46, 2303.

Liu, Y., Zhang, L., Watanasiri, S. "Representing Vapor-Liquid Equilibrium for an Aqueous MEA-CO_2 System Using the Electrolyte Nonrandom-Two-Liquid Model", *Ind. Eng. Chem. Res.* **1999**, 38, 2080.

Lyudkovskaya, Liebush, A. G., *J Appl. Chem. (U.S.S.R.),* **1949**, 23, 145.

Mason, J. W., Dodge, B. F., "Equilibrium Absorption of Carbon Dioxide by Solutions of the Ethanolamines", Proceedings of AIChE Meeting, Columbus, OH, November 13-15, 1935.

Maurer, G., "On the Solubility of Volatile Weak Electrolytes in Aqueous Solutions. In Thermodynamics of Aqueous Systems with Industrial Applications; Newman, S. A., Ed.,; ACS Symposium Series 133; American Chemical Society: Washington, DC, 1980; pp 139-186.

Meissner, R. E., "A Low Energy Process for Purifying Natural Gas", *Proceedings of the gas conditioning Conference, University of Oklahoma, Norman, OK* **1983**

Meissner, R. E., Wagner, U., *Oil and Gas J.*, Feb. 7, pp55-58, **1983**

Mshewa, M., Rochelle G. T., "Carbon Dioxide Desorption/Absorption with Aqueous Mixture of Methyldiethanolamine and Diethanolamine at 40°C to 120°C". Ph.D Dissertation, The University of Texas at Austin, **1995**.

Muhlbauer, H. G., Monaghan, P. R., "Sweeting Natural Gas with Ethanolamine Solutions", *Oil and Gas J.* **1957**, 55(17), 139.

Murzin, V. I., Leites, I. L., *Zhur. Fiz. Khim.* **1971**, 45, 2652.

Nasir, P., Mather A. E., "The Measurement and Prediction of the Solubility of Acid Gases in Monoethanolamine Solutions at Low Partial Pressures", *Can, J. Chem. Eng.* **1977**, 55, 715.

Pacheco, M. A., "Mass Transfer, Kinetics and Rate-Based Modeling of Reactive Absorption", Ph.D Dissertation, The University of Texas at Austin, **1998**.

Pacheco, M. A., Kaganoi, S., Rochelle, G. T., "CO_2 Absorption into Aqueous Mixtures of Diglycolamine® and Methyldiethanolamine", *Submitted to Chem. Eng. Sci.*, July 5, 1999.

Pezold, L. R., "A Description of DDASSL: a Differential/Algebraic System Solver", In Scientific Conputing; Stepleman, R. S., Eds.; IMACS/North-Holland Publishing Co.: Amsterdam, The Netherlands, 1983.

Posey, M. L., Rochelle, G. T., "A Nonrandom Two-Liquid Model for Alkanolamine-Water Systems". Presented at the 44th Canadian Chemical Engineering Conference, Calgary, Alberta, Oct 2-5, **1994**

Posey, M. L., Rochelle, G. T., "A Thermodynamic Model of Methyldiethanolamine-CO_2-H_2S-Water", *Ind. Eng. Chem. Res.* **1997**, 36, 3944.

Posey, M. L., Tapperson, K. G., Rochelle, G. T., "A Simple Model for Prediction of Acid Gas Solubility in Alkanolamines", *Gas. Sep. Purif.* **1996**, 10(3), 181.

Reed, Wood, *Trans. Am. Inst. Chem. Engrs.* **1941**, 37, 363.

Ribker, E. B., Ashour, S. S., Sandall, O. C., "Kinetics and Modelingof Carbon Dioxide Absorption into Aqueous Solutions of *N*-Methyldiethanolamine. *Chem. Eng. Sci.* **1995**, 50, 755.

Rochelle, G. T., "Research Needs for Acid Gas Kinetics and Equilibria in Alkanolamine Systems", Paper presented at the 70th Annual GPA Convention, March 11-12, 1991, San Antonio, Texas.

Secor, R. M., Beutler, J. A., "Penetration Theory for Diffusion Accompanied by a Reversible Chemical Reaction with Generalized Kinetics", *AIChE J.* **1967**, 13, 365.

Shen, K-P., Li, M-H., "Solubility of Carbon Dioxide in Aqueous Mixtures of Monoethanolamine with Methyldiethanolamine", *J. Chem. Data.* **1992**, 37, 96.

Versteeg, G. F., van Swaaij, W. P. M. "Solubility and Diffusivity of Acid Gas (CO_2, N_2O) in Aqueous Alkanolamine Solutions", *J. Chem Eng. Data.* **1988**, 33, 29.

Weiland, R., Chakravarty, T., Mather A., "Solubility of Carbon Dioxide and Hydrogen Sulfide in Aqueous Alkonolamines". *Ind, Eng. Chem. Res.* **1993**, 32, 1419. Also see correction: *Ind. Eng. Chem. Res.* **1995**, 34, 3173.

Weiland, R. H., Dingman, J.C., Cronin, D. B., Browning, G. J., "Density and Viscosity of Some Partial Carbonated Aqueous Alkanolamine Solutions and Their Blends", *J. Chem. Eng. Data.* **1998**, 43, 378.

Xu, G-W., Zhang, C-F., Qin S-J., Gao, W-H., Liu, H-B., "Gas-Liquid Equilibrium in CO2-MDEA-H2O System and the Effect of Piperazine on It", *Ind. Eng. Chem. Res.*, **1998**, 37, 1473-1477.

Xu, G-W., Zhang, C-F., Qin S-J., Wang, Y-W., "Kinetics Study on Absorption of Carbon Dioxide into Solutions of Activated Methyldiethanolamine", *Ind. Eng. Chem. Res.*, **1992**, 31, 921-927.

Xu, G-W., Zhang, C-F., Qin S-J., Zhu, B-C., "Desorption of CO_2 from MDEA and Activated MDEA Solution", *Ind. Eng. Chem. Res.*, **1995**, 34, 874-880.

Zuo, Y-X., Fürst, W., "Use of an Electrolyte Equation of State for the Calculation of Vapor-Liquid Equilibria and Mean Activity Coefficients in Mixed Solvent Electrolyte Systems". *Fluid Phase Equilibria.* **1998**, 115, 267.

Vita

Hongyi Dang was born in Wudalianchi City, Heilongjiang Province, China on March 19, 1975, the daughter of Datong Dang and Xiuyun Fang. After graduation from the Wudalianchi High School in China in July 1993, Hongyi entered the Tianjin University in China. In June 1997, she earned her B.S. degree in Chemical Engineering. Hongyi worked as a research assistant for Chemical Engineering Department of Tianjin University from September 1997 to January 1999. She entered the Graduate School of the University of Texas at Austin in August 1999.

Full time employment has been accepted with The MEMC Southwest in Sherman, Texas.

Permanent address: 231 Wudalianchi, Heilongjiang Province, China 164100

This thesis was typed by the author.